TECHNICAL REPORT STANDARD TITLE PAGE

1. Report No. TX - 01 4188-2	**2. Government Accession No.**	**3. Recipient's Catalog No.**
4. Title and Subtitle A Methodology for Optimizing Opening of PCC Pavements to Traffic		**5. Report Date** August 2003 **6. Performing Organization Code**
7. Authors D. Yuan, S. Nazarian and A. Medichetti		**8. Performing Organization Report No.** Research Report 4188-2
9. Performing Organization Name and Address Center for Highway Materials Research The University of Texas at El Paso El Paso, Texas 79968-0516		**10. Work Unit No.** **11. Contract or Grant No.** Project No. 0-4188
12. Sponsoring Agency Name and Address Texas Department of Transportation Office of Research and Technology Implementation P.O. Box 5080 Austin, Texas 78763-5080		**13. Type of Report and Period Covered** Interim Report 9/00– 8/01 **14. Sponsoring Agency Code**
15. Supplementary Notes Research Performed in Cooperation with TxDOT Research Study Title: Development of Methods and Materials to Accelerate Construction and Opening of PCC Pavements		

16. Abstract

Due to difficulties associated with the maintenance of highways constructed in urban settings, the expedited construction of durable portland cement concrete (PCC) pavement has become a necessity. To obtain a durable PCC pavement, a number of parameters should be considered. One important parameter is the adequate curing of a proper mix before opening the road. Since most urban roads experience excessive traffic, the tendency of highway agencies is to open a newly constructed highway to traffic as soon as possible. A rational method to assess the minimum time required to gain a desired strength before opening it to traffic is proposed here. Two reliable and easy-to-use test methods, maturity method and seismic method, are combined to improve the determination of the readiness of a road to be opened to traffic.

17. Key Words Portland Cement Concrete, Early age, Opening, Seismic Nondestructive Testing, Maturity		**18. Distribution Statement** No restrictions. This document is available to the public through the National Technical Information Service, 5285 Port Royal Road, Springfield, Virginia 22161	
19. Security Classified (of this report) Unclassified	**20. Security Classified (of this page)** Unclassified	**21. No. of Pages** 128	**22. Price**

Form DOT F 1700.7 (8-69)

A Methodology for Optimizing Opening of PCC Pavements to Traffic

by

Deren Yuan, Ph.D.
Soheil Nazarian, Ph.D., P.E.
and
Anitha Medichetti, BSCE

Research Project 0-4188

Conducted for

Texas Department of Transportation

Research Report 4188-2

August 2003

The Center for Highway Materials Research
The University of Texas at El Paso
El Paso, TX 79968-051

Deren Yuan. Ph.D.
Soheil Nazarian, Ph.D., P.E. (69263)
Anitha Medichetti, BSCE

Acknowledgments

The authors would like to express their sincere appreciation to Jim Hunt of the TxDOT Dallas District for ever-present support on this project. We would also like to thank Mr. Gerald Lankes of Construction Division and Mr. Tomas Saenz of El Paso District for their interest in the project.

As usual the staff of El Paso District Lab, especially Hector Zuniga, Luis Randon and Ray Guerra were available to help us. The student involved in this project was Fai Chi.

Executive Summary

Several TxDOT districts throughout the state rely almost solely on portland cement concrete pavement (PCCP) (especially continuously reinforced concrete pavement, CRCP) for heavily traveled metropolitan highways and the urban and suburban sections of the interstate. The goal of most urban projects is to provide smooth and maintenance-free roads to the public with a minimal closure time. Timely opening of the roads to traffic is extremely important. However, if the traffic, especially truck traffic, is allowed on the road before the PCC has gained adequate strength, the pavement performance may be compromised. Understanding the significance of this subject, TxDOT has incorporated new quality control procedures to facilitate estimating the strength of concrete based on the maturity concept. Even though the maturity concept can vastly contribute to that goal, it may be desirable to take advantage of newer technologies that can potentially provide faster, more accurate and more frequent data. In this project, we have evaluated and implemented the seismic technology in conjunction with maturity testing.

The advantage of this procedure is that the same specimens used for laboratory calibration of the maturity data can be used for seismic calibration; however, instead of placing thermocouples at isolated places during construction, a portable device can be used to test a large number of points. In that way, the variability in the curing of concrete due to possible differences in the materials, curing procedures, workmanship and construction equipment can be measured and considered.

In this report the preliminary protocol to be followed as well as the technical and operational feasibility of implementing this procedure is explored.

Implementation Statement

This project, which is tailored towards developing procedures and equipment that can be immediately implemented, is an important missing link towards developing a rational criterion for opening of PCC roads to traffic. To implement the methods and the technology recommended by this research, the guidelines for proper use of these methods and technology has been established, which should be feasible for both TxDOT and contractor.

Most of the laboratory and field equipment are already available for immediate limited implementation and evaluation.

Table of Contents

List of Figures

List of Tables

Chapter 1

Introduction

Several TxDOT districts throughout the state rely almost solely on portland cement concrete pavement (PCCP) (especially continuously reinforced concrete pavement, CRCP) for heavily traveled metropolitan highways and the urban and suburban sections of the interstate. The goal of most urban projects is to provide smooth and maintenance-free roads to the public with a minimal closure time. Timely opening of the roads to traffic is extremely important. However, if the traffic, especially truck traffic, is allowed on the road before the PCC has gained adequate strength, the pavement performance may be compromised. Understanding the significance of this subject, TxDOT has incorporated new quality control procedures to facilitate estimating the strength of concrete based on the maturity concept. Even though the maturity concept can vastly contribute to that goal, it may be desirable to take advantage of newer technologies that can potentially provide faster, more accurate and more frequent data. In this project, we have evaluated and implemented the new technologies that have been recently developed in this field in Texas, the United States, and the world. We have focused particularly on the use of seismic technology in conjunction with maturity testing.

The advantage of this method is that the same specimens used for laboratory calibration of the maturity data can be used for seismic calibration; however, instead of placing thermocouples at isolated places during construction, a portable device can be used to test a large number of points. In that way, the variability in the curing of concrete due to possible differences in the materials, curing procedures, workmanship and construction equipment can be measured and considered.

Organization

Chapter Two contains a brief description of various nondestructive techniques along with their advantages, disadvantages and equipment costs.

Chapter Three describes in detail the two test methodologies used in this study, namely the maturity and seismic methods.

Chapter Four contains the protocols for the two test methods, i.e. the maturity and seismic methods along with an illustrative example.

Chapter Five describes all the four case studies used in this study to determine the feasibility of the procedures in detail along with the mix designs used and test frequencies.

Chapter Six describes the mix related parameters and discusses the studies made on the impact of aggregates and admixtures. It also summarizes the results from all the case studies relevant to the parameters.

Chapter Seven describes the impact of environmental parameters like temperature on concrete with the aid of experimental studies made for the purpose.

Chapter Eight describes the impact of construction parameters on concrete in detail.

The report is summarized and the conclusions are drawn in Chapter Nine. Several appendices supplement the results shown in the report.

Chapter 2

Background

INTRODUCTION

To produce a durable and maintenance-free PCCP, several steps have to be followed. These steps include:

- An appropriate design procedure based on a realistic mechanistic or mechanistic-empirical model
- Concrete mixes using high-quality aggregates, appropriate amount of cement, and other additives that provide the desired design strength and stiffness rapidly without adverse side effects such as shrinkage cracking.
- An appropriately prepared site with favorable climatic condition during construction where the environmental parameters are monitored.
- A means of quality control that not only assures proper construction but will also provide information about the proper timing for saw cutting and opening of the highway to traffic.

Highway agencies face major challenges from increasing traffic volumes on existing roadways and urban streets. Agencies must repair or replace deteriorated aging pavements and add capacity to existing roadways while maintaining traffic on these structures. Traditional pavement construction, repair or replacement solutions are no longer acceptable due to increasing traffic volumes and associated user costs induced by construction work zones. Traditional solutions are especially inappropriate in urban areas where congestion is severe. Accelerated PCC pavement construction, which is suitable for new construction, reconstruction or resurfacing projects, resolves these problems by potentially providing high-quality, long-lasting pavements with quick public access.

One of the primary ways to decrease PCCP construction time for early opening to traffic is to use concrete mix designs that develop strength rapidly. Special care should be exercised with the use of accelerated strength gain mixes to guarantee long-term durability by carefully controlling curing procedures as affected by temperature variations and evaporation rates. Shilstone (2000) has an excellent description of different parameters that should be considered.

The most recent semi-mechanistic approaches for predicting the remaining life of a rigid pavement are based upon inputting the thickness, modulus of elasticity, and tensile strength or flexural strength of the PCC slab as well as a composite modulus of subgrade reaction. Huang (1993) eloquently describes the effects of each of these parameters on the performance of pavements. In the field, the thickness of a PCC slab is determined through coring the slab at pre-determined intervals. The modulus of elasticity is typically measured on cores or laboratory-cured cylinders or through empirical correlations. The tensile strength or flexural strength once again is determined either directly (based on tests on cores, laboratory-cured cylinders or beams), or indirectly (based on correlations with other parameters).

TxDOT's procedure for quality control and decision process for opening a PCC project to traffic is primarily based on flexural or compressive strength testing (Tex-448-A or Tex-418-A) of standard specimens and time. Questions have been raised regarding the decision making process based on this type of testing since it only represents the potential strength of the concrete as delivered to a construction site. It is not intended for determining the strength of the concrete in structure since it makes no allowance for the effects of placement, compaction, and curing. It is almost impossible for the concrete in a structure to have the same strength or stiffness as a standard-cured specimen.

Direct measures of the strength of the concrete in a structure can be obtained through field-cured cylinder or drilled cores. The results of tests on field-cured cylinders are often significantly different from the strength of concrete in place because it is difficult and often impossible to assure identical bleeding, compaction, and curing conditions in the cylinders and in the structure (ACI, 1989). Improper handling or inappropriate storage of these cylinders may result in misleading data for critical construction operations. Core testing is costly, limited in number, and cannot provide the early-age information of the concrete in a structure because drilling can be carried out only on hardened concrete. For these reasons, in-place tests are needed to determine or estimate the strength of the concrete in the structure in the locations and at the time required for various construction operations.

The most feasible in-place methods are based on measuring a property or parameter of concrete that bears some relationship to its strength. An essential step for using these methods to estimate the in-place strength is the development of a correlation between strength and the quantity measured by the in-place test. Usually, such a relationship is empirically established based on testing of standard-cured specimens (Malhotra and Carino, 1991; Bickley, 1993). This relationship is then used to estimate the strength of concrete based on the result of the in-place testing. The accuracy of the estimated strength depends directly on the degree of correlation between the strength of concrete and the quantity measured by the in-place test.

One of the most important factors in accelerated concrete pavement construction is determining when traffic can begin to use the new pavement. The basis for this decision should be made on the concrete strength and not arbitrarily on the time from placement. Strength directly relates to load carrying capacity and provides certainty that the pavement is ready to accept loads by construction or general traffic.

For most concrete pavement applications, flexural strength (ASTM C78) is the most appropriate structural strength criterion to evaluate load capacity. Flexural strength values provide an assessment of the tensile strength at the bottom of the slab where wheel loads induce tensile stresses. However, flexural strength tests are sensitive to the test beams and testing procedures. Many agencies realize this shortcoming and use the more consistent compressive strength test (ASTM C39) to evaluate concrete for acceptance and opening. Strengths from maturity, and other nondestructive tests are evaluated by this research project for use as opening criteria.

The criteria necessary to allow vehicles onto a new pavement depend on the following factors:

- Type, weight and number of anticipated loads during early-age period
- Location of loads on slab
- Concrete modulus of elasticity
- Pavement structure (new construction, bonded or unbonded overlays, tied shoulders, etc.)
- Slab thickness
- Foundation support (layer moduli)
- Edge support condition (widened lane or tied curb & gutter or tied concrete shoulder)

As slab support or pavement thickness increases, stress in the concrete will decrease for a given load. This relationship allows different opening strength criteria for different pavement designs and early traffic loads. An opening strength as low as 150 psi in third-point loading is acceptable if the pavement will carry only automobiles. If the pavement will carry trucks, strength of up to 650 psi may be necessary for thin slabs (Okamoto et al., 1993; FHWA, 1993).

Wheel load location also influences the magnitude of stress. Critical flexural stresses occur from wheels that ride directly on the pavement edge away from a slab corner. Wheel loads that ride near the center of the slab induce considerably lower stresses.

Currently two traffic categories exist for early opening assessment: construction and general traffic. The opening to either type of traffic can be timed based on nondestructive test results that are correlated to the strength of concrete.

Nondestructive Testing

Nondestructive testing (NDT) methods are the techniques used to obtain information about the properties or the internal condition of an object without damaging the object. NDT methods are extremely valuable in assessing the condition of structures, such as pavements, bridges and buildings.

In this study, all the existing and developing nondestructive test methods were reviewed for use in estimating the early age strength of concrete. The study focuses on maturity and seismic methods, as these are the only methods that can monitor the early age behaviors of concrete. The seismic method is the only truly nondestructive test method that can directly measure the elastic modulus of concrete. This characteristic is particularly significant as the same specimens can be subsequently tested at any other required time. Both these tests are affected very little by the localized differences in the composition of the concrete being tested (Ramaiah et al., 2001). Thus the repeatability of these two tests is expected to be much better than others. Other tests are described for completeness.

Surface Hardness Methods

Figure 2.1 – Rebound Hammer

Surface hardness methods measure the hardness of a concrete specimen. Indentation methods and the rebound method constitute the surface hardness methods, out of which, the rebound method is the most widely used and accepted method.

Rebound hammer (Schmidt, 1950) test method is the foremost surface hardness test method, which measures the rebound number that is indicative of the surface hardness of concrete. Though there is no unique relationship between concrete strength and rebound number, certain experimental relationships have been developed between them that depend on several factors such as smoothness of surface (Kolek, 1958; Greene, 1954), carbonation (Kolek, 1969), etc. An accuracy of ±15 to ±20% can be obtained for concrete specimens that are cast, cured and tested under the same conditions. The rebound hammer method is relatively inexpensive and quick. Possible inhibitors to this test are factors such as smoothness of surface, (Kolek, 1958; Greene, 1954) size of concrete (Mitchell and Hoagland, 1961), age of concrete (Kolek, 1958), etc.

According to Carette and Malhotra (1984), the method is not suitable for estimating the early age strength of concrete because of large variations within the tests.

Penetration Resistance Methods

Figure 2.2 – Windsor Probe

The penetration resistance methods consist of the probe penetration and pin penetration test systems out of which the Windsor probe test is considered to be the best one.

The foremost factor affecting the relationship between the strength of concrete and the penetration resistance is the hardness of the coarse aggregate. The relationship between the two is obtained by developing certain correlation curves for each specific type of concrete (Malhotra, 1974). The accuracy and precision of this method is not clearly known though it can be said that the variations are large compared to the variations obtained from the standard cylinder tests (Cantor, 1970). The device commonly used for this test is the Windsor probe at a cost of about \$3000. The advantage of this test is that it is not influenced by local surface conditions unlike in the pin penetration system (Al-Manaseer, 1987). The accuracy of this method in estimating the early age strength of concrete is reasonable (Carrette and Malhotra, 1984) and thus is applied to find out the safe stripping times for the removal of formwork in concrete constructions (Bartos, 1979). This method is also of limited use in this study because of the qualitative nature of the method.

Pull Out Test

Figure 2.3 - Pull Out Test System

The pull out test measures the ultimate load required to pull an embedded metal insert whose enlarged head has been cast into a concrete specimen or structure to a certain depth.

The load measured can be converted to an equivalent compressive strength by means of a relationship advocated by ASTM E178. The pull out test subjects the concrete to static loading unlike the penetration and surface hardness tests. Various studies have been done to analyze the failure mechanism of the pull out test (Jensen and Braestrup, 1976). Though the results have differed, it has been generally concluded that the circumferential cracking begins in the highly stressed region next to the insert head at a pull out load that is a fraction of the measured value. The main advantages of this method are its repeatability and the good correlation between the pull out strength and the compressive strength of concrete (Bickley, 1982). The main disadvantage of this test is the test speed and the destructive nature of the method.

Break Off Test Method

Figure 2.4 - Break Off Test System

The break off test method (Johansen, 1976) is currently the only available test method that measures the flexural strength of the in-place concrete. The test method involves breaking off an in-place cylindrical concrete specimen at a failure plane parallel to the finished surface of the concrete element. The stress measured in this way is related to compressive or flexural strength using a relationship established before hand. The degree of accuracy of the test method is acceptable and the test is reproducible.
The main application of this method is the estimation of time for safe form removal; hence the method is reliable for estimating early age strength. The major limitation of this method is that the damage done to the specimen must be repaired.

Ultrasonic Pulse Velocity Method

Figure 2.5 – Ultrasonic V-Meter

The ultrasonic pulse velocity method determines the velocity of propagation of ultrasonic energy pulse through a concrete member.

The operational principle of the equipment involves sending a short duration, high voltage signal by a pulser to a transducer to vibrate at its resonant frequency (ASTM C597). The pulse travels through the member and is detected by a receiving transducer coupled to the opposite concrete surface. When the pulse is received the timer is turned off and the elapsed travel time is displayed. The pulse velocity is obtained by dividing the direct path length between the transducers by the travel time. For a given concrete mixture, as the compressive strength increases with age, there is a proportionally smaller increase in the pulse velocity (Jones, 1954). Thus at early ages, the pulse velocity is sensitive to the gain in strength. The accuracy of measurements depends on factors such as moisture content (Jones and Facaoaru, 1969) and steel reinforcement (Chung, 1978) in the member. The devices commonly used for pulse velocity measurement are V-meters at a cost of about $4500. The limitation of this method is that the results are operator dependent and for longer travel paths the results are not constant.

Other Methods

The following are some of the other nondestructive methods used for testing concrete. The parameters measured with these methods are difficult to be related to the strength parameters of concrete. Magnetic and electrical nondestructive methods of testing concrete are used to evaluate properties of concrete such as moisture content, corrosion potential of reinforcement, etc.

Current excitations and magnetic response are the underlying principles of the magnetic methods. Magnetic nondestructive techniques can be used only on ferromagnetic materials. The magnetic method is used for concrete evaluation because of the magnetic properties of reinforcement and the response of hydrogen nuclei to such fields. Electromagnets are used in most of the cases. Its applications include determination of the depth of concrete cover (Rebut, 1962), detection of flaws in reinforcement (Kusenberger and Barton, 1981) and determination of moisture content (Matzkanin et al., 1982).

Electrical resistance, dielectric constant and polarization resistance are the three electrical properties of concrete on which the electrical methods for evaluating concrete are based on. Properties of concrete such as moisture content (Hammond and Robson, 1955) and pavement thickness (Vassie, 1978) are measured using the electrical methods. The accuracy of the measurements depends on the variations in the parameters measured.

Radioactive and nuclear methods refer to test methods that use the interaction of wave or particle radiation with matter to evaluate the properties of concrete such as reinforcement, density, etc. Radiometry (Malhotra, 1976), radiography (Barton, 1976) and neutron gamma techniques

(Malhotra, 1976) are the three methods generally used for testing concrete out of which gamma radiometry is the most popular. The main principle of these methods is the usage of radiation from different sources to bombard concrete specimens. The radiation transmitted or emitted by concrete is then collected and analyzed and thus the properties are determined. These methods are very accurate and quick but are not widely used because of their complex technology, high initial costs and training and licensing requirements.

Short pulse radar methods are primarily used for nondestructive detection of delamination and other types of defects in reinforced concrete decks. The main principle of these methods is the propagation of electromagnetic energy through materials of different dielectric constants. The other applications of these methods include the determination of hydration of cement (Clemena, 1983), water content of concrete (Clemena, 1987) and the thickness of concrete (Clemena and Steele, 1988).

Chapter 3

Maturity and Seismic Concepts

Maturity Method

The strength of a given concrete mixture, which has been properly placed, consolidated and cured, is a function of its age and temperature history (Saul, 1951). At early age, temperature has a dramatic effect on strength development. The maturity method, which accounts for the combined effects of time and temperature on the strength development of concrete, is used during the curing period only. The temperature history obtained from the maturity method is used to calculate the maturity index, which is then related to strength by a strength-maturity curve.

Saul (1951) gave the following expression to calculate the maturity with respect to a "datum temperature," which is defined as the lowest temperature at which the gain in strength of concrete is observed:

$$M(t)=\Sigma(T_a-T_o)\Delta t \tag{3.1}$$

where M(t) = time-temperature factor (TTF) at age t, Δt = time interval between consecutive measurements, T_a = average concrete temperature during time interval, Δt, and T_o = datum temperature. This equation has become known as the Nurse-Saul function. Saul recommended a datum temperature of 10.5°C for Equation 3.1, while Plowman (1956) recommended a temperature of -12°C. A datum temperature of -10°C is currently being used for the function.

Alternatively, the equivalent age is used to define maturity. The equivalent age is defined as the duration of the curing period at the reference temperature resulting in the same maturity value as the curing period at any other temperatures. The Nurse-Saul function for calculating the equivalent age is:

$$t_e=\Sigma(T_a-T_o)/(T_r-T_o)\,\Delta t \tag{3.2}$$

where t_e =equivalent age at the reference temperature, T_r = reference temperature

Equation 3.2 can also be written as:

$$t_e = \Sigma \alpha \Delta t \tag{3.3}$$

where

$$\alpha = (T_a - T_o)/(T_r - T_o) \tag{3.4}$$

and is known as age conversion factor and it converts Δt to the equivalent curing interval at the reference temperature.

Weaver and Sadgrove (1971) gave the following equation for equivalent age at 20°C:

$$t_e = \Sigma (T_a + 16)^2 \Delta t / 1296 \tag{3.5}$$

Freisleben et al. (1977) gave the following expression for the equivalent age based on the Arrhenius equation:

$$t_e = \Sigma e^{-E/R[(1/273+Ta)-(1/273+Tr)]} \Delta t \tag{3.6}$$

where T_r = reference temperature, E = activation energy, and R = universal gas constant. They also suggested the following values for E:

For T≥20°C	E=33500 J/mol
For T<20°C	E=33500+1470(20-T) J/mol

Equation 3.2, the Nurse-Saul function, was mostly used in this study to represent the maturity parameter.

The device used to measure the maturity is known as the maturity meter. Maturity meters are used to monitor and record the temperature history of concrete needed for strength predictions. Maturity measurement in the field consists primarily of monitoring the internal temperature of the concrete with respect to time. Maturity meters are basically temperature-measuring devices that automatically compute the TTF and the equivalent age of the concrete with time. The temperature is monitored by attaching thermocouple wires inserted into the fresh concrete to the maturity meter. The numbers of thermocouples used for on a project depend on several factors such as type of structure, weather conditions, etc.

Several maturity meters are commercially available in the market. Two of them, namely the Humboldt H-2686 and James M-3056 maturity meters (see Figure 3.1) were used in this study. The cost of a 4-channel Humboldt model H-2686 maturity meter is about $1,200 and the cost of a 6-channel James M-3056 maturity meter is about $3,000. Less expensive alternative devices that can also be used for maturity monitoring are digital data loggers. The major difference between the maturity meters and the temperature recorders is that the maturity meters give the values of equivalent age and the temperature time factor directly, whereas the temperature recorders record the temperature only, hence the equivalent age and the temperature-time factor

a) Humboldt H-2686 Maturity Meter

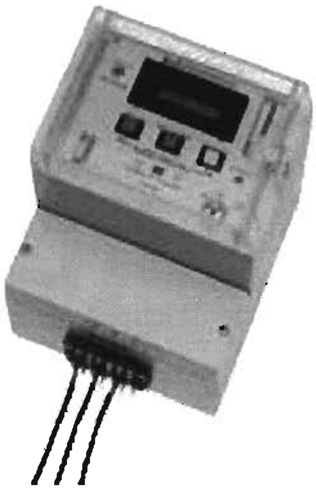

b) James M-3056 Maturity Meter

Figure 3.1 – Typical Maturity Meters Used in This Study

are calculated later using the maturity functions. Ramaiah et al., (2001) also discusses several inexpensive, disposal temperature data loggers.

Various strength-maturity relationships have been proposed. Nykanen (1956) proposed the following exponential relationship:

$$S = S_{\infty} (1 - e^{-KM}) \qquad (3.7)$$

where S = compressive strength at a given maturity, S_{∞} = ultimate compressive strength of mixture, M = TTF and K= a mix-related constant that depends on the initial rate of strength gain and water-cement ratio.

Plowman (1956) proposed the following empirical relationship:

$$S = a + b \log(M) \qquad (3.8)$$

The two constants a and b are related to the water-cement ratio and the type of cement. Chin (1971) gave the following hyperbolic function for the strength-maturity relationship:

$$S = M / (1 / A + M / S_{\infty}) \qquad (3.9)$$

where A is the initial slope of strength-maturity curve. Carino (1984) found that Equation 3.9 is not appropriate for small maturity values; hence it was modified into the following:

$$S = (M - M_0) / [1 / A + (M - M_0) / S_{\infty}] \qquad (3.10)$$

Where M_o is the offset maturity. The concept of offset maturity (Carino, 1981) was introduced to account for the strength development that does not start until a finite value of maturity is reached.

Freiesleben and Pederson (1985) recommended the following relationship based on the relationship between the heat of hydration and maturity:

$$S = S_{\infty} e^{-[\tau/M]^{a}} \tag{3.11}$$

where τ = characteristic time constant and a = shape parameter.

All the above-proposed relationships are useful in representing the relationship between strength and maturity. However, irrespective of the relationship used, the coefficients that define the exact shape of the curves depend on the particular concrete mixture.

Seismic Method

Seismic methods rely on generation and detection of elastic waves within a medium and measuring the velocity of propagation of these waves. The measured velocity can be converted to the modulus of elasticity (also called the seismic modulus) based on theory of elasticity. A summary of wave propagation principles is included in Appendix A for the benefit of the readers. Three types of waves (i.e., compression wave, shear wave, or surface wave) are typically used in the civil engineering applications. Seismic tests can be carried out in the laboratory as well as in the field.

The free-free resonant column (impact resonance) tests of specimens (ASTM C215) is particularly suitable for measuring the seismic modulus of concrete in the laboratory. When a cylindrical specimen is subjected to an impulse load at one end, seismic energy over a large range of frequencies will propagate within the specimen (see Figure 3.2). Depending on the dimensions and the stiffness of the specimen, energy associated with one or more frequencies are trapped and resonate as they propagate within the specimen. The goal with this test is to determine these resonant frequencies. Since the dimensions of the specimen are known, if one can determine the resonant frequencies, one can readily determine the modulus of the specimen using principles of wave propagation in a solid rod (Richart et al., 1970).

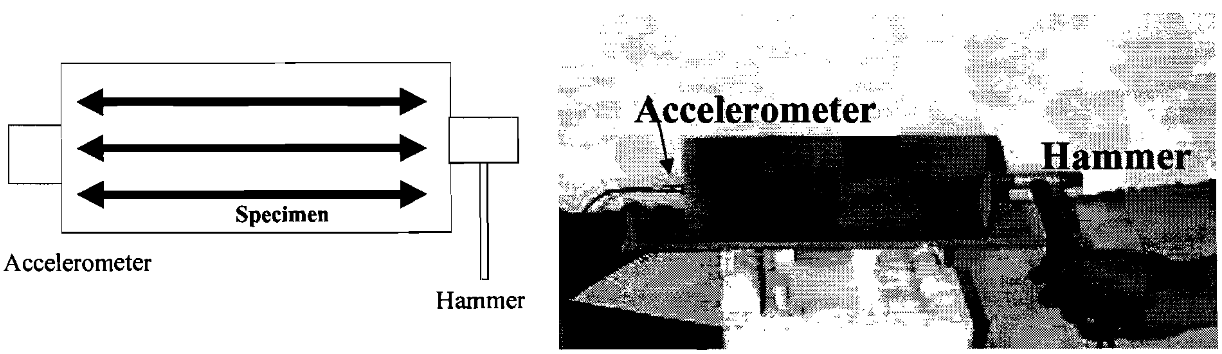

Figure 3.2 – Resonant Column Concept

Results from a typical test are shown in Figure 3.3. Resonant frequencies appear as peaks in a so-called amplitude spectrum. Two peaks are evident, one corresponding to the longitudinal propagation of waves in the specimen, and the other corresponding to the shear mode of vibration. It is simple to distinguish the two peaks, because for typical concrete specimens, the longitudinal resonance occurs at a higher frequency than the shear resonance.

Once the longitudinal resonant frequency, f_L, and the length of the specimen, L, are known, laboratory Young's modulus, E_{lab}, can be found from the following relation:

$$E_{lab} = \rho \ (2 \, f_L \, L)^2. \tag{3.12}$$

where ρ is mass density. The mass density is calculated from:

$$\rho = M/(L \, A_s) \tag{3.13}$$

where A_s is the cross-sectional area of the specimen. Poisson's ratio, ν, is determined from

$$\nu = (0.5\,\alpha - 1) / (\alpha - 1) \tag{3.14}$$

where

$$\alpha = (f_L / f_S)^2 \, C_{L/D} \tag{3.15}$$

with $C_{L/D}$ being a correction factor when the length-to-diameter ratio differs from 2 and f_s=shear (or torsional) resonant frequency.

Under Project 0-1735, we have simplified the above test and have delivered two prototypes for implementation (see Figure 3.4). The test can be performed in less than 30 seconds. The set up and software developed has been modified for ease of use with this project. One of the advantages of this method is that it provides properties that can also be directly measured in the

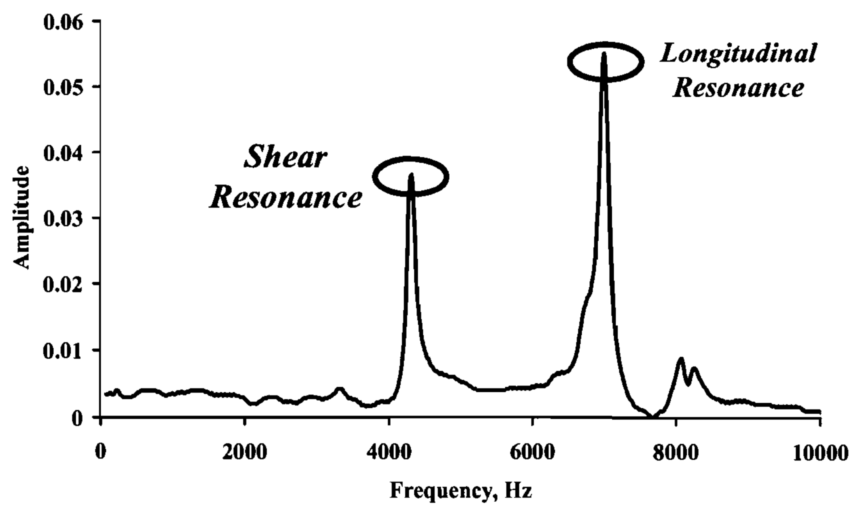

Figure 3.3– Typical Response from a Concrete Cylindrical Specimen

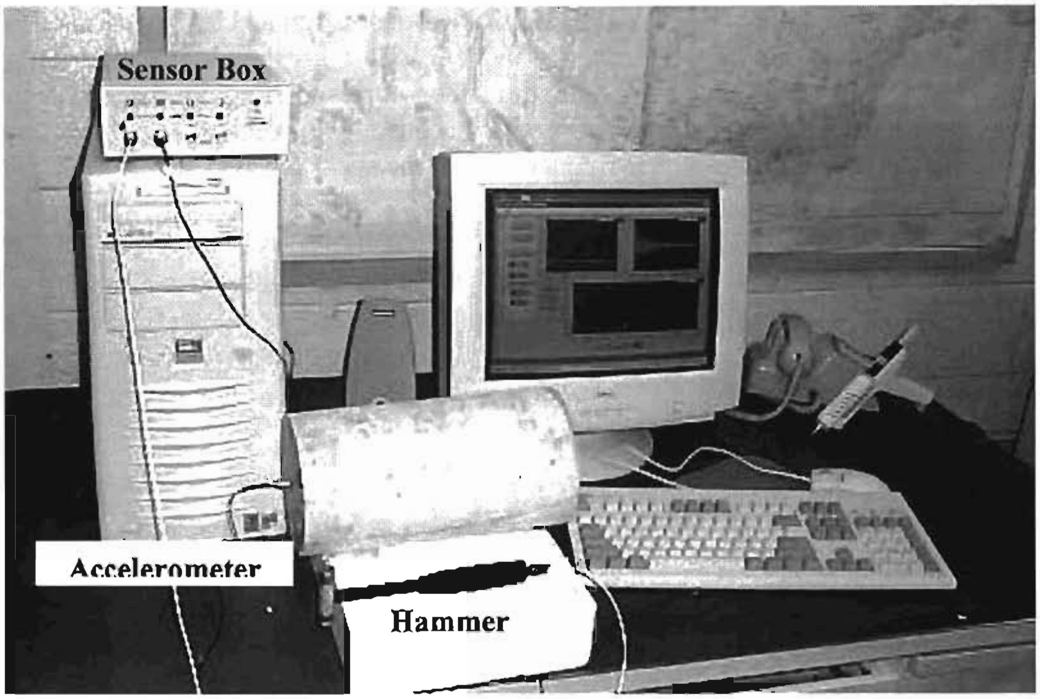

Figure 3.4 – Free-Free Resonant Column Test

field with a nondestructive testing device called the Portable Seismic Pavement Analyzer (PSPA). The PSPA estimates the in-place seismic modulus of a PCC slab. The PSPA (see Figure 3.5) consists of two transducers and a source packaged into a hand-portable unit. The device is operable from a computer. This computer is tethered to the hand-carried transducer unit through a cable that carries power to the accelerometers and hammer and returns the measured signals to the data acquisition board in the computer.

The major mechanical components of the PSPA sensor unit, as depicted in Figure 3.6, are near and far accelerometers, and an electric source. The data collected with the PSPA can be processed using signal processing and spectral analysis to determine the modulus of the layer. The analysis can be conducted by either inspecting the time-domain records, or can be performed in the frequency-domain via the Ultrasonic Surface Waves (USW) tests.

Theoretically, compression, shear or surface wave velocity of the upper layer of pavement, can be measured from the time records. A typical record is shown in Figure 3.7. Once the wave velocity of a material is known, its Young's modulus can be readily determined.

In the time-domain analysis, one relies on identifying the time at which different types of energy arrive at each sensor. The velocity of propagation, V, is typically determined by dividing the distance between two receivers, ΔX, by the difference in the arrival time of a specific wave, Δt. In general, the relationship can be written in the following form:

$$V = \frac{\Delta X}{\Delta t} \tag{3.16}$$

Figure 3.5 – Portable Seismic Pavement Analyzer

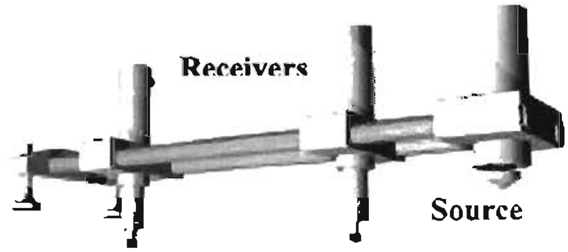

Figure 3.6 – Sensor Unit of PSPA

In the equation, V can be the propagation velocity of any of the three waves [i.e. compression wave, V_P; shear wave, V_S; or surface (Rayleigh) wave, V_R]. Knowing wave velocity, modulus can be determined in several ways. Young's modulus, E, can be determined from shear modulus, G, through Poisson's ratio (ν) using:

$$E = 2(1+\nu)G \tag{3.17}$$

Shear modulus can be determined from shear wave velocity, V_S, using:

$$G = \rho V_S^2 \tag{3.18}$$

To obtain modulus from surface wave velocity, V_R is first converted to shear wave velocity using:

$$V_S = V_R(1.13 - 0.16\nu) \tag{3.19}$$

The shear modulus is then determined by using Equation 3.18.

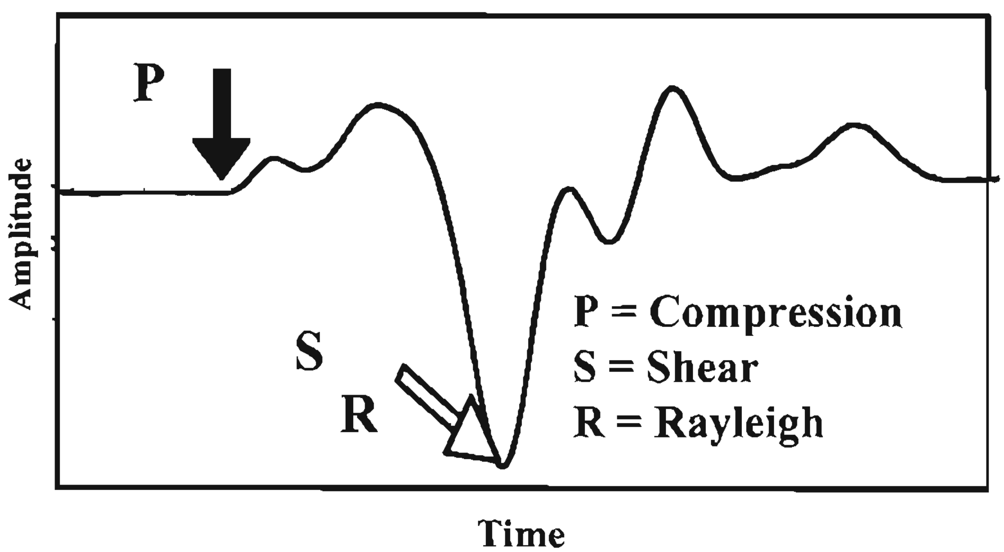

Figure 3.7 – Typical Time Record Used in UBW Method

As an example, the arrivals of compression, shear and surface waves are marked on Figure 3.7. The compression wave (or P-wave) energy is reasonably easy to identify because it is the earliest source of energy to appear in the time record. Since only less than 10% of the seismic energy propagates in this form, the peak compression wave energy in the signal sometimes is only several times above the inherent background noise. This limitation may make it difficult to always reliably estimate the arrivals of these waves.

The shear wave (or S-wave) energy is about one-fourth of the seismic energy, and as such it is better pronounced in the record. The practical problem with identifying this type of waves is that they propagate at a speed that is close to that of the surface waves. As such, the separation of the two energies, at least for short distances from the source, may be difficult.

Surface (Rayleigh) waves contain about two-thirds of the seismic energy. As marked in Figure 3.7, the most dominant arrivals are related to the surface waves; as such it should be easy to measure them. If a layer does not have surface imperfections, and if the impact is sharp enough to generate only waves that contain energy for wavelengths shorter than the thickness of the top layer, this method can be readily used to determine the modulus. However, it may be difficult to observe these two restrictions. The USW method, even though more complex to implement, it is by far more robust for the user than the time-domain analysis.

The ultrasonic-surface-wave (USW) method[1] is an offshoot of the SASW method. The major distinction between these two methods is that in the ultrasonic-surface-wave method the modulus of the top pavement layer can be directly determined without using an inversion algorithm.

As sketched in Figure 3.8, at wavelengths less than or equal to the thickness of the uppermost layer, the velocity of propagation is independent of wavelength. Therefore, if one simply generates high-frequency (short-wavelength) waves, and if one assumes that the properties of the uppermost layer are uniform, the shear wave velocity of the upper layer, V_s, can be determined from the velocity of surface waves, V_{ph}, using Equation 3.19.

By combining Equations 3.17, 3.18 and 3.19, the modulus of the top layer, E_{field}, can be determined from

$$E_{field} = 2 \rho V_s^2 (1 + \nu). \tag{3.20}$$

The wavelength at which the phase velocity is not constant anymore is closely related to the thickness of the top layer.

1 Some organizations involved in seismic tests do not differentiate between the USW and the SASW methods. In our terminology the SASW test is a comprehensive test that requires the development of an experimental dispersion curve and determining the modulus profile through an inversion process. The USW simply provides the modulus of the top layer without need for an inversion process, and as such is much simpler to perform.

It can be shown theoretically that the laboratory and field moduli, E_{lab} and E_{field}, are related through Poisson's ratio, ν, (Richart et al., 1970). The relationship is in the form of:

$$E_{field} / E_{lab} = (1 + \nu)(1 - 2\nu) / (1 - \nu) \qquad (3.21)$$

For a typical concrete (Poisson's ratio=0.2) the ratio of the two moduli is about 0.9. This means that the modulus from the PSPA determined in the way discussed above has to be divided by 0.9 to obtain the modulus of the identical material tested with the free-free resonant column test.

Alexander (1996) demonstrated that the velocities measured with the PSPA and free-free resonant column tests are highly correlated. The results of the evaluation of the seismic laboratory and field tests performed by Alexander (1996) are included in Table 3.1. He concluded that the repeatability of the tests was better than those carried out by traditional strength tests.

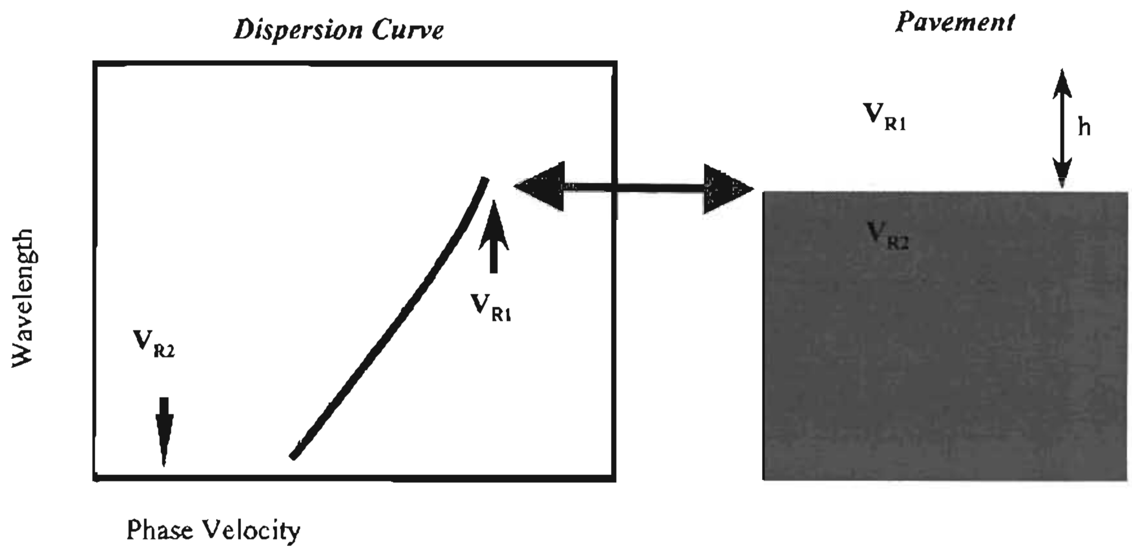

Figure 3.8 – Schematic of USW Method

Table 3.1 – Evaluation of Repeatability of Free-Free Resonant Column and PSPA (from Alexander, 1996)

Test Type	No. of Data Sets [Replicates]	Range of Means	Range of Std. Dev.	Average and [Range] for CV(%)
Free-Free P-Wave Velocity for Sawn Beams - between replicates on a single beam	63 [3]	11545 to 14230 fps	0 to 845 fps	1.2 [0 to 6.9]
Free-Free P-Wave Velocity for Sawn Beams - between beams for a single mixture	16 [4]	11670 to 14090 fps	39 to 465 fps	1.6 [0.3 to 3.6]
Free-Free P-Wave Velocity for Field Cores[a] - between replicates on a single core	24 [10]	12725 to 17265 fps	0 to 110 fps	0.2 [0.0 to 0.8]
Free-Free P-Wave Velocity for Field Cores[a] - between cores for a single mixture	6 [4]	12875 to 15880 fps	45 to 1020 fps	2.0 [0.4 to 6.4]
Free-Free P-Wave Velocity for Lab-Molded Beams - between replicates on a single beam	33 [3]	9870 to 14535 fps	7 to 270 fps	0.6 [0.1 to 1.9]
Free-Free P-Wave Velocity for Lab-Molded Beams - beams for a single mixture	12 [3]	9980 to 14390 fps	13 to 430 fps	1.0 [0.1 to 4.1]
Free-Free P-Wave Velocity for Lab-Molded Cylinders[b] - between replicates on a single cylinder	72 [3]	9650 to 14110 fps	0 to 480 fps	0.8 [0.0 to 3.7]
Free-Free P-Wave Velocity for Lab-Molded Cylinders[b] - between beams for a single mixture	24 [3]	12400 to 14020 fps	8 to 340 fps	1.0 [0.1 to 2.6]
PSPA R-Wave Velocity for Slabs[c] - between readings at the same location	2 [30]	7360 to 8090 fps	31 to 40 fps	0.5 [0.4 to 0.5]
PSPA R-Wave Velocity for Slabs[c] - between locations in close proximity	48 [3 to 5]	6020 to 8640 fps	10 to 250 fps	0.8 [0.1 to 3.5]

[a] includes 6-, 4-, and 3-inch diameter specimens
[b] 6x12-inch cylinders only
[c] 6-inch thick slabs

Chapter 4

Maturity-Seismic Test Protocols

Introduction

As indicated before, the combination of maturity and seismic methods complement one another quite readily. The calibration process for relating strength and maturity can be readily adapted for laboratory seismic testing. In fact, the same specimens can be used for both tests.

The seismic method has several advantages over the maturity concept. Since in the current specifications, two thermocouples per 1000 yd^2 of PCC poured are required, approximately one sample for every 375 ft of a 12-ft wide standard lane is considered. As such, any variability in the strength of concrete due to batching errors, construction, equipment-related problems or the curing process might not be found with the maturity tests. A proposed protocol that combines the two methodologies is included in this chapter. The protocol is illustrated using an example.

Specimen Preparation

Both ASTM (C1074) and TxDOT (Tex-426-A) have standard methods for preparing the specimens. The specimen preparation adopted here is identical to that recommended by the Tex-426-A (see Appendix B). For compressive strength, a total of 12 standard 6 in. (diameter) by 12 in. (length) specimens are prepared. For flexural strength, a similar number of specimens but in the shape of standard beams is poured. It should be mentioned that if one would be interested in only establishing relationships between the seismic modulus and maturity only three specimens are necessary. During specimen preparation, thermocouples are inserted into 3 cylinders. The specimens are then cured in a curing tank.

Test Procedure

Testing consists of four phases: maturity measurement, strength tests, seismic modulus tests, and development of the correlations. Each is discussed below.

I. Maturity Tests: As usual, the specimens equipped with thermocouples are either connected to a maturity meter or a temperature data-logger. Both the devices record the variation in temperature with time automatically when they are turned on. The temperature is continuously measured for 28 days. The temperature time history is converted to the time-temperature factor or to the equivalent age using Equations 3.1 and 3.2, respectively.

II. Seismic Tests: Shortly before a specimen is subjected to strength test, the free-free resonant column test will be carried out on it. Since the test is nondestructive, this activity should not impact the results from the strength tests. In this case, the modulus and optionally the Poisson's ratio of the specimen is determined for correlation to strength and maturity.

III. Strength Tests: Standard compression or three point bending tests are performed on at least 3 cylinders or beams at ages of 1, 3, 7 and 28 days. The average compressive strength or the flexural strength from the three tests is obtained.

IV. Development of Correlations: A plot between the average compressive or flexural strengths and average maturity values at corresponding times is made and a best-fit curve is drawn through the plot. The curve is then used for estimating the strength of concrete based on maturity as it has been traditionally done. Similarly, a plot between the average compressive or flexural strengths and average seismic moduli is developed. A best-fit curve is also drawn through this data. This relationship can be readily used with the PSPA for predicting the strength of the concrete at any location on the slab or other structures.

An example will illustrate this simple procedure.

Illustrative Example

The results from tests on the so-called Small Slab I Study carried out in El Paso are included here. Even though two types of aggregates (limestone and siliceous river gravel) were used in this study, we will focus on the limestone mixture typically used in that region. The concrete mixture is summarized in Chapter 5.

Typical variations in compressive strength from standard cylinders with maturity parameters are shown in Figure 4.1. The time-temperature factor (TTF), as defined in Equation 3.1, is used to represent the maturity parameter in Figure 4.1a. A good correlation is observed between the compressive strength and TTF as judged by a coefficient of determination (R^2 value) of about 0.97. Alternatively, the variation in compressive strength with the equivalent age using Equation 3.2 can be used (see Figure 4.1b). Naturally, this relationship is adequate as well. Since the two maturity parameters demonstrate essentially the same information, we will concentrate on TTF from here on.

Indirect split tensile and three-point bending tests were also carried out on cylinders and beams cured under standard conditions. The variations in tensile strength and flexural strength with TTF are shown in Figures 4.2 and 4.3, respectively. The tensile strength is reasonably (R^2 = 0.82) and the flexural strength is strongly (R^2 = 0.96) correlated to the TTF.

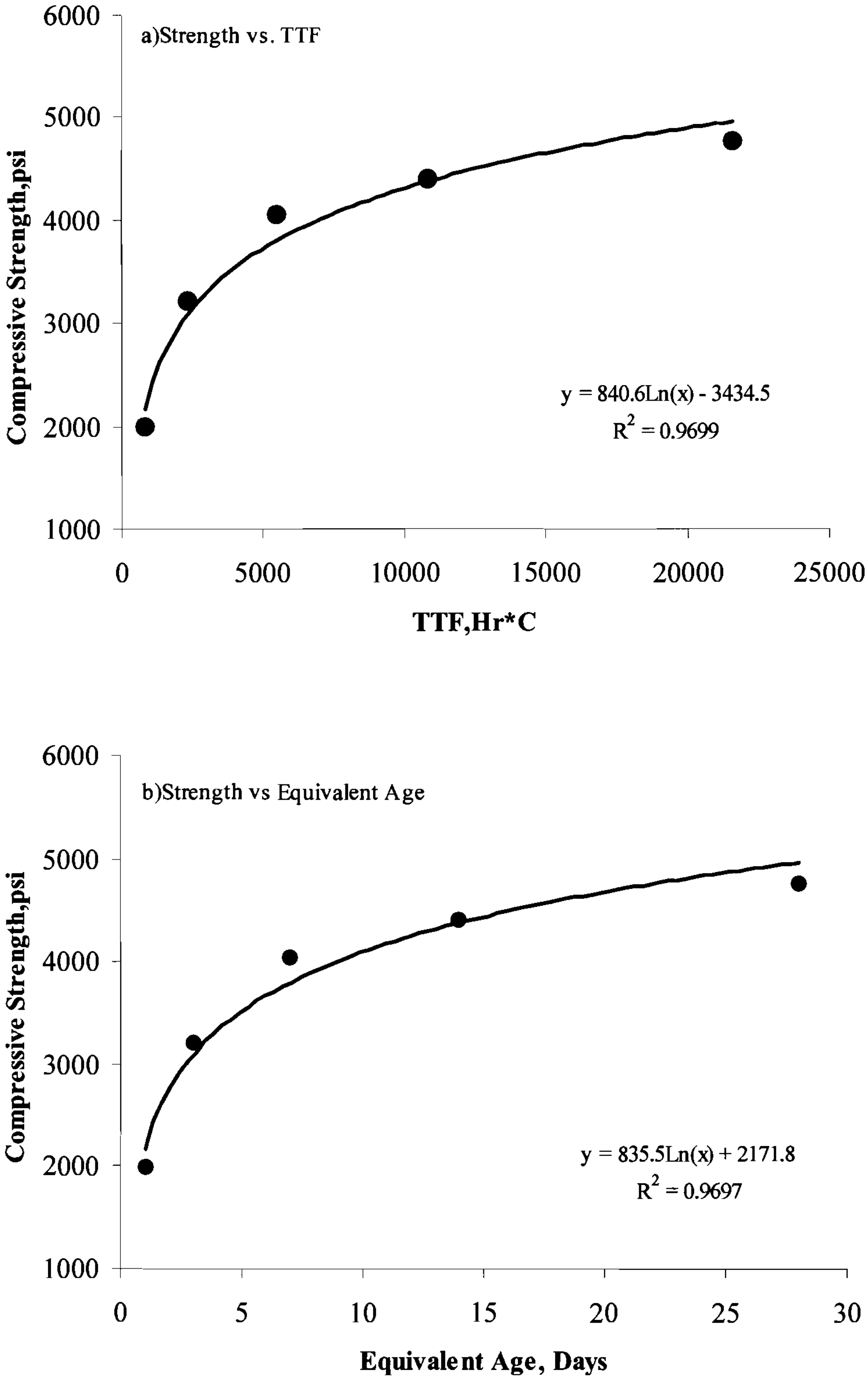

Figure 4.1 – Variations in Compressive Strength with Maturity Parameters

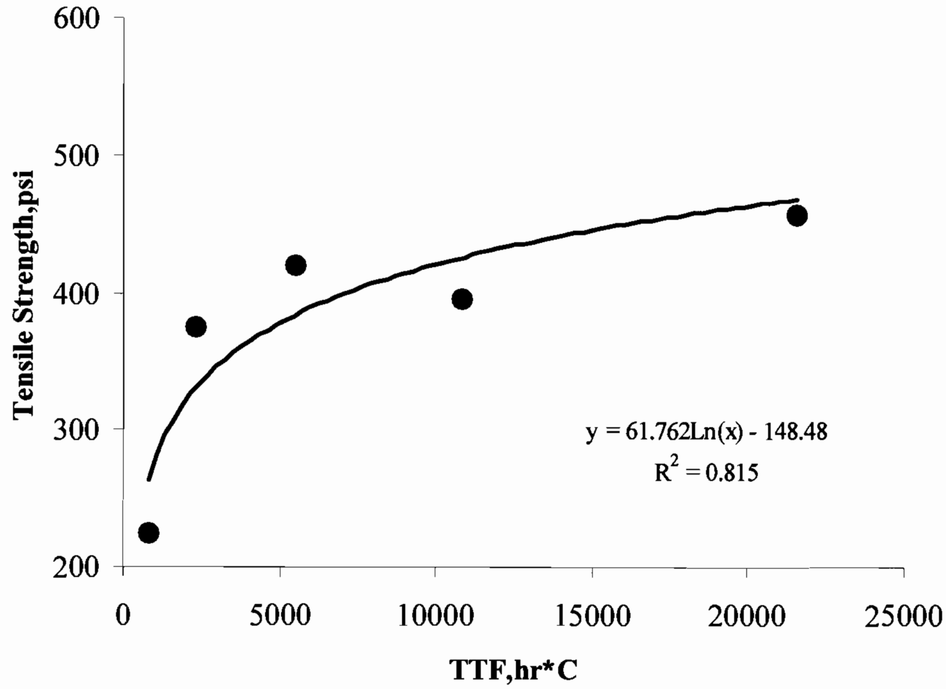

Figure 4.2 – Variation in Tensile Strength with Maturity Parameter

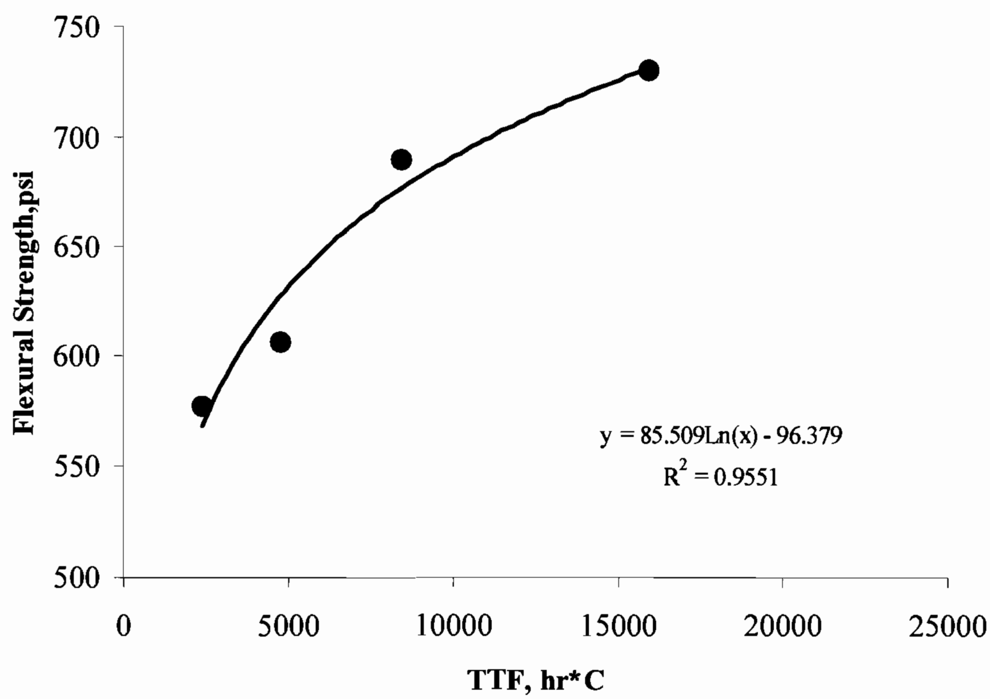

Figure 4.3 – Variation in Flexural Strength with Maturity Parameter

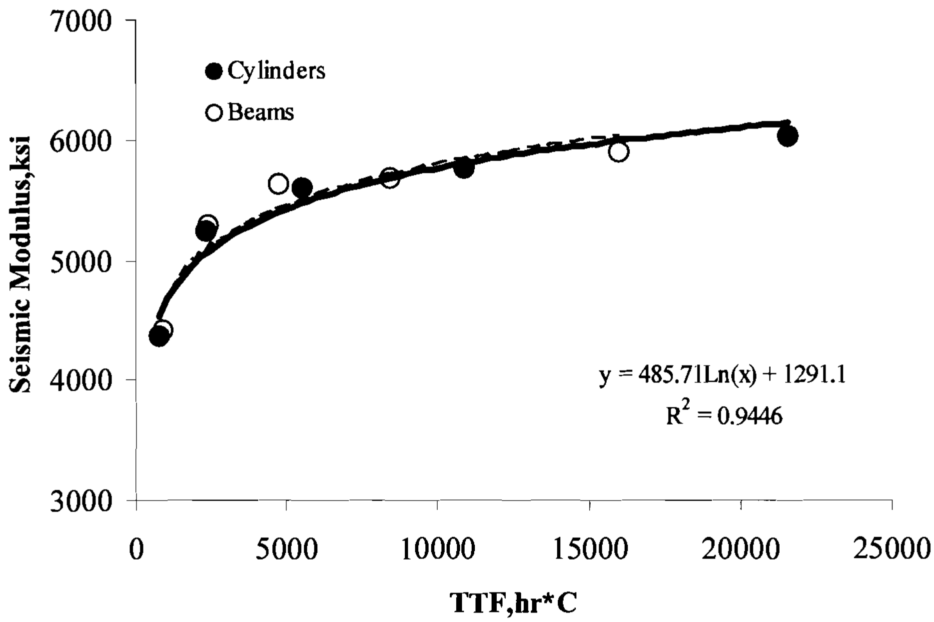

Figure 4.4 – Variation in Seismic Modulus with Maturity Parameter

The variation in seismic modulus with TTF on the cylinders, used for determining the compressive strength shown in Figure 4.1, is shown in Figure 4.4. A high correlation between the seismic modulus and TTF is obtained. Also included in the figure is the variation in the seismic modulus with TTF for the beams tested for flexural strength. Since the results from the cylinders and beams follow one another closely, the seismic modulus is practically independent of the shape of the specimen being tested (See Ramaiah et al., 2001 for a detailed statistical analysis). Figure 4.4 can be readily used to project the modulus of concrete as a function of time as typically done with the strength-maturity relationship.

In the next step, the seismic moduli measured at different times are related to the compressive, tensile and flexural strengths. The results from this exercise are shown in Figure 4.5. The compressive and tensile strengths are highly correlated to the seismic modulus. The flexural strength is more moderately correlated since the R^2 value is about 0.84. This occurs because only four data points are available, and none of them belong to the early ages of the concrete. These three relationships can in turn be used to predict the strength of materials as a function of seismic moduli measured in the field with the PSPA.

Unfortunately, most cores were 4 in. in diameter and only six 6-in.-diameter cores were made for compressive tests at this site. Three of these cores were made after 7 days of curing and the other three after 28 days. The average compression strength of each of these cores is plotted against the seismic modulus in Figure 4.5a with open symbols. Both data points lie fairly close

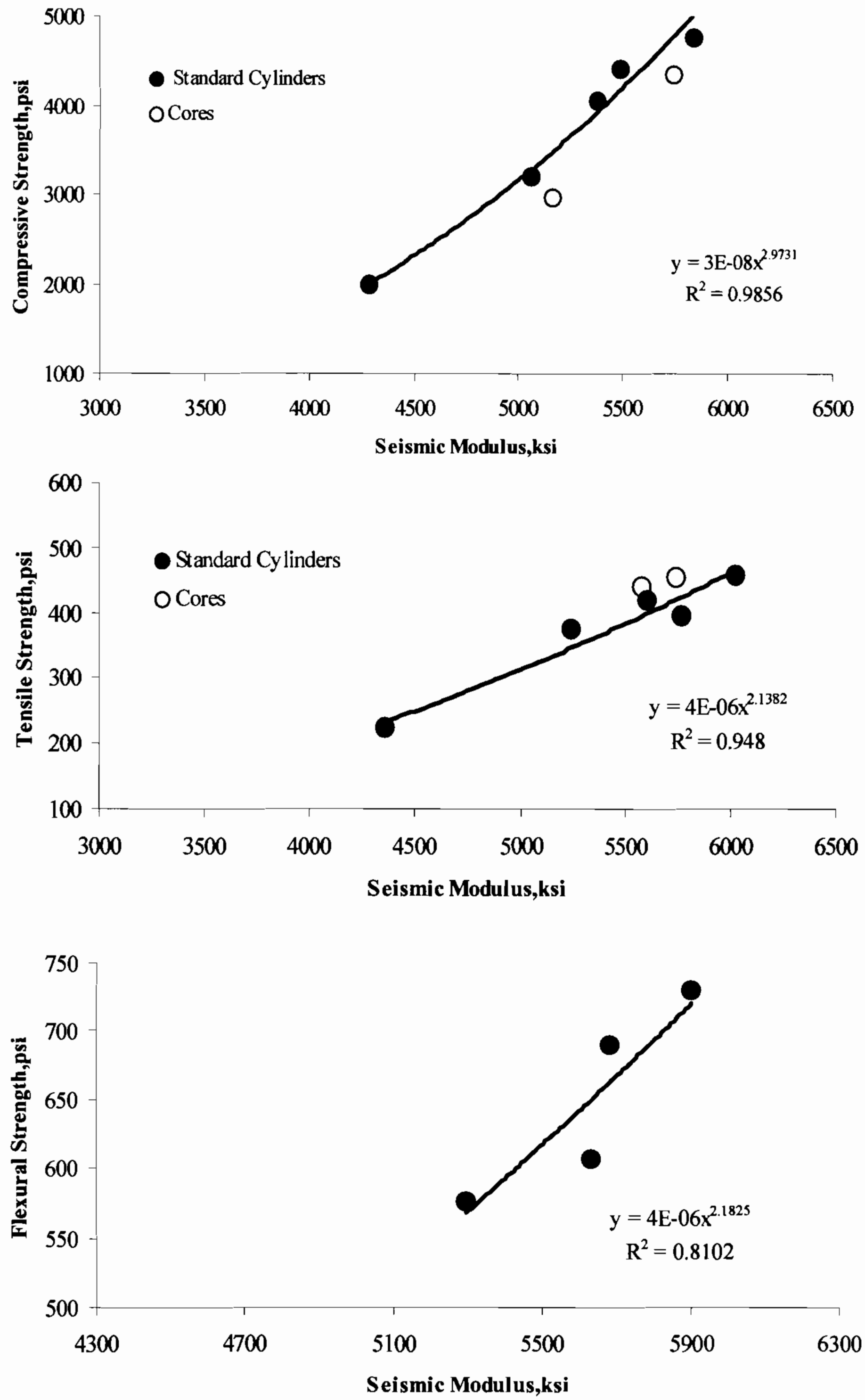

Figure 4.5 – Variations in Strength Parameters with Seismic Modulus

to the trend line. This means that, by conducting a PSPA measurement and using the equation of the trend line, the strengths are estimated by an accuracy of better than 10% to 15%. Similar exercise was carried out for the tensile strength. Once again, the tensile strengths using the seismic modulus and the relationship developed from the laboratory study will predict the modulus with an accuracy of better than 10%.

Similarly, the results from the traditional maturity model are shown in Figure 4.6. As anticipated, the compressive strength is predicted reasonably well with an accuracy of better than 20% for the seven-day strength and 10% for 28-day strength.

The protocol described here is comprehensively written in the TxDOT specification format in Appendix B.

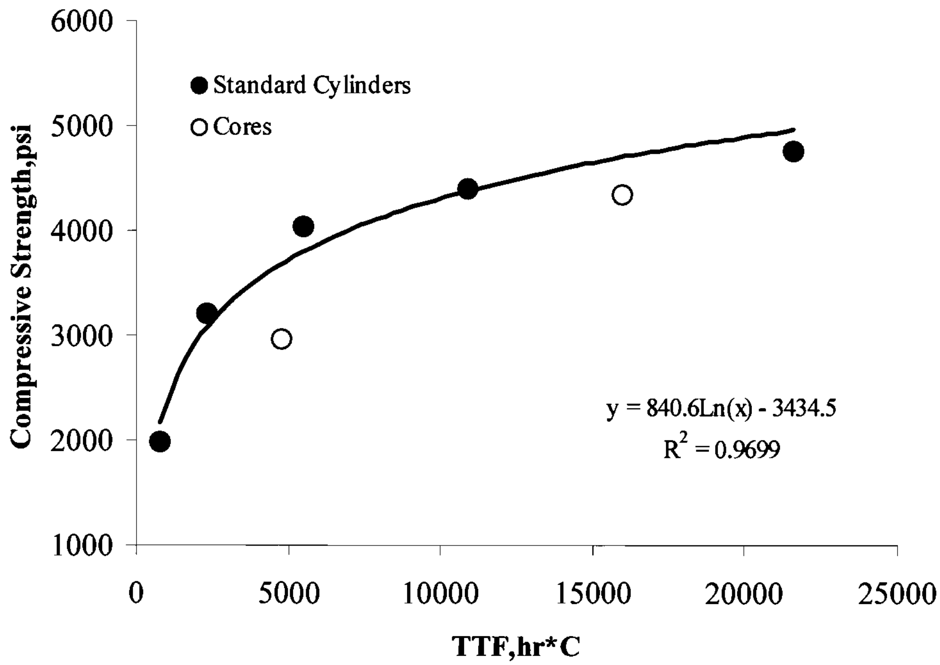

Figure 4.6 – Comparison of Laboratory and Field Results Relating Compressive Strength with Maturity Parameter

Chapter 5

Case Studies

Introduction

Developing a universal relationship that relates either the maturity parameters or seismic moduli to strength parameters of concrete is very desirable. This is typically not possible because of vast variety of aggregates, cements and additives that are utilized in the concrete industry. Through several case studies, we attempted to study the impact of three categories of parameters on these relationships. These categories include mix-related parameters, environment related parameters and construction-related parameters. The parametric studies are included in the next few chapters. However, the case studies are reported here first.

Four case studies are primarily used here. The first case study was related to the impact of the additives, and was carried out in conjunction with the staff of El Paso District. This case study will be called the Laboratory Study from this point on. Two other studies were carried out in conjunction with the strategic research project for improving concrete properties (Project 0-1700). These two studies are called the Small Slab 1 (SSI) Study and Small Slab 2 (SSII) Study. Ramaiah et al. (2001) extensively describes these two case studies. The last study, which will be called the Environmental Study, was primarily carried out at UTEP.

Laboratory Study

Standard nondestructive and destructive tests were performed on two concrete mixtures to identify the effect of admixtures on the strength and stiffness development of concrete: one with air-entraining agent, and the other without an air-entraining agent. The mix proportions are included in Table 5.1.

For the mix with air-entraining agent, 24 standard 6 in. diameter by 12 in. length concrete cylinders were poured simultaneously. Thermocouples for monitoring the maturity of the concrete were inserted into three of the cylinders. The other cylinders were kept in the district's concrete curing room.

Table 5.1- Mixture Proportions Used in Laboratory Case Study

Material	Amount	
	C	C1
Type I-II Cement (lb)	315	305
Sand (lb)	1280	1280
Coarse Aggregate (lb)	1785	1765
GGBF (lb)	307.5	307.5
Water (gal)	178	173
Air Entraining Agent (oz)	6.25	Not Added
Water Reducer (oz)	61.25	61.25

* GGBF denotes Ground Granulated Blast Furnace Slag.

Seismic and strength tests were performed on the cylinders in the District's lab at the ages of 1, 2, 3, 7, 14 and 28 days. At each age, the seismic moduli of three randomly selected cylinders were determined. Since seismic tests were nondestructive, the same three cylinders were immediately tested for compressive strength using a standard compression-testing machine. At the same time, the maturity parameters were noted using the three cylinders equipped with thermocouples. The three cylinders equipped with thermocouples were tested for compressive strength and seismic modulus last, so that the maturity could be monitored throughout the 28 days of the test. In summary, at the completion of that test series, the variation in the maturity parameters, seismic modulus and compressive strength with time were obtained for a period of 28 days.

A similar procedure was followed for the mixture without the air-entraining agent. The frequency at which the seismic and strength tests conducted on the cylinders was slightly different in this case. Additional tests were also carried out at an age of 5 days.

Small Slab I Study

This study is comprehensively described in Ramaiah (2001). Nondestructive and destructive tests were performed on several slabs and cores extracted from them to study the impact of aggregate type on the development of the strength and stiffness of in-place concrete. In addition, the strength and stiffness parameters were measured on cylinders and beams cured in a curing tank and in a sand bed. The impact of the reinforcing bars and the texture of the concrete (grooved vs. smooth) on the seismic measurements made with the PSPA were also studied on the slabs poured for this purpose.

A general layout of the slab is shown in Figure 5.1. The slab poured consisted of three 15 ft by 24 ft sections with a nominal thickness of 14 in. Two sections had a mix prepared with limestone aggregates (called the LS sections), while the third section contained a mix prepared with siliceous river gravel aggregates (called the SRG section). As shown in the figure, an area in the middle of the slab was reserved for nondestructive testing (called the NDT area). To study the effect of curing compound, two small areas (about 2 ft by 3 ft) within the NDT area were covered with cardboard to protect them from the curing compound. One area was located in the LS section and another in the SRG section. These sections were repeatedly tested for seismic moduli with the PSPA.

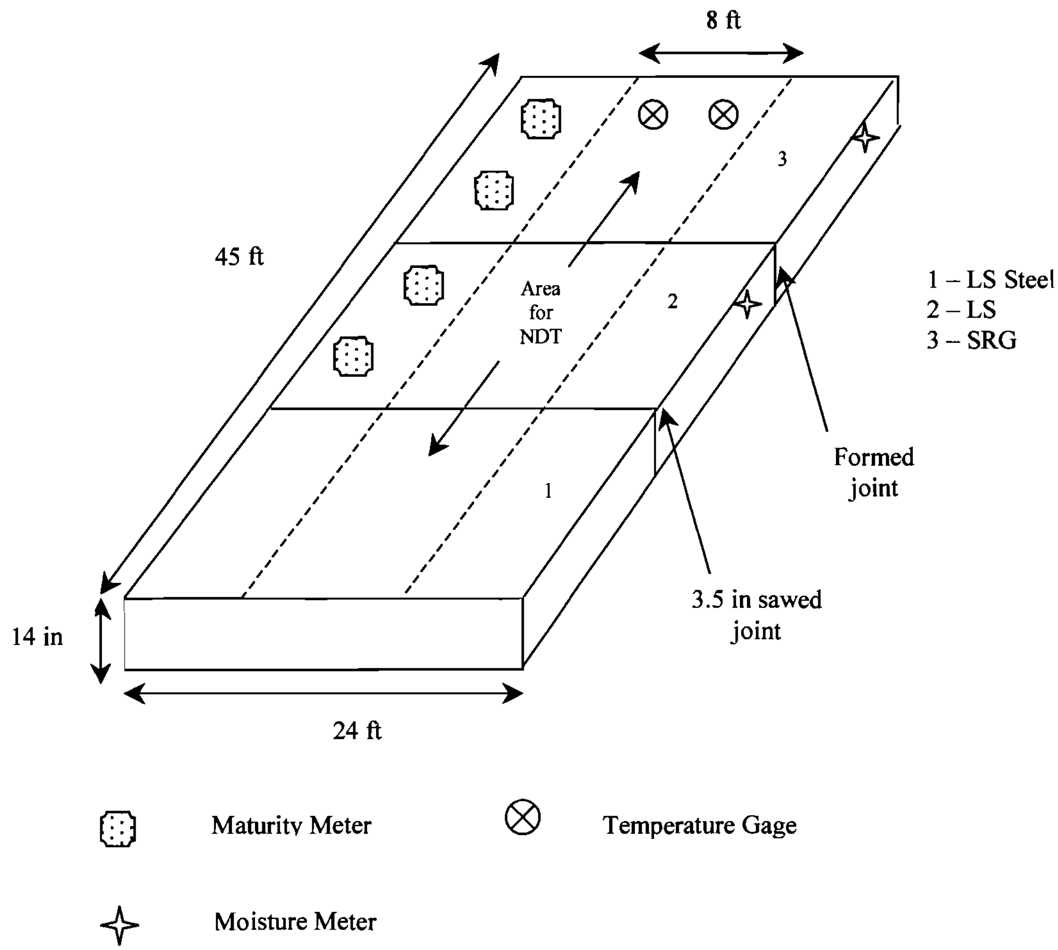

Figure 5.1 – General Layout of the Small Slab I Study

The mixture proportion for the Small Slab I study is shown in Table 5.2. Essentially, the same proportions were used for both aggregate types. The top aggregate size was 1 in.

Standard 6 in.-diameter cylinders of both aggregates were molded while pouring concrete for the slabs. The cylinders were cured in two ways so that the effect of curing method on the strength and modulus development can be studied. Some specimens were cured in water, while others were cured in a sand bed near the slab. The maturity parameters of the cylinders during curing were monitored throughout the 28 days of testing. The free-free resonant column tests were performed on the specimens at the ages of 1, 3, 7, 14 and 28 days. As before, the specimens tested with the seismic method were also tested for compressive strength (as per ASTM C39-86), splitting tensile strength (as per ASTM C496-96) and static modulus of elasticity (as per ASTM 469-94).

The slabs were also cored for strength and modulus tests. Shortly before coring, the slabs were tested with the PSPA. Cores were either nominally 4 in. or 6 in. in diameter. The slabs were monitored for maturity throughout the 28 days of testing.

Four-in.-diameter cores were obtained and tested at the ages of 1, 3, 7, 14 and 28 days. Six-in.-diameter cores were only retrieved and tested at the ages of 7 and 28 days. Every core was subjected to the free-free resonant column tests followed by either compressive strength, splitting tensile strength or static modulus.

Also, water cured beams were poured and tested at the ages of 3, 7, 14 and 28 days for flexural strength (as per ASTM C293-00). The free-free resonant column tests were performed on the beams at the ages of 1, 3, 7, 14 and 28 days.

Table 5.2- Mixture Proportions Used in Small Slab I Study

Material	Amount	
	Limestone	Siliceous River Gravel
Type I-II Cement (lb)	564	564
Sand (lb)	1031	1040
¾" Aggregate (lb)	1700	-
1" Aggregate (lb)	423	-
1 ½" Aggregate (lb)	-	1946
Water (gal)	29	29
Air Entraining Agent (oz)	9.5	9.5
Water Reducer (oz)	5.6	5.6

In summary, a total of 40 cylinders, 10 beams, 20 4-in.-diameter cores and 8 6-in.-diameter cores were tested to develop relationships amongst the strength parameters (tensile and compressive), moduli (seismic and static) and maturity parameters under three curing conditions (water-cured, sand-cured and naturally-cured). Ramaiah et al., (2001) has an excellent summary of the strengths and weaknesses of the seismic procedure.

Small Slab II Study

Nondestructive and destructive tests were performed on a slab, which was cured in six different ways to study the impact of the curing method on the strength and stiffness development of a PCC slab. This study is comprehensively described in Ramaiah et al., (2001) as well.

A general layout of the experiment is shown in Figure 5.2. The slab, which was 30 ft long by 10 ft wide with a nominal thickness of 14 in., was divided into six sections to simulate a range of field curing conditions from excellent to poor. In addition to curing compound, monomolecular film (MMF) was used in some of the slab sections. The varying conditions of the six sections are given below:

1. Covered with plastic sheeting as soon as it was possible.
2. Curing compound was applied at the sheen loss with MMF.
3. Curing compound was applied at the sheen loss without MMF.

4. Curing compound was applied two hours after the concrete placement with MMF.
5. Curing compound was applied eight hours after the concrete placement with MMF.
6. No curing compound or MMF applied.

Mixture proportions for this study are shown in Table 5.3. The only differences among the six sections were essentially the curing method.

The test plan for this case study was similar to the Small Slab I Study. Thirty standard cylinders were molded while pouring the slab. The cylinders were then cured in a water bath for 1, 3, 7, 14 or 28 days. As enumerated for the Small Slab I Study, the cylinders were tested for

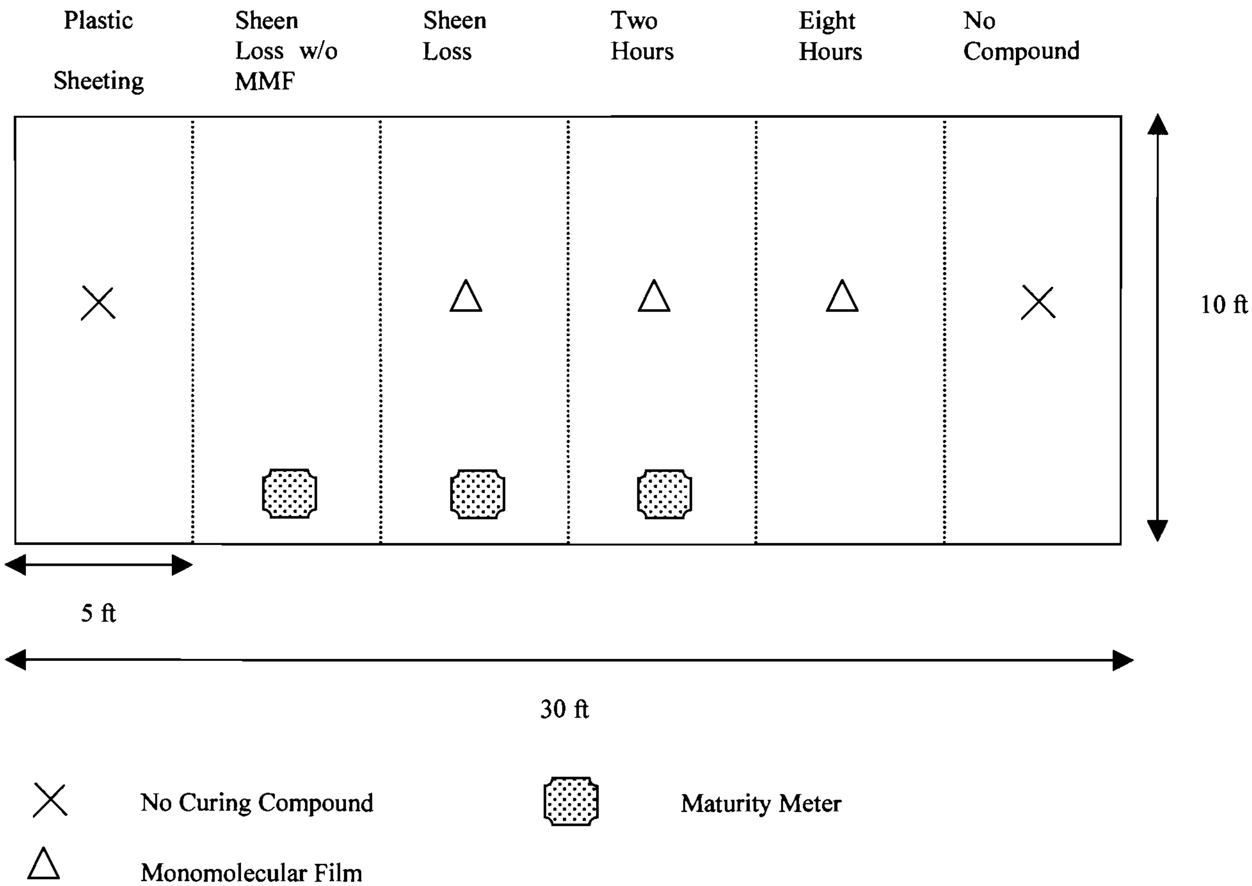

Figure 5.2 – General Layout of the Small Slab II Study

Table 5.3 - Mixture Proportions Used in Small Slab II Study

Material	Amount	
	Batch1	Batch2
Type I-II Cement (lb)	2135	2130
Sand (lb)	10120	10120
¾" Aggregate (lb)	12285	12260
Fly Ash (lb)	903	930
Water (gal)	1033	882
Air Entraining Agent (oz)	22	14
Water Reducer (oz)	304	304

compressive and tensile strengths, and static moduli shortly after their seismic moduli were determined. On each testing day, 6 specimens were randomly selected. A half of the specimens was used for compressive strength and static modulus determination, while the other half was used for tensile strength determination. The maturity parameters were also noted using the readings from 6 cylinders that were equipped with thermocouples.

At the ages of 3, 7 and 28 days, each of the six slabs was also cored. The cores, which were nominally 6 in. in diameter, were drilled using a truck-mounted machine. Six cores for each condition were drilled on each testing day; hence a total of 36 cores were drilled throughout the test period. Shortly before coring, the PSPA was used to determine the modulus of the slab in place. To minimize damage to the slab, coring started at the outer edge of the slab, moving inward. A half of the cores was used for splitting tensile tests and the other half for static modulus and compressive strength determination. The seismic modulus of each core was determined shortly before they were subjected to the strength tests. The maturity meters were turned off and the thermocouples were removed from the slabs after 28 days of testing and the data was downloaded.

Environmental Study

Nondestructive and destructive tests were performed on PCC slabs of the same mix that were cured under varying environmental conditions to study the impact of temperature and moisture on the strength and modulus development of these slabs. The mix design, as shown in Table 5.4, was similar to that used in the Small Slab I Study.

Seven 2-ft by 3-ft slabs were constructed for this study. Almost immediately after pouring, five of the slabs were placed in different environmental conditions. All these slabs were 14 in. thick. The environmental conditions are summarized in Table 5.5. Slab No. 1a was placed inside an air-conditioned laboratory with a nominal temperature of 25°C (77°F) and a humidity of about 35%. Slab No. 2 was placed in a standard concrete curing room (temperature of 25°C and humidity of 100%). Slabs No. 4 and 5 were placed in two environmentally controlled chambers, one set at a temperature of 4°C (39°F) and the other at 40°C (104°F). Both rooms had humidity similar to the laboratory where Slab 1 was placed. Finally, Slab No. 3 was placed outside the building and allowed to cure under the natural conditions.

Table 5.4 - Mixture Proportions Used in Environmental Study

Material	Amount
Type I-II Cement (lb)	564
Sand (lb)	1031
¾" Aggregate (lb)	1700
1" Aggregate (lb)	423
Water (gal)	29
Air Entraining Agent (oz)	9.5
Water Reducer (oz)	5.6

Table 5.5 – Curing Conditions of Slabs Used in Environmental Study

Slab No.	Nominal Thickness, in.	Nominal Temperature, °C	Location
1a	14	25	Air Conditioned Laboratory
1b	10	25	Air Conditioned Laboratory
1c	18	25	Air Conditioned Laboratory
2	14	25	Curing Room
3	14	Variable	Outside the Building
4	14	5	Temperature Control Room
5	14	40	Temperature Control Room

As a second objective, two extra slabs (Slabs No. 1b and 1c in Table 5.5) were poured and cured similar to Slab No. 1a. The only difference among the three slabs was the thickness. While Slab No. 1a was 14 in. thick, the other two slabs were 10 in. and 18 in., so that the impact of the slab thickness on the development of the strength and stiffness can be studied.

For each environmental condition, five standard cylinders were poured and placed besides its corresponding slab. The cylinders were first tested for seismic modulus at the ages of 1, 3, 7 and 28 days and then immediately tested for compressive strength. Thermocouples were inserted into one of the cylinders in each group and into the slabs to determine their respective maturity parameters. The air temperature was monitored near each slab using an extra thermocouple.

Several 4-in.-diameter (nominal) cores were retrieved as well. At the age of 7 days, 2 cores were extracted from Slabs 2 and 3. At the age of 28 days, 2 cores were extracted from each of the seven slabs. The cores were trimmed, tested for seismic modulus and subjected to compressive strength tests shortly after drilling.

Chapter 6

Mix-Related Parameters

The impact of several mix-related parameters on the development of strength and modulus was studied in this chapter. The major parameters considered were the type of aggregates used in the concrete mixtures and the impact of the admixtures.

Impact of Aggregate Type

The impact of aggregate type can be best determined from the laboratory and the field test results from the Small Slab I Study described in Chapter 5. In that chapter we indicated that two different types of aggregates, limestone and siliceous river gravel, were used. The results are summarized here.

Three types of specimens, namely water-cured standard cylinders, sand-cured cylinders and 4-in.-diameter cores were drilled from the slab. Figures 6.1 through 6.5 contain the results in a graphical format, while the relationships developed are included in Appendix C.

The variation in compressive strength with maturity parameter (TTF) for water-cured specimens prepared with LS aggregates with that of similar specimens prepared with SRG aggregates is compared in Figure 6.1. The best-fit curves through both data sets are also included in the figure. The coefficients of determination (R^2-values) for both mixtures were above 0.97 indicating that the curves describe the data well. The two curves depicted in Figure 6.1 are quite similar. This is anticipated because the mixtures were designed for this purpose.

Similar relationships but for tensile strength and flexural strength are shown in Figures 6.2 and 6.3. Once again the trends are similar for the LS and SRG mixtures. However, due to the variability associated with the indirect tensile and flexural strength tests, the relationships detailed based on the best-fit curves are not as strong as those from the compressive strength. Nevertheless, the R^2 values, as depicted in Appendix C, is above 0.90 for most cases with a low of about 0.82 for tensile strength of LS. The trends for flexural strength are similar for both mixtures as shown in Figure 6.3 with R^2 values greater than 0.90 indicating a good correlation.

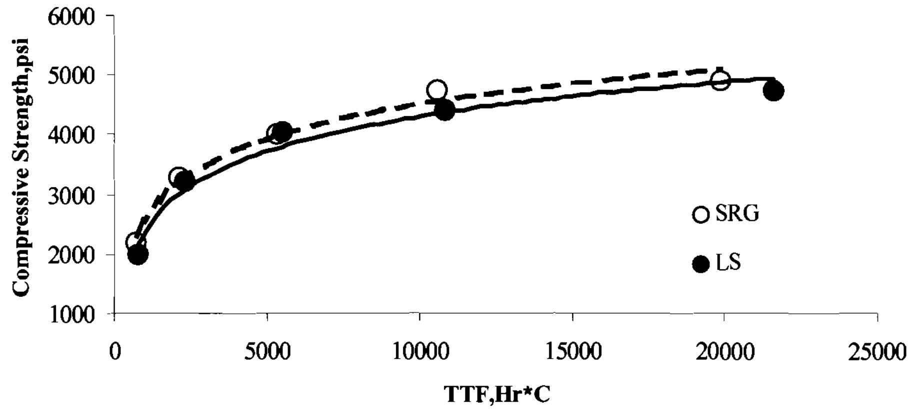

Figure 6.1 – Variation in Compressive Strength with Maturity for Water-cured Specimens

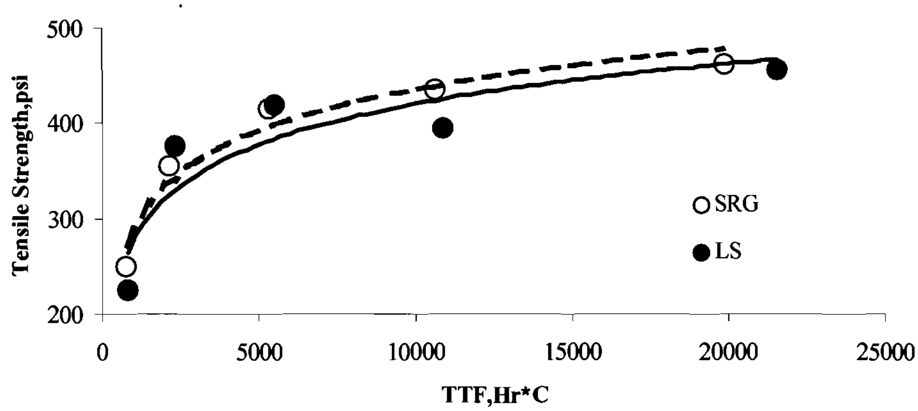

Figure 6.2 – Variation in Tensile Strength with Maturity for Water-cured Specimens

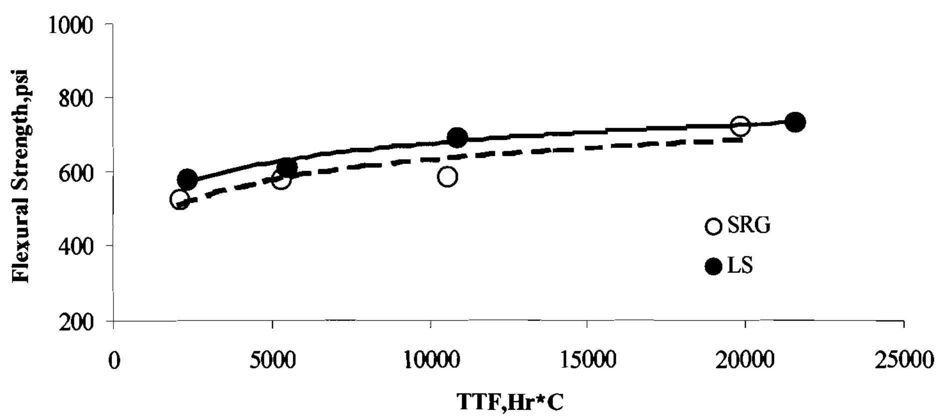

Figure 6.3 – Variation in Flexural Strength with Maturity for Water-cured Specimens

Seismic moduli obtained from the free-free resonant column are related to the maturity in Figure 6.4. The best-fit curves to the data for both mixtures yield R^2 values of about 0.94. As such, the curve fits are representative of the measured data. Unlike the compressive strengths, the moduli measured on limestone are higher than those from the gravel. This trend indicates that it may not be prudent to use the strength parameters to estimate stiffness of mixtures.

The compressive, tensile and flexural strengths from the two mixtures are related to seismic modulus in Figure 6.5. The strength parameters and moduli are highly correlated in all cases since the minimum R^2 value is 0.94. Even though unique relationships are apparent for the limestone and gravel mixtures, the power terms for both mixtures are similar.

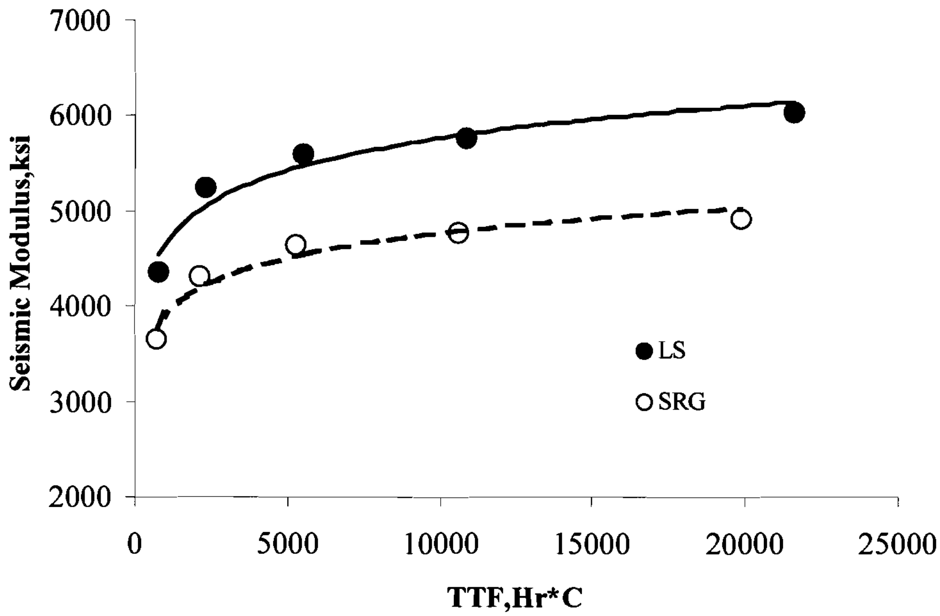

Figure 6.4 – Variation in Seismic Modulus with Maturity for Water-cured Specimens

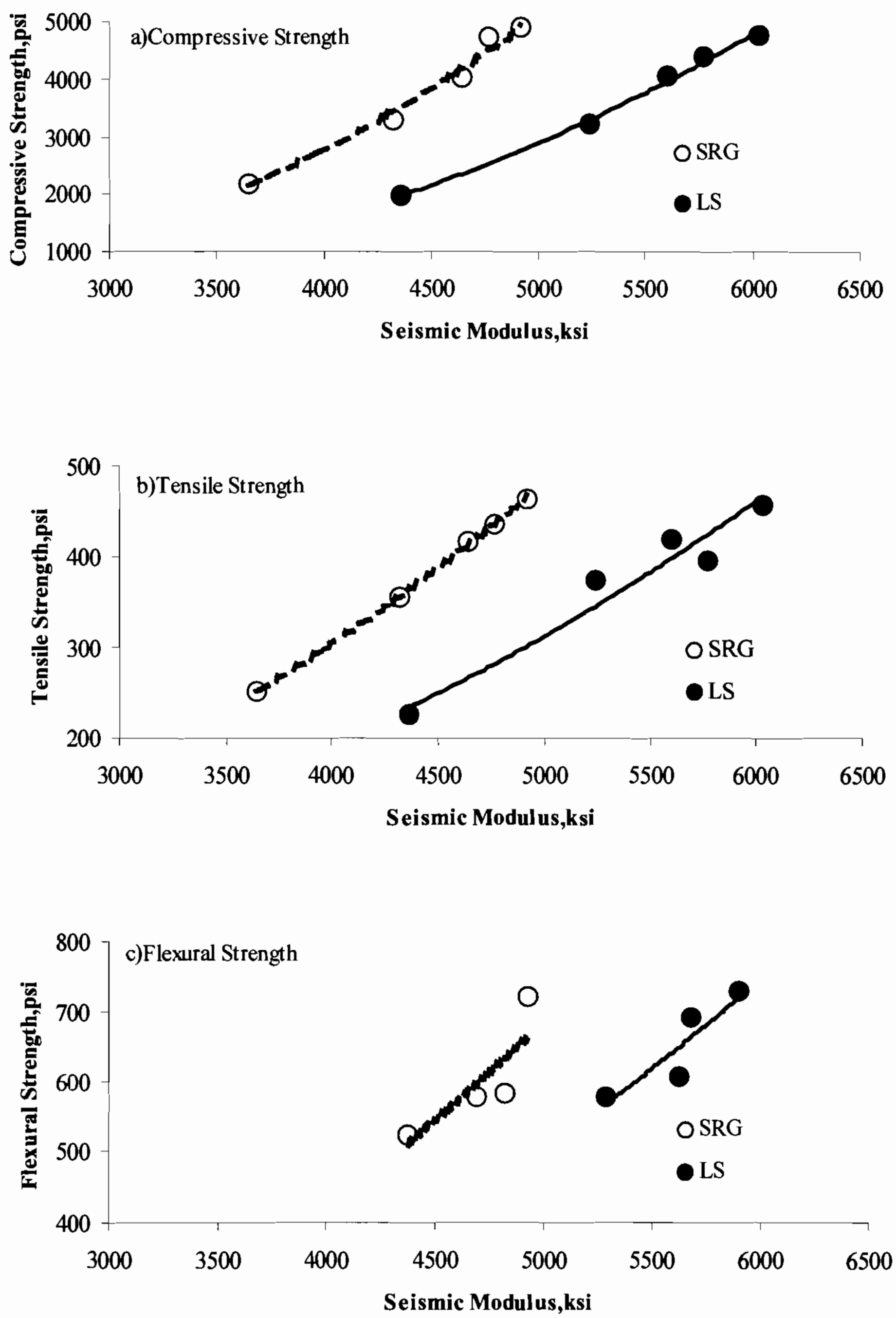

Figure 6.5 – Variations in Strength Parameters with Seismic Modulus for Water-cured Specimens

Similar trends were observed for the sand-cured cylinders and 4-in.-diameter cores as shown in Appendix D. A comprehensive comparison of the results as a function of curing is carried out later in this report. In summary, the sand-cured specimens and cores did not gain as much strength as the water-cured specimens, and the results from the cores demonstrated more variability. Same conclusions can be drawn from the tensile tests as well. For the seismic modulus, the gain in modulus was less pronounced for the water-cured and cores. However, the results seem to demonstrate less test-related variability as compared to others.

Impact of Admixtures

The impact of admixtures is determined through the laboratory case study described in Chapter 5. In that study, two similar mixtures with differences in air entraining agent were tested to show the impact of admixtures on concrete properties. As indicated in Chapter 5, only standard cylinders were prepared in this study. Appendix C contains a detailed description of the results.

The variations in compressive strength with the maturity parameter of the specimens prepared with the mixture containing air-entraining agent is compared with that of similar specimens prepared with the mixture without an air-entraining agent in Figure 6.6. The best-fit curves have R^2 values of 0.99 indicating that the strength is highly correlated to maturity. The mix without the air-entertainer exhibits higher strength at a given TTF. A trend similar to that of the compressive strength was observed for the variation in seismic modulus with maturity (see Figure 6.7). A good correlation between the modulus and maturity exists for both mixtures.

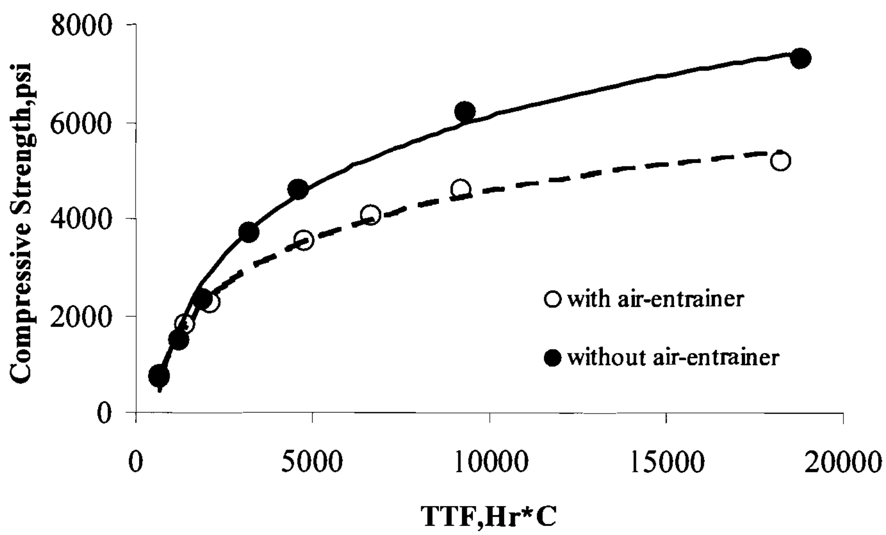

Figure 6.6 – Variation in Compressive Strength with Maturity for Mixtures Used in Laboratory Study

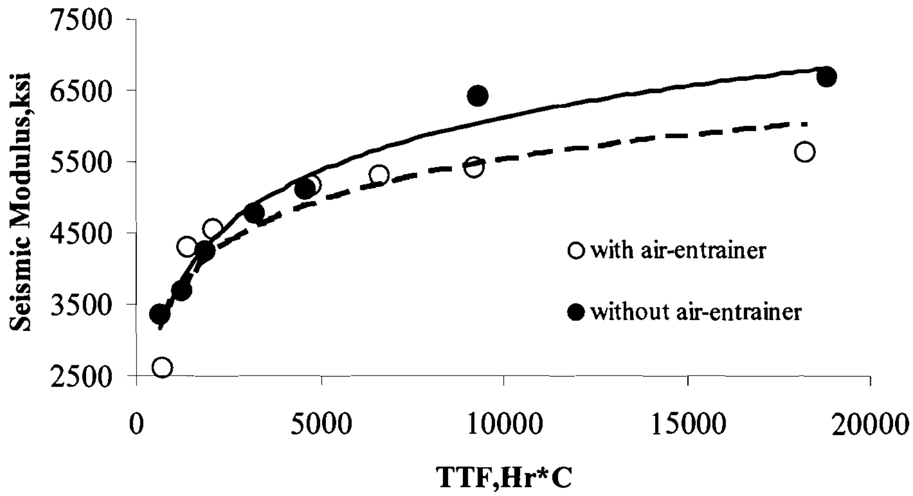

Figure 6.7 – Variation in Seismic Modulus with Maturity for Mixtures Used in Laboratory Study

Figure 6.8 contains the variation in compressive strength with seismic modulus. The R^2 values for the best-fit curves through the data for both mixtures are above 0.93. Also from Figure 6.8, the relationship between the compressive strength and seismic modulus seems to be independent of the mixture. This phenomenon has quite a significant practical implication. If this trend holds true for other mixtures, one can anticipate less effort in calibrating the relationships.

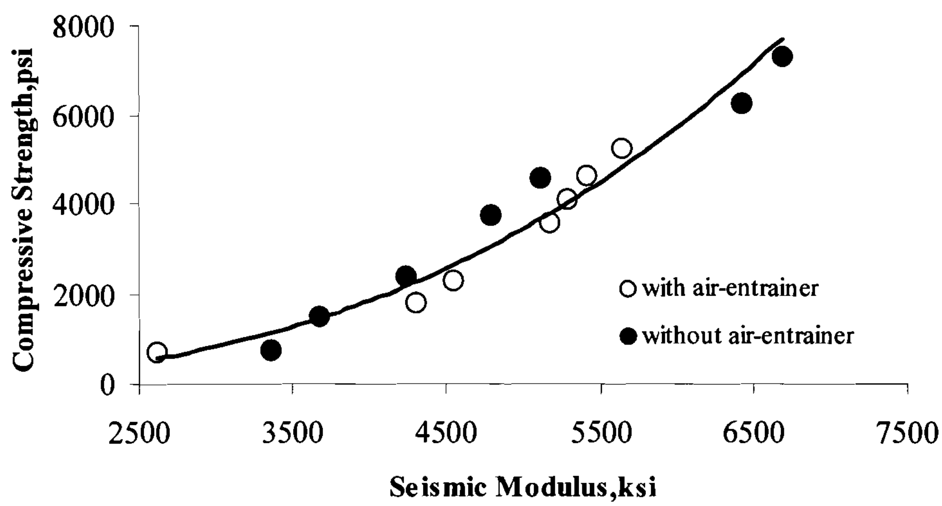

Figure 6.8 – Variation in Compressive Strength with Seismic Modulus for Mixtures Used in Laboratory Study

To study the feasibility of developing a preliminary unique relationship between the compressive strength and seismic modulus, the results from all four mixtures tested in this study are accumulated in Figure 6.9. The results from the Small Slab I Study constructed with the siliceous river gravel (marked as SRG) demonstrate one pattern. However, the trends from all other mixtures follow a similar pattern. All these mixtures have one thing in common; they are made from the limestone aggregates from El Paso area. The global best-fit curve through all data points from all four case studies is shown in Figure 6.9. The R^2 value of the global best-fit curve is about 0.90. This data trend indicates that it may be possible to develop a unique calibration curve for preliminary assessment of the concrete work in a given district. This may not be possible with the maturity. The variations in compressive strength with maturity parameter for the same mixtures are shown in Figure 6.10. Large variability is observed amongst the trends from different mixtures.

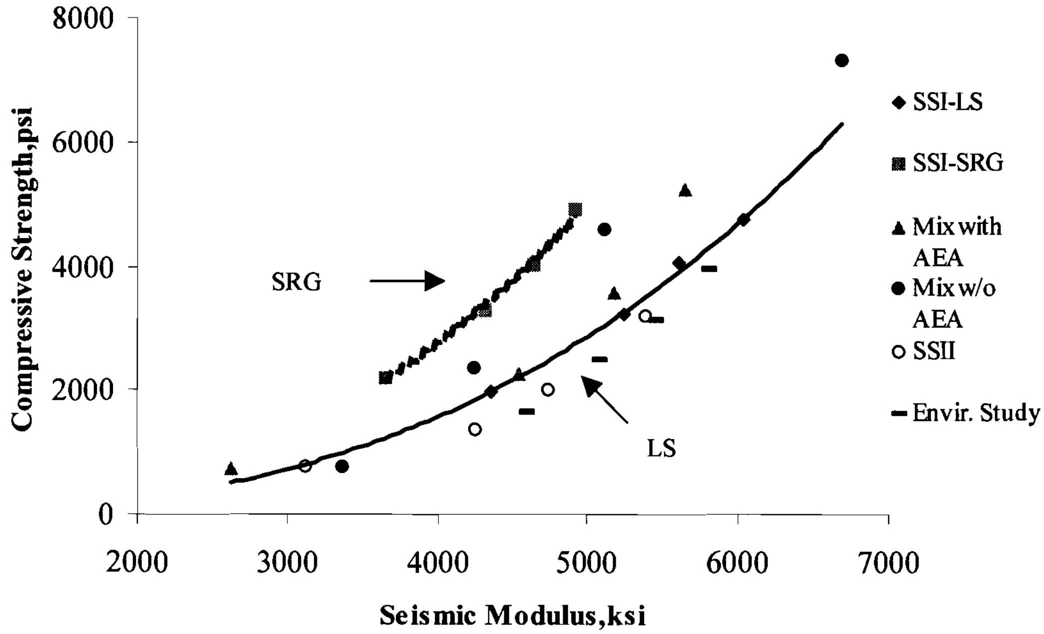

Figure 6.9 – Variation in Compressive Strength with Seismic Modulus for All Mixtures Studied

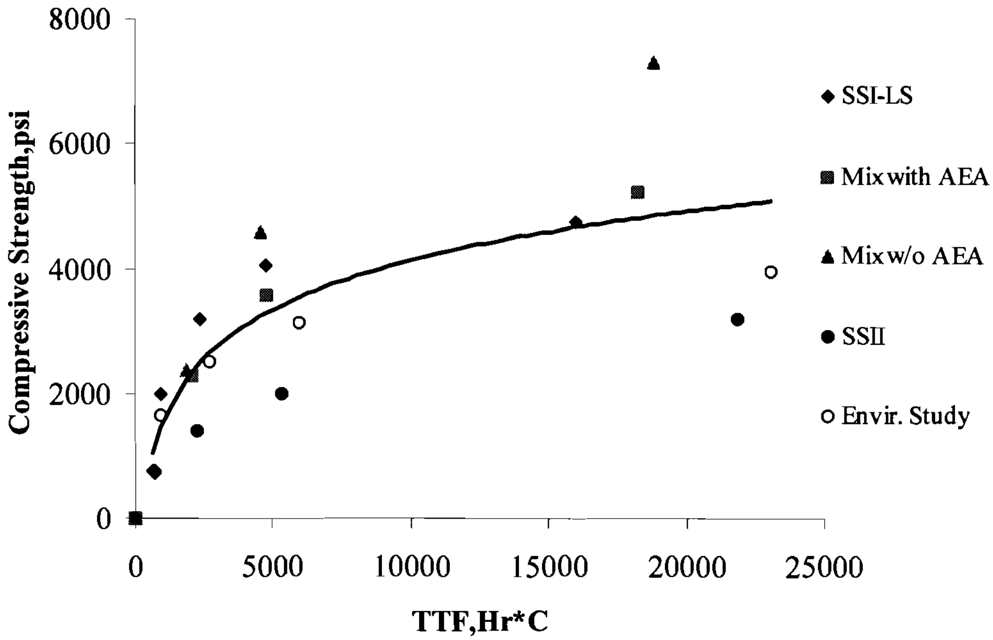

Figure 6.10 – Variation in Compressive Strength with Maturity for All Limestone Mixtures Studied

Chapter 7

Environmental Parameters

The impact of various environmental parameters on the development of strength and modulus of concrete is studied in this chapter. The environmental parameters considered were the temperature, moisture and the combination of the two.

Impact of Temperature

The impact of temperature can be best determined from the laboratory results from the environmental study described in Chapter 5. The variations in concrete properties with time at nominal temperatures of 5°C, 25°C and 40°C are studied here.

The variations in compressive strength with the actual age, equivalent age and TTF of the standard cylinders maintained at three different constant temperatures (i.e. 5°C, 25°C and 40°C) are shown in Figure 7.1. As a reminder, the specimens were sprayed with curing compound before they were placed in appropriate temperature control rooms with similar relative humidities. From Figure 7.1a, the compressive strengths of the specimens maintained at the three temperatures are different at early ages. The lower the temperature is, the slower the developed strength will become. However, after 28 days, the compressive strengths become similar for all specimens. The variations in compressive strength with TTF for the same specimens are shown in Figure 7.1b. The curve developed from the measurements at 25°C may require an adjustment factor, especially for the early ages, to be applicable as an accurate predictive tool for other temperatures. Inspecting Figure 7.1c, this statement is also applicable when the equivalent age is used as the independent variable.

The variations in seismic modulus with actual age, equivalent age and TTF for the same cylinders are shown in Figures 7.2. The patterns observed for the variations in strength are also applicable to this case. At early actual age, the rate of gain in modulus is quite variable amongst the cylinders cured at different temperatures. However, after 28 days, the moduli are similar for all three cases. Once again, an adjustment factor maybe needed to use the relationship developed at one temperature for another one.

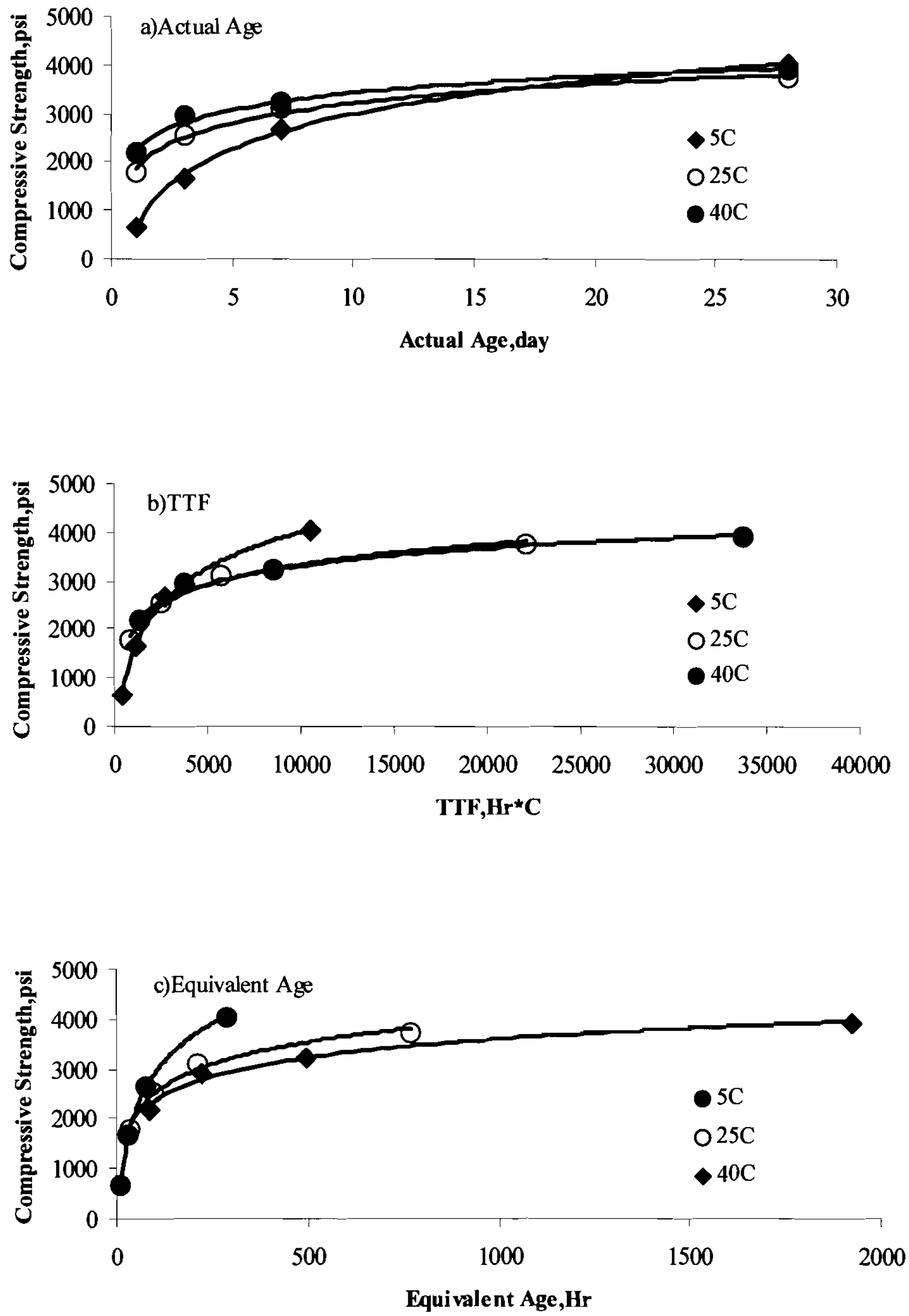

Figure 7.1 – Variation in Compressive Strength with Time and Maturity Parameters for Cylinders Cured at Different Temperatures

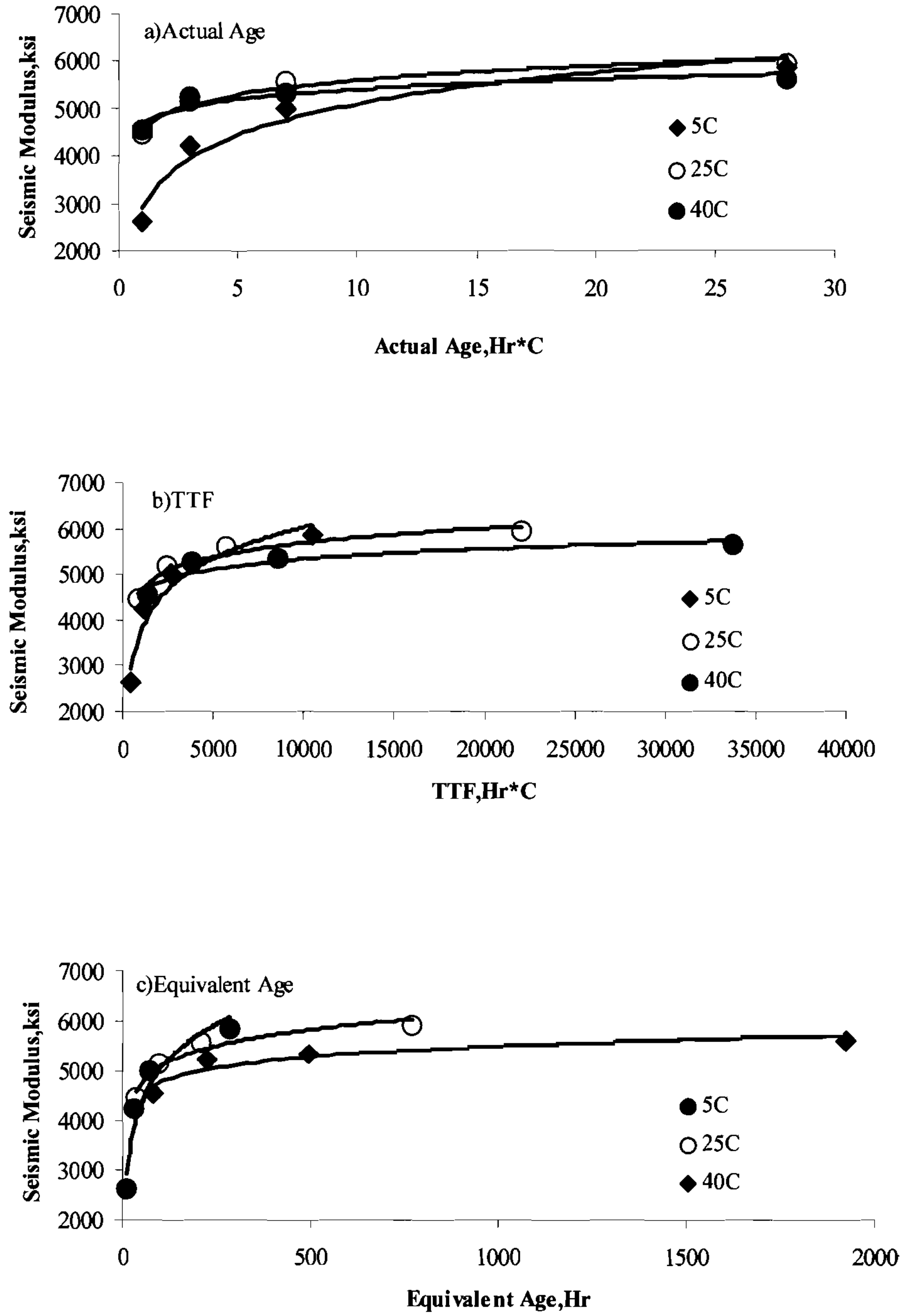

Figure 7.2 – Variation in Seismic Modulus with Time and Maturity Parameters for Cylinders Cured at Different Temperatures

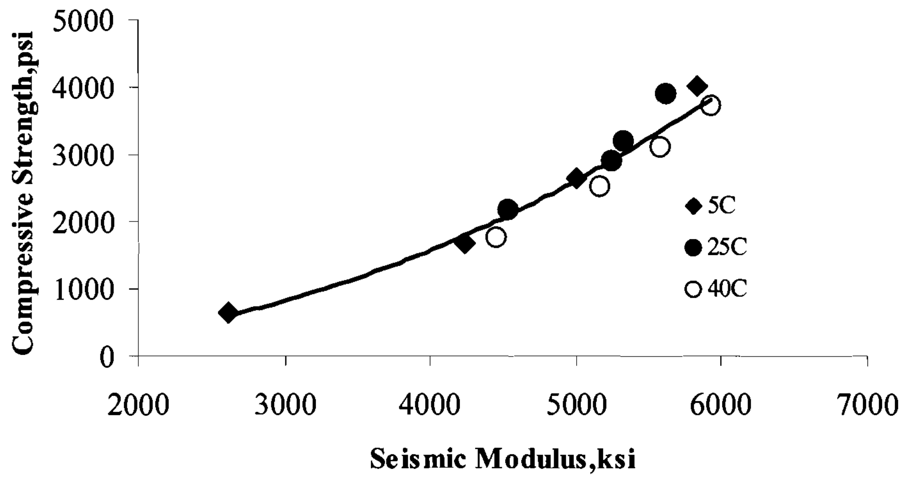

Figure 7.3 – Variation in Compressive Strength with Seismic Modulus for Cylinders Cured at Different Temperatures

The variations in compressive strength with seismic modulus for the three temperatures are presented in Figure 7.3. A reasonably unique relationship between the compressive strength and the modulus is observed with an R^2 value of about 0.97.

The variation in seismic modulus measured on the slab with maturity parameter is shown in Figures 7.4. The slab in 40°C chamber exhibits a lower modulus than the other two slabs. A comparison between Figures 7.2 and 7.4 indicates that the variation in modulus with temperature differs between the cylinders and the slabs for almost all temperatures. This can be attributed to the significantly different mass of materials that are involved in the cylinders as opposed to the slab. This matter will be discussed later on.

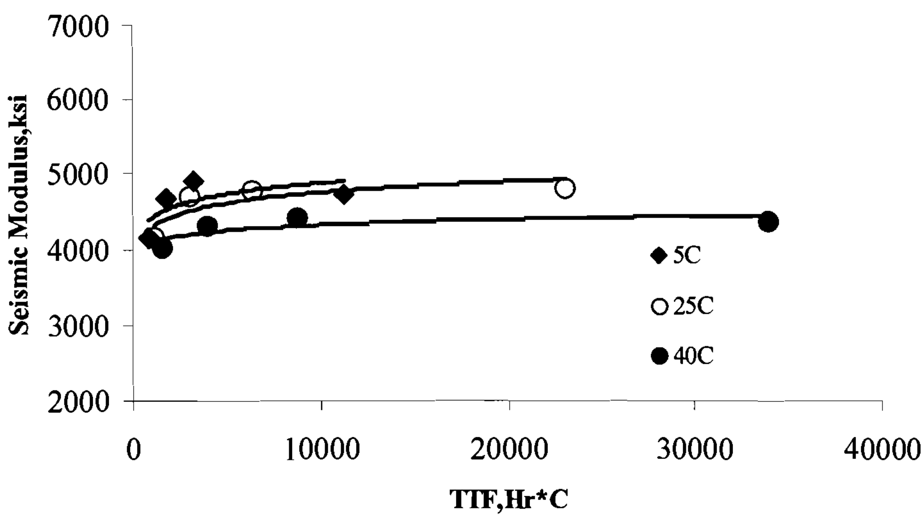

Figure 7.4 – Variation in Seismic Modulus with Maturity for the Slabs Cured at Different Temperatures

Impact of Humidity

To study the impact of humidity, the specimens and slabs kept inside the curing room representative of 100% moisture and the specimens kept outside the curing room representative of 35% moisture are compared. For both conditions, the ambient temperatures were almost the same; as such, any changes in the curing patterns can be primarily attributed to differences in moisture.

The variation in compressive strength with maturity parameter for the cylinders in 100% humidity conditions is compared with that of the cylinders in 35% humidity conditions in Figure 7.5. The trends followed by the specimens from the two different curing regimes are similar. After 28 days, the compressive strength of the cylinders maintained under 100% humidity is slightly higher than that of the cylinders under 35% humidity. As such, the impact of moisture on the gain in strength of the cylinders is small.

The variations in seismic modulus with maturity parameter for the cylinders are shown in Figure 7.6. The impact of moisture on the gain in the stiffness of the specimens is similar to that of the gain in strength. Once again, the results from the two methods yield similar trends. The variation in compressive strength with seismic modulus is again reasonably unique and is less dependent on the moisture regime.

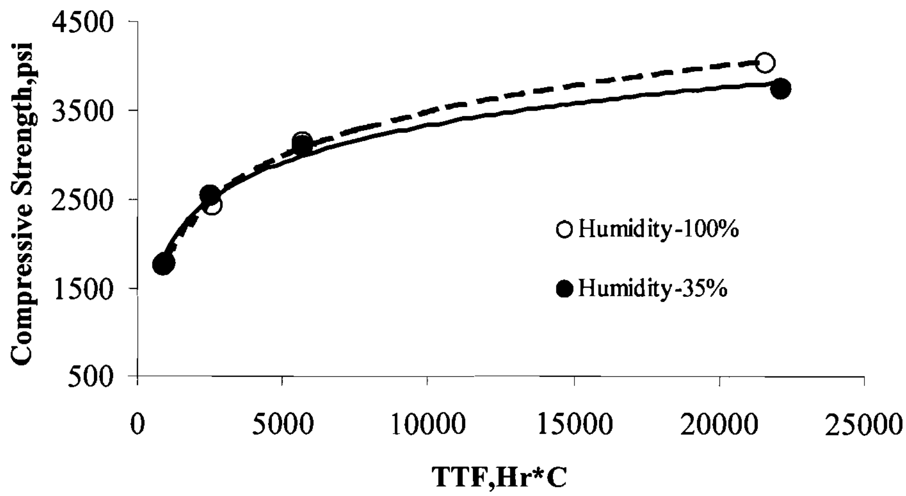

Figure 7.5 – Variation in Compressive Strength with Maturity for Cylinders Maintained Under Different Humidity Conditions

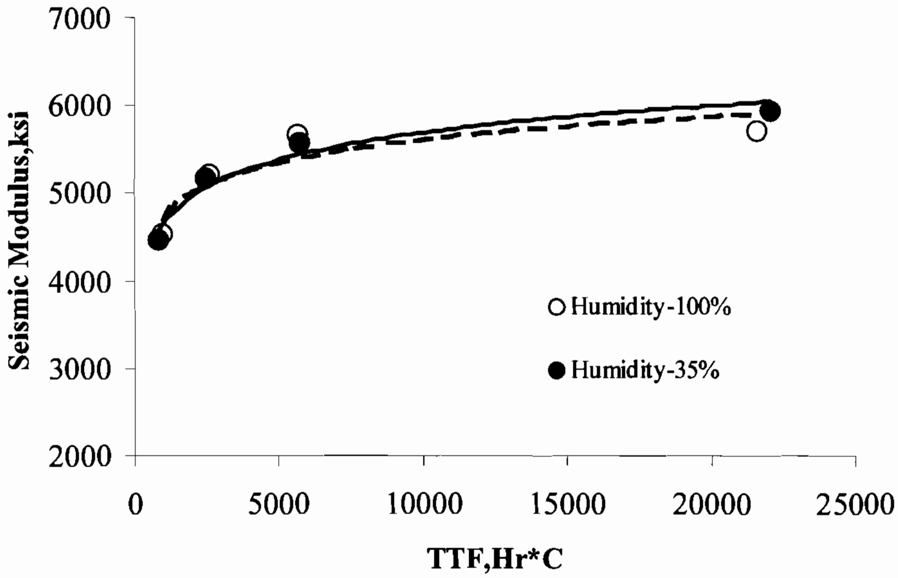

Figure 7.6 – Variation in Seismic Modulus with Maturity for Cylinders Maintained Under Different Humidity Conditions

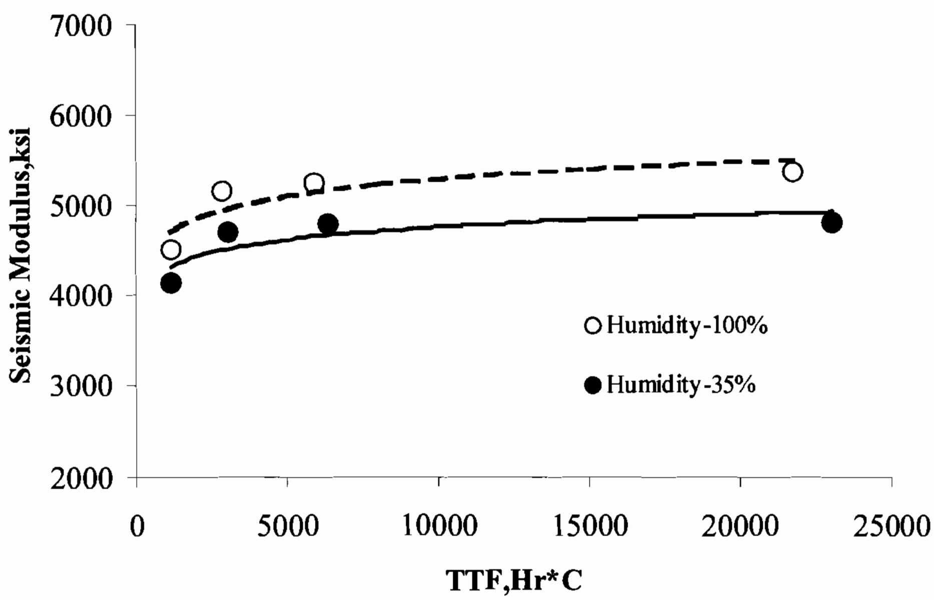

Figure 7.7 – Variation in Seismic Modulus from PSPA with Maturity for the Slabs Maintained Under Different Humidity Conditions

Figure 7.7 shows the variation in seismic modulus measured from the PSPA with maturity for the slabs. Unlike for the strength or stiffness of the cylinders, the moisture significantly impacts the gain in stiffness of the slab with age. Unfortunately, the gain in strength with the TTF of the slab cannot be established because the two slabs were cored only after 28 days. However, the average strength of the cores after 28 days was about 4300 psi and 5600 psi for the slabs maintained in the low humidity and high humidity rooms, respectively. Once again, this demonstrates a close correlation between the strength and seismic modulus of the concrete.

Impact of Combined Parameters

The impact of combined parameters is determined by comparing the trends observed from the slabs and the cylinders maintained inside the curing room with those maintained outside the building.

The variation in compressive strength, with maturity parameter for the cylinders in ideal curing conditions, is compared with that of the cylinders in natural curing conditions in Figure 7.8. The trends followed by the specimens maintained under different curing regimes are practically the same. This shows that there is almost no impact of type of curing on compressive strength for specimens of very small volume. Figure 7.9 provides the variation in seismic modulus with maturity parameter for the same cylinders used in the strength tests. Once again, the two trends are similar.

However, when the gain in seismic modulus from the slabs is compared, the moduli measured on the ideally cured slab are consistently higher than those from the slab cured outside. The strength tests on cores from the slabs indicate a difference in compressive strength of about 15% between the two curing regimes.

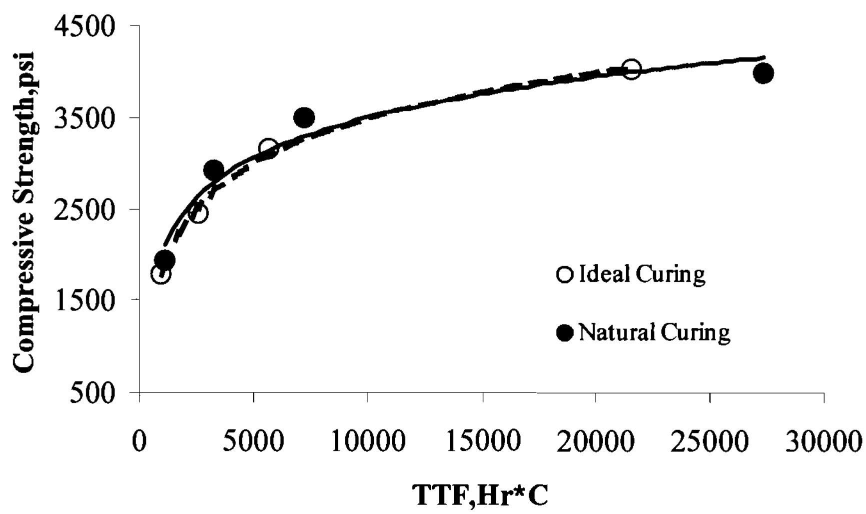

Figure 7.8 – Variation in Compressive Strength with Maturity for Cylinders Maintained Under Different Curing Conditions

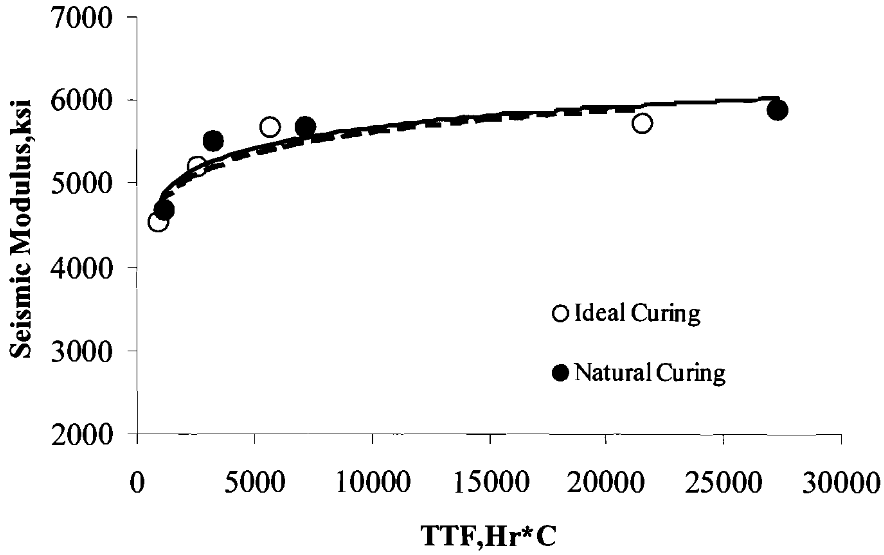

Figure 7.9 – Variation in Seismic Modulus with Maturity for Cylinders Maintained Under Different Curing Conditions

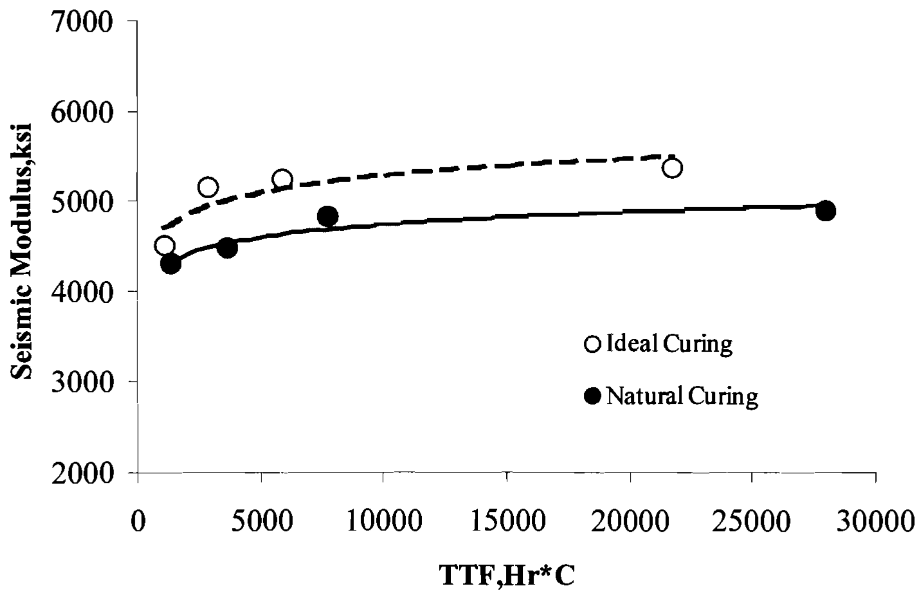

Figure 7.10 – Variation in Seismic Modulus from PSPA with Maturity for the Slabs Maintained Under Different Curing Conditions

The variation in seismic modulus, with strength from cores extracted from all five slabs, is compared with the trend observed for the cylinders in Figure 7.11. For cores, the results from ages of 7 days and 28 days are shown in the figure because these were the only two dates that the slabs were cored. At a given seismic modulus, the compressive strength developed in the slab is greater than those obtained from the cylinders by about 10% to 15%. This can partially be attributed to the differences in the specimen size and partially to the mass of concrete cured. As indicated before, the cores were 4 in. in diameter, whereas the cylinders were 6 in. in diameter. To investigate the curing regime, the cores were divided into two halves and individually tested. The variations in strength and modulus for all specimens are included in Figure 7.12. The bottom half of all specimens demonstrates higher seismic moduli and strengths as compared to the top half. The harsher the curing trend, the greater the differences in properties between the top and bottom halves. For the ideal curing condition, the top and bottom halves provide reasonably close strength and stiffness. However, the largest differences are in the elevated temperature and low humidity. The practical implication of this matter is that perhaps the QA/QC as well as the opening criteria should be based on the properties of the top half of the slab.

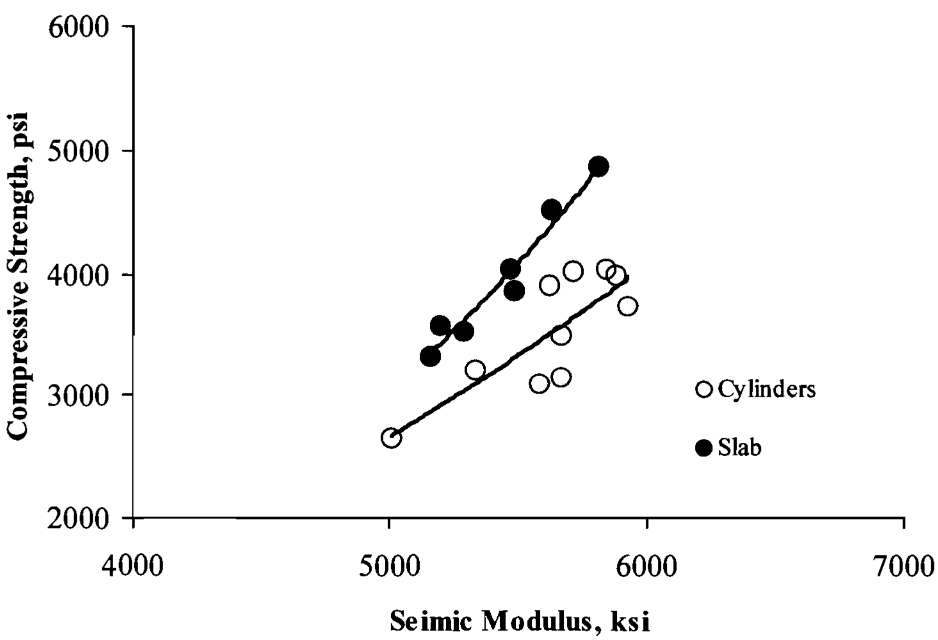

Figure 7.11 – Comparison of Variations in Compressive Strength with Seismic Modulus from All Slabs and Cylinders Used in Environmental Study

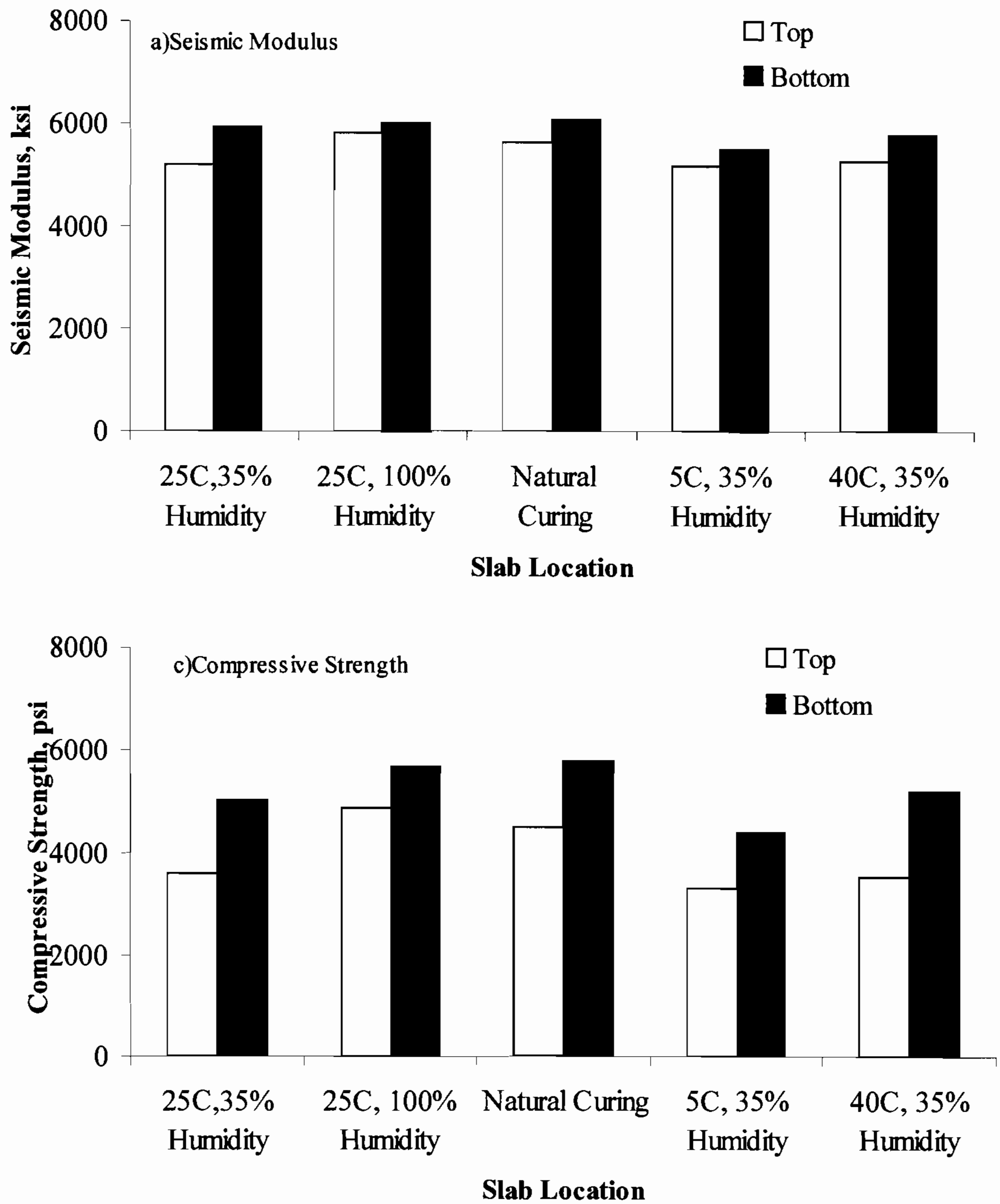

Figure 7.12 – Impact of Location of Concrete on Strength and Modulus

Chapter 8

Construction Parameters

The impact of the construction parameters on the development of strength and stiffness is represented in this chapter. The construction parameters considered are the thickness of the slab and the curing method. In addition, the impact of grooving and reinforcing bars were also studied. Since the goal is to study the impact of the construction parameters, the results reported are mostly related to those from the PSPA.

Impact of Thickness

The impact of thickness is evaluated from the test results from the Environmental Study described in Chapter 5. Three slabs with different thickness were poured and maintained in the same ambient conditions. The three slabs were 10 in., 14 in. and 18 in. thick.

Figure 8.1 shows the variations in seismic modulus with maturity parameter for the three slabs considered. The trends followed by the three slabs are very similar. As such, the impact of the thickness on the properties of concrete is small.

Impact of Curing

The impact of curing is best determined by using the laboratory and field test results from the Small Slab I Study and Small Slab II Studies. In the Small Slab I Study, two small areas (about 2 ft by 3 ft) within the NDT area shown in Figure 5.1 were covered with cardboard to protect them from the curing compound. One area was located in the limestone (LS) section and another in the siliceous river gravel (SRG) section. These sections were repeatedly tested for seismic moduli with the PSPA to investigate the effect of curing on the gain in concrete stiffness.

The variations in seismic modulus with the actual age of the slab for the two sections, with and without curing compound, are shown in Figure 8.2. For both types of aggregates, the gain in stiffness is significantly impacted by the presence of the curing compound. However, after about two weeks, the measured moduli are less dependent on the application of the curing compound.

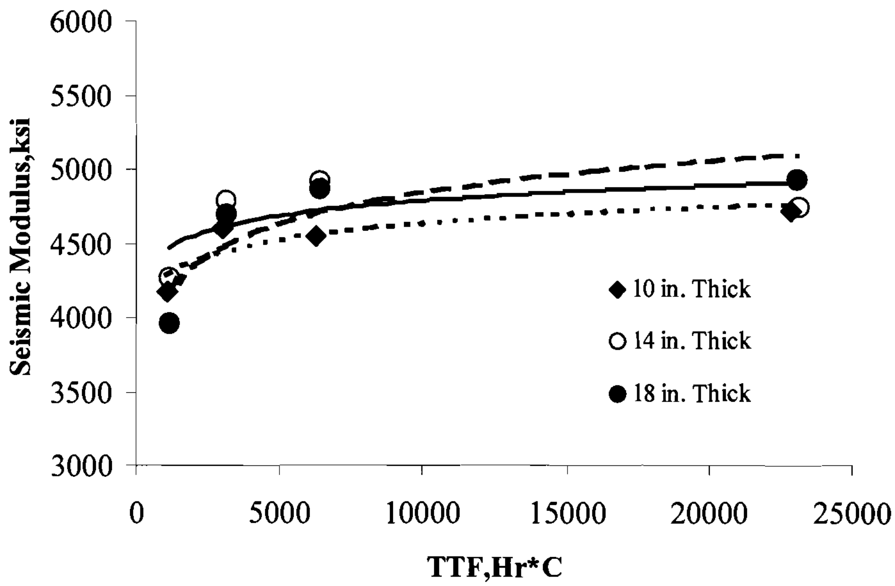

Figure 8.1 – Variation in Seismic Modulus with Maturity for Slabs of Different Thickness

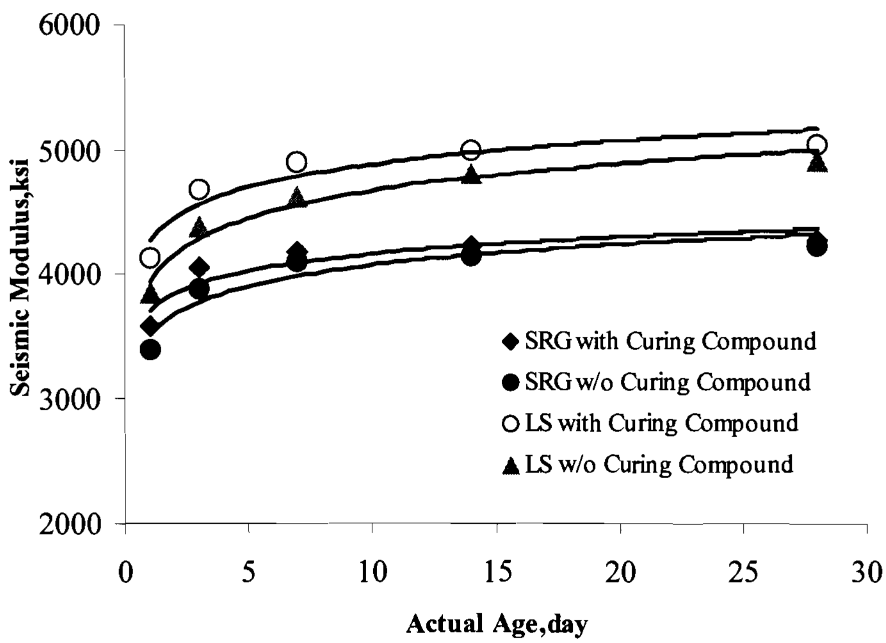

Figure 8.2 – Impact of Curing Compound on Gain in Stiffness for Limestone and Siliceous River Gravel Aggregate Mixes

As reflected in Figure 8.2, the gain in stiffness for the limestone aggregates is more affected by the presence of the curing compound. Ramaiah et al. (2001) contains advance statistical analysis that confirms the results indicated above.

A more comprehensive study of the effect of curing method on the stiffness and strength gain of concrete was carried out during the Small Slab II Study discussed in Chapter 5. As mentioned, the slab was cured in six different manners as follows:

1. No curing compound or MMF applied (a.k.a. Section N).
2. Curing compound was applied at the sheen loss with MMF (a.k.a. Section S).
3. Curing compound was applied at the sheen loss without MMF (a.k.a. Section O).
4. Curing compound was applied two hours after the concrete placement with MMF (a.k.a. Section 2).
5. Curing compound was applied eight hours after the concrete placement with MMF (a.k.a. Section 8).
6. Covered with plastic sheeting as soon as it was possible (a.k.a. Section P).

The variations in compressive strength, with maturity parameter for the cores drilled from the six different sections of the slab described above, are shown in Figure 8.3a. The trends from all sections are similar. For Section P (i.e. the section covered with a plastic sheeting) the maturity data was available only for the first 14 days. As shown in Appendix C, the R^2 values are all above 0.96 indicating a strong correlationship between the compressive strength and maturity. Similar graph but for tensile strength is included in Figure 8.3b. Again, the trends are similar, except that more scatter in the data is apparent.

The variations in seismic modulus, with maturity parameter for the cores, are shown in Figure 8.4a. The gain in seismic modulus of the P section is higher than that of the other five sections, perhaps because of better curing process. Similar results but from tests with PSPA are shown in Figure 8.4b.

The variations in compressive and tensile strengths with seismic modulus for the cores are shown in Figure 8.5. As all the sections follow a similar trend, a global curve was fitted to all of them. The R^2 values for the compressive and tensile strengths are 0.90 and 0.74, respectively. The compressive strength-seismic relationships yield a better fit because of higher repeatability associated with the compressive test.

The variations in compressive and tensile strengths with seismic modulus for the slabs are shown in Figure 8.6. Here too, a global curve was fitted to the data from all six sections. The R^2 values are 0.76 and 0.64 for the compressive strength and the tensile strength, respectively. The small R^2 value for tensile strength is due to the precision associated with those test series.

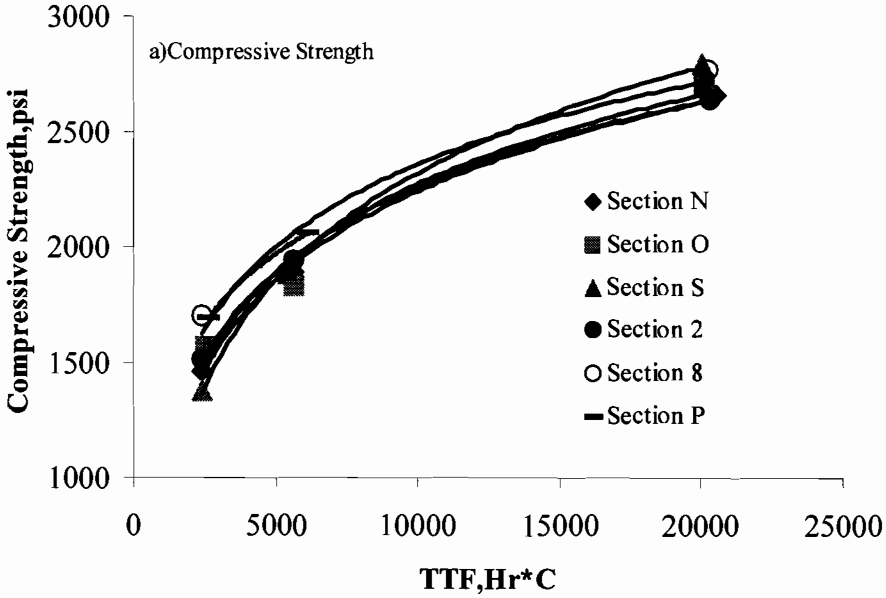

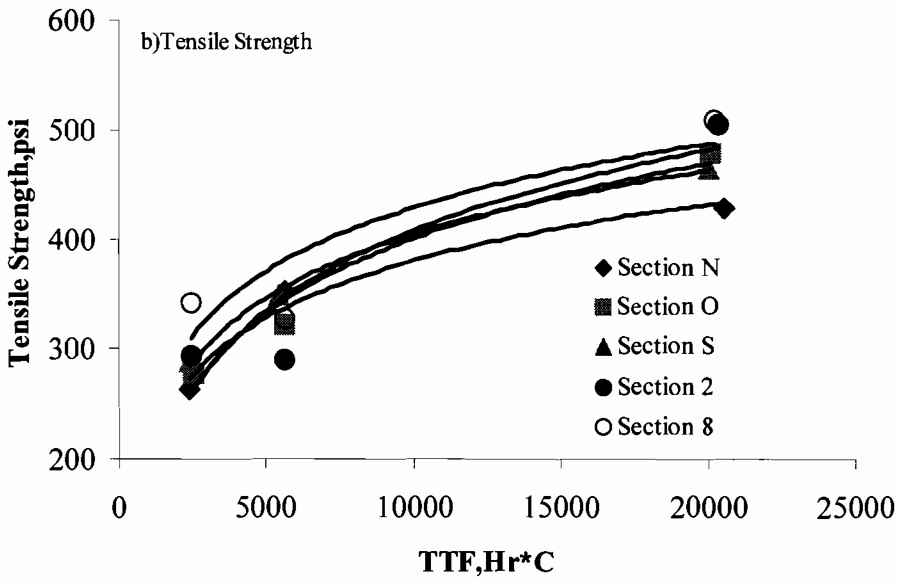

Figure 8.3 – Variation in Compressive and Tensile Strengths with Maturity for Cores from the Slab Poured for Small Slab II Study

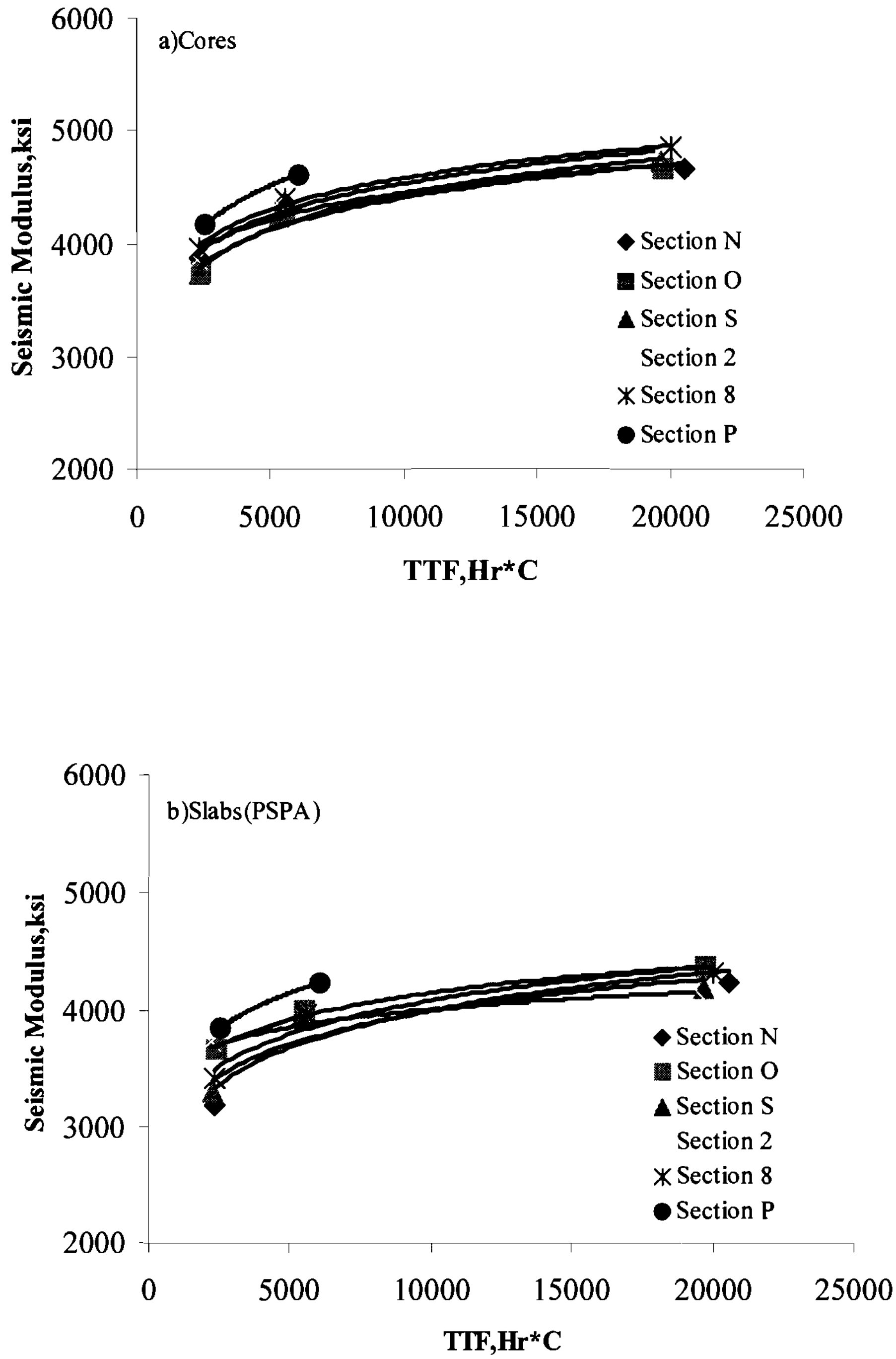

Figure 8.4 – Variation in Seismic Modulus with Maturity for the Slab Poured for Small Slab II Study

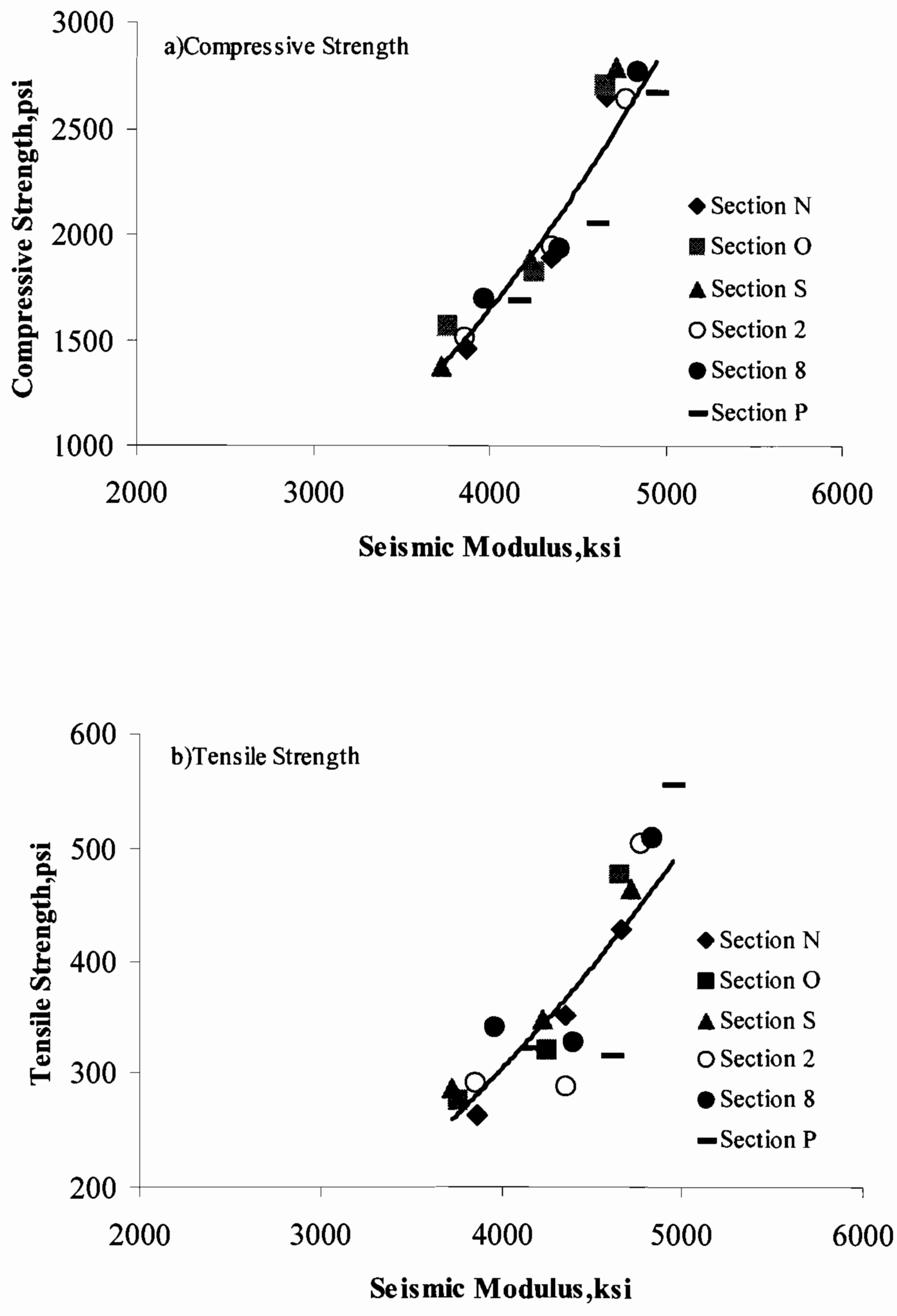

Figure 8.5 – Variation in Compressive and Tensile Strengths with Seismic Modulus for Cores from the Slab Poured for Small Slab II Study

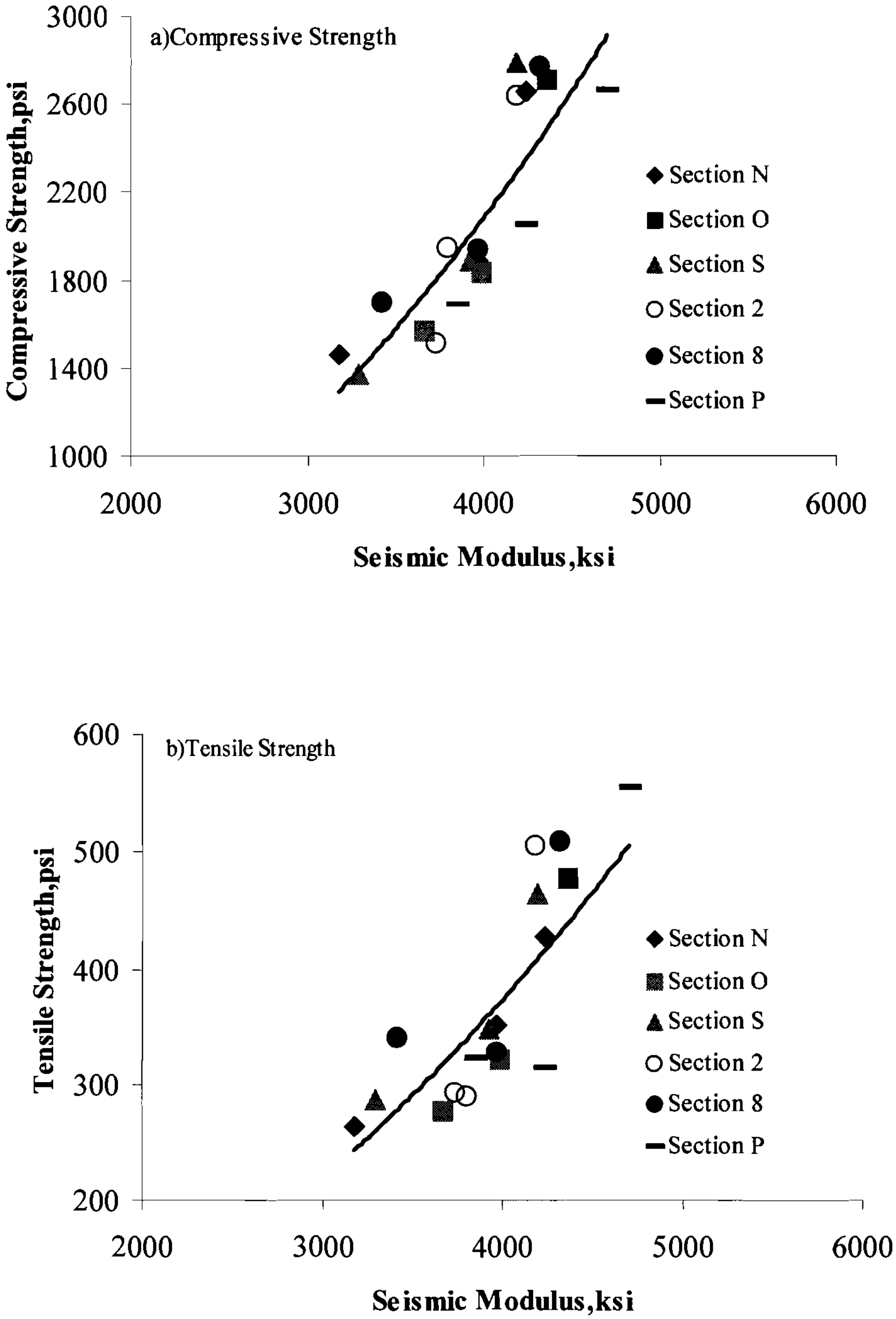

Figure 8.6 – Variation in Compressive and Tensile Strengths with Seismic Modulus for the Slab Poured for Small Slab II Study

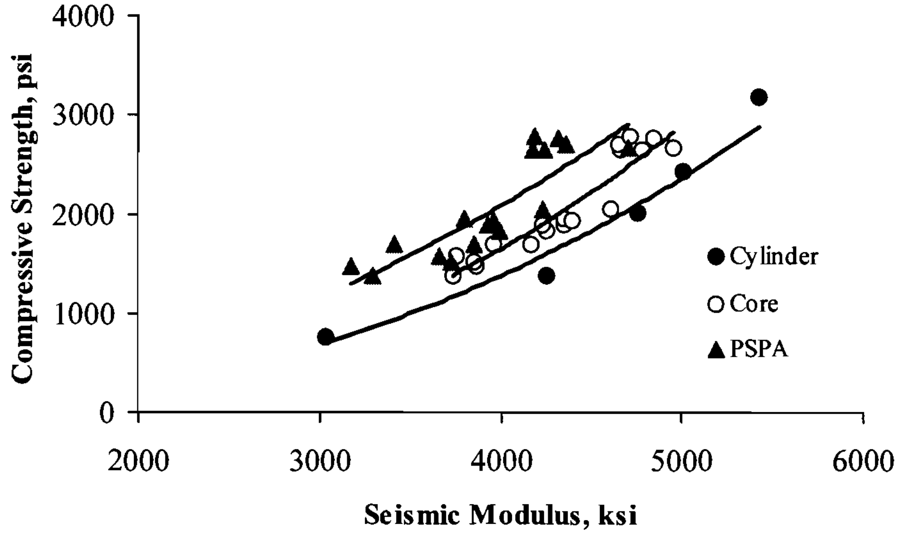

Figure 8.7 – Variation in Compressive Strength with Seismic Modulus for the Cylinders, Cores and Slabs for Small Slab II Study

The variations in compressive and tensile strengths with seismic modulus for the cylinders, cores and slabs are summarized in Figures 8.7 and 8.8, respectively. The relationships developed for the cores and for the slabs are parallel but differ by about 10%. The difference can be for most of the part explained by Equation 3.21. From that equation, one should expect an 8% to 10% difference between the two curves. Appropriate adjustment factors had been applied, the two relationships would have been similar. The relationships for the cores and cylinders are somewhat different. However the differences are not as great as those developed based on maturity. The differences are more pronounced for the tensile strengths (Figure 8.8), because of large variability in the static test results.

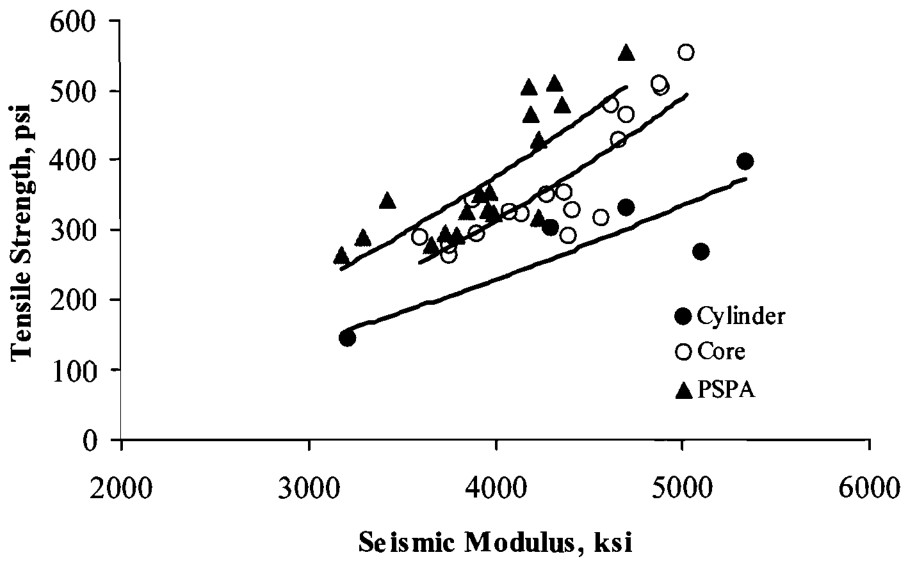

Figure 8.8 - Variation in Tensile Strength with Seismic Modulus for the Cylinders, Cores and Slabs for Small Slab II Study

Impact of Grooving

Grooved concrete slabs constitute a far larger proportion of rigid pavement construction. The major question to be answered was whether reliable interpretations of stress waves could be made on grooved pavements. If reliable interpretations can be made, the secondary issue is the sensitivity of the measurement, and its accuracy to the presence, size, and orientation of the grooves.

We utilized the slab built for the Small Slab I Study. Six 2 ft by 3 ft sections within the area with limestone aggregate of the slab were selected for this study. One of them was reinforced with steel bars. As shown in Table 8.1, the six sections were grooved in a manner that the impacts of the spacing, width and depth of grooves as well as the existence of rebars can be studied. The grooving pattern applied to Sections 1 and 6 contains extreme cases so that the impact of the grooves can be well appreciated. Section 5 is perhaps the most representative of grooves found on highways.

A series of tests took place on all of six sections just before and after grooving, respectively. Perpendicular and parallel placements of the sensor unit of the triangle geometry, as defined in Figure 8.9, were used in these tests. This geometry is of interest because currently all TxDOT PSPAs utilize this triangular geometry. Six points distributed evenly on each section were tested with each sensor alignment. A second series of tests took place with the in-line source-sensor geometry. Tests were performed in parallel to grooves, in perpendicular to grooves, and outside the grooved area. Unfortunately, only section 6 of the slab was available during the last tests.

Table 8.1 - Grooving Patterns Used in This Study

Section	Grooving Pattern, inch		
	Spacing	Width of Groove	Depth of Groove
1	1.5	0.25	0.25
2	1.5	0.25	0.50
3	1.0	0.25	0.25
4	2.0	0.25	0.25
5	1.5	0.125	0.25
6 (rebar)	1.5	0.25	0.25

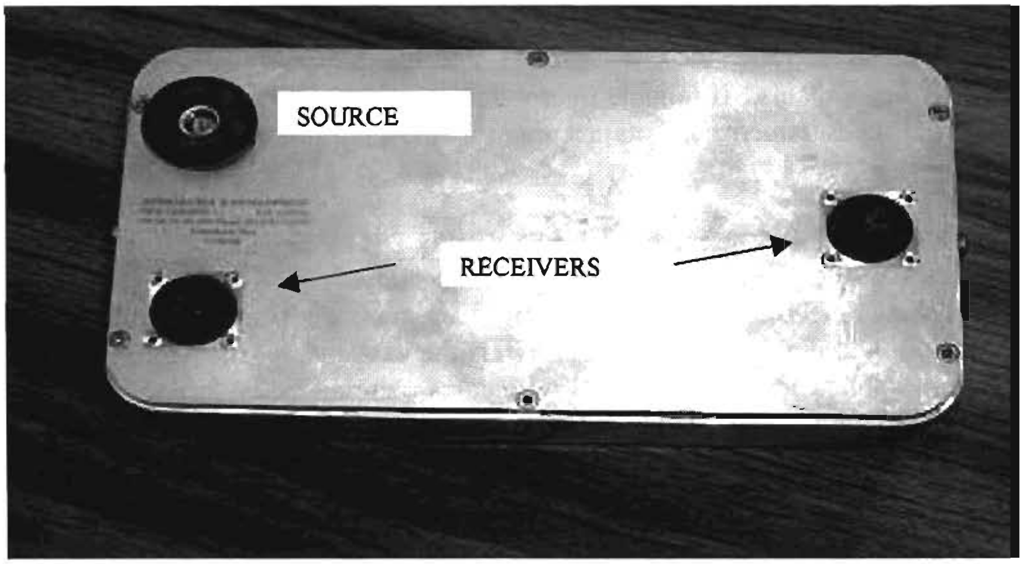

Figure 8.9 - Triangular Geometry of TxDOT's PSPA

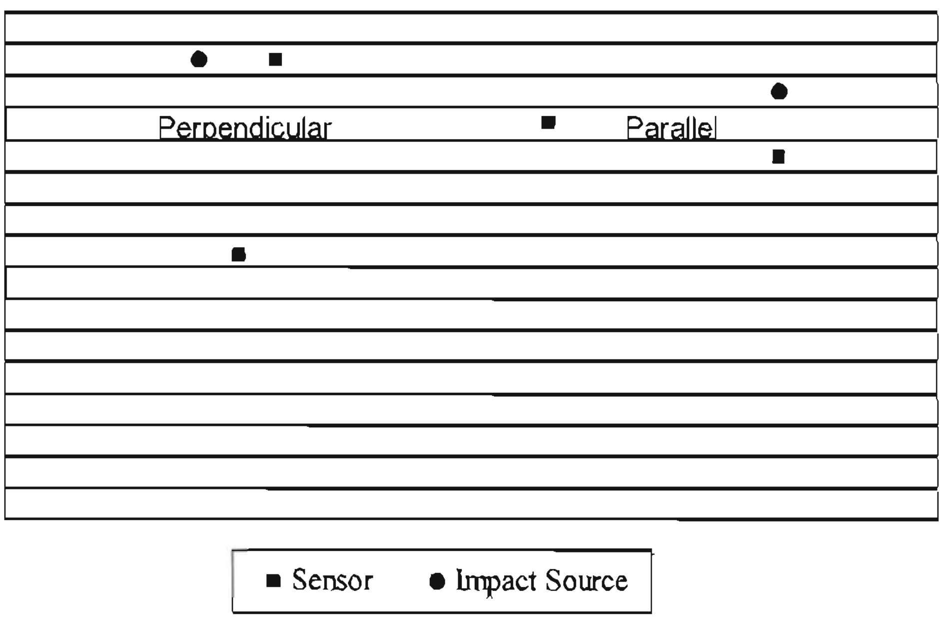

Figure 8.10 –Measurement Positions Used in Grooved Concrete Slab

Since the present study is focused on the effect of grooves on measurements, we first discuss the results from the five sections without rebar. Moduli for all of the five sections obtained before and after grooving are summarized in Table 8.2. The ratio of moduli before and after grooving for each section is shown in Figure 8.11. The moduli demonstrate a dependence on placement position of the source-sensor array relative to the grooves. Moduli measured with parallel position (see Figure 8.10) are quite comparable to those measured before grooving. On the other hand, moduli measured with the source and the near sensor on the same groove (termed perpendicular position because the longer axis of the source-sensor unit is perpendicular to the grooves in this case) show about 6% to 20% decrease depending on the grooving pattern.

Table 8.2 - Effects of Grooving Pattern on Measured Seismic Moduli

Section	Average Modulus, ksi		
	Before Grooving	Perpendicular Position	Parallel Position
1	5457	4930	5427
2	5441	4340	5469
3	5425	4621	5404
4	5553	5014	5381
5*	5497	5112	5469
Average	5475	4803	5430

* Most Representative of Highways

Since the newer PSPAs are manufactured with the inline configuration with adjustable source-receiver configuration, another set of experiments was carried out with this configuration. Unfortunately, for this experiment only Section 6 was available. The USW analysis was made on a 6-in. transducer spacing with the source-to-near-receiver spacings of 3 in. (similar to the existing PSPA) and 6 in. (proposed as a rule of thumb). As summarized in Table 8.3, the parallel orientation gives a measured modulus, which is only slightly different from the ungrooved case. For the perpendicular case, the differences in moduli relative to ungrooved case are greater as compared to the parallel case. In any case, the impact of the grooves is less pronounced with an in-line sensor array relative to the triangular configuration.

Table 8.3 – Impact of Grooving on Measured Moduli

Source-to-Receiver Spacing, in.	Modulus Ratio (grooved/ungrooved)	
	Perpendicular to Grooves	Parallel to Grooves
3	0.97	1.02
6	0.95	1.01

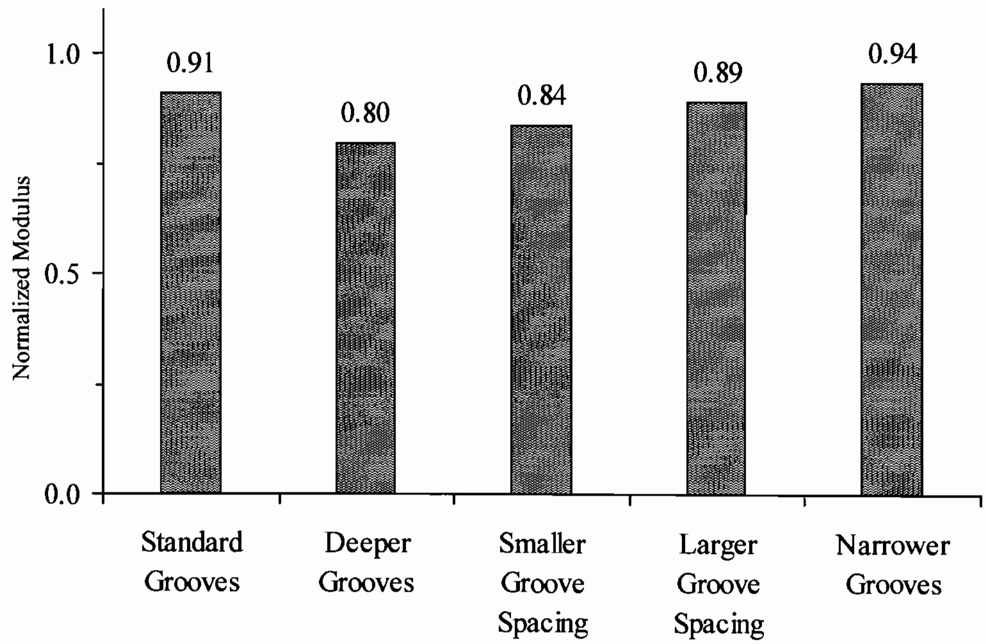

a) Perpendicular

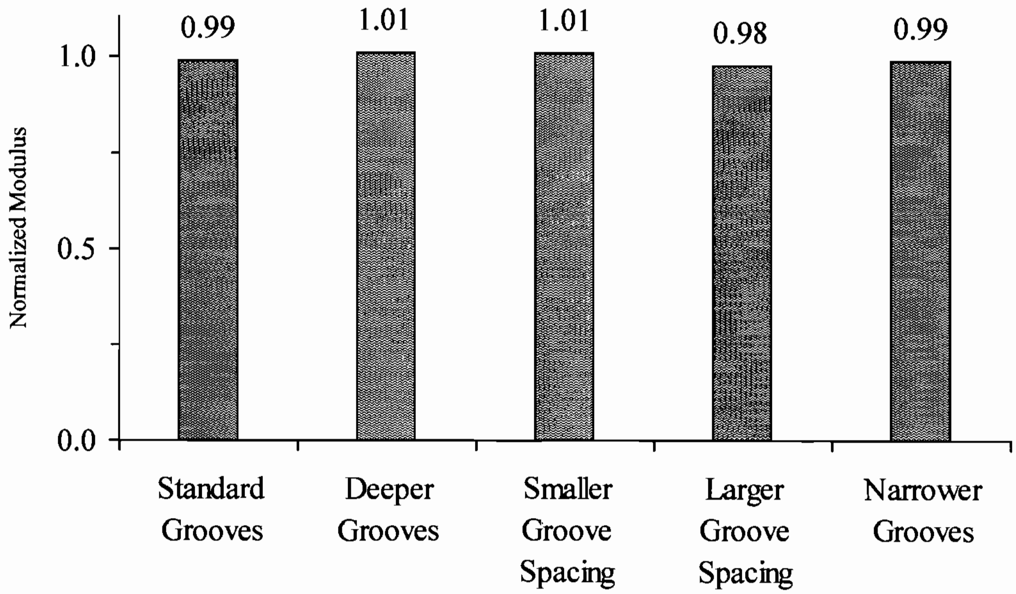

b) Parallel

Figure 8.11 – Effects of Grooving Pattern on Measured Seismic Moduli

Impact of Rebar

Ramaiah et al. (2001) contains a discussion on the impact of the rebar on the modulus of the slab measured with seismic methods for Small Slab I Study. They indicate that neither the presence nor the amount of steel in a specimen caused a statistically significant change in the seismic modulus measured. To pursue this further, the amount and position of steel in the specimens were gradually increased until the seismic modulus of specimens with rebars deviated from the case when no rebars were used. The results are reported here.

Five sets of standard cylinders were poured. Each set consists of 10 cylinders with eight cylinders retrofitted with rebar in four configurations. As such the ten specimens contained the following arrangements (see the schematic in Figure 8.12):

1. No rebar in the specimen, control specimen (2 cylinders)
2. One rebar at mid-height of the specimen (2 cylinders)
3. One rebar at quarter height of the specimen (2 cylinders)
4. Two parallel rebars at quarter height and three-quarter height (2 cylinders)
5. Two perpendicular rebars at quarter height and three-quarter height (2 cylinders).

The only difference between the five sets of ten cylinders was the size of the rebar. The rebars used were 4 (0.50 in. diameter), 5 (0.62 in. diameter), 6 (0.75 in. diameter), 8 (1 in. diameter) and 10 (1.27 in. in diameter). It should be noted that the area of the rebar, as a percentage of the concrete cross-sectional area, in many cases are much larger than those allowed by the state of practice.

As in the case of Ramaiah et al., the use of rebars No. 4, 5 and 6 did not impact the results. The impact of the number and location of rebar on the seismic modulus for specimens made with No. 8 and No. 10 rebars are shown in Figure 8.13. A slight increase in the modulus of the specimens prepared with one rebar at mid-height is observed. The reason for such an increase, aside from the variability in the specimen preparation and accuracy of the test method, is unknown. For the other three cases, a decrease in modulus in the range of 3% to 7% is observed.

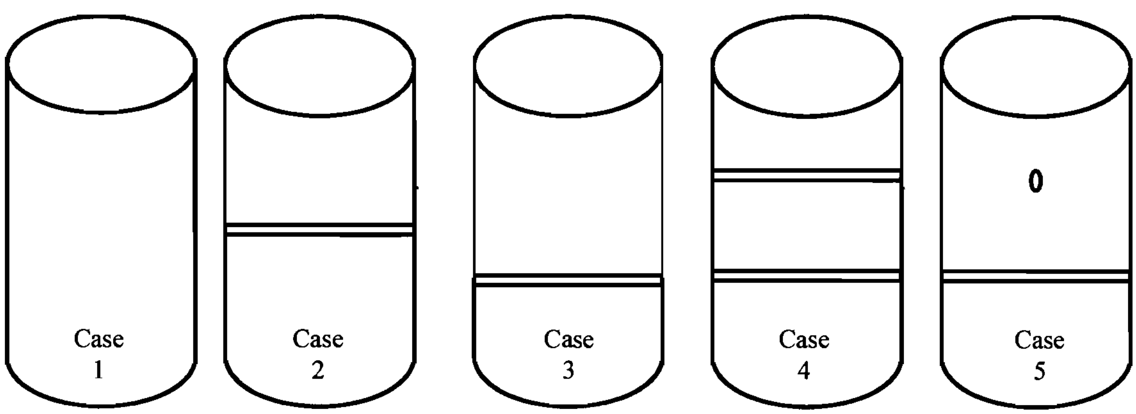

Figure 8.12 – Schematic of Cylinders Poured for Rebar Study

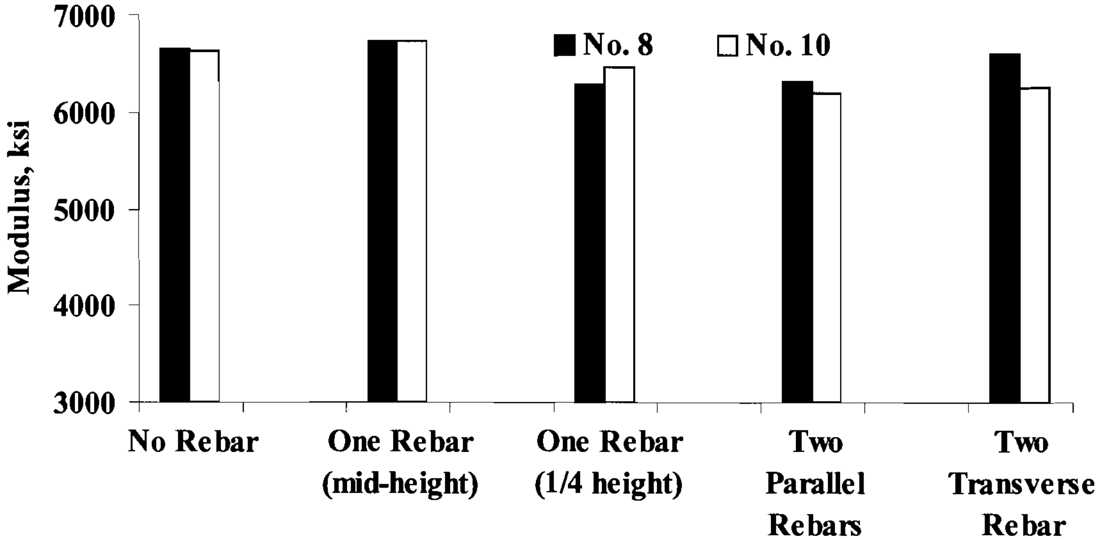

Figure 8.13 – Impact of Rebar on Seismic Modulus of Cylinders

Shortly after the seismic tests were completed, the specimens were subjected to compressive tests. The compressive strengths measured for the same specimens presented in Figure 8.13 are shown in Figure 8.14. Some variability in the results is evident. This can be attributed to the fact that the specimens containing rebar did not fail in the classical form. For the specimens with two sets of rebar, the failure plain was vertical, passing through the two locations where the rebars were placed. For the specimens with one rebar, the failure planes were for the most part dictated by the rebars. The reason for a large variability between the strengths of the specimens without rebar from the two sets of specimens is unknown. All the cylinders used in this study were poured simultaneously.

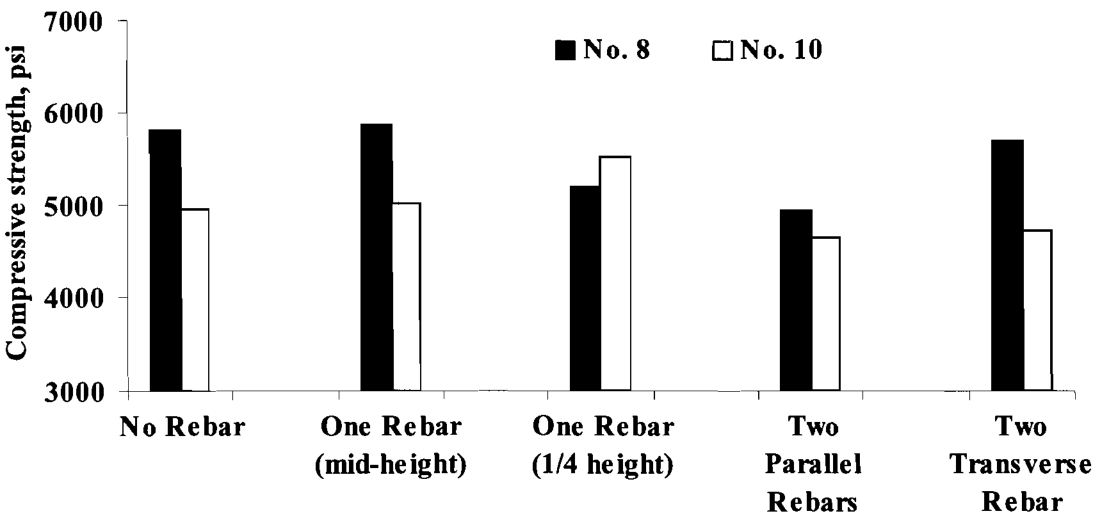

Figure 8.14 – Impact of Rebar on Static Strength of Cylinders

Chapter 9

Summary and Conclusions

Summary

The main goal in urban construction is to provide smooth and maintenance free roads with a minimal closure time. TxDOT procedures for quality control and decision process for opening a PCC project to traffic are primarily based on strength testing of standard specimens and time. Since it is almost impossible for the concrete in a structure to have the same strength or stiffness as a standard-cured specimen, in-place tests are used to measure a property of concrete that bears relationship with its strength and then estimate the in-place strength by developing a relationship between the measured property and the in-place strength. The solution for this lies in nondestructive testing. Nondestructive tests are widely being used to assess the condition of pavements. Though a large number of NDT tests are available, the maturity and seismic tests are the only tests that can monitor the early age behaviors of concrete. The seismic method is the only truly nondestructive test method that can measure the modulus of concrete. This characteristic is particularly significant as the same specimens can be subsequently tested at any other required time. In this report a protocol for determining the in-place strength of concrete base on combined maturity-seismic concepts is proposed.

To further evaluate the feasibility and limitations of the method, three broad ranges of parameters were studied. These parameters fall under one of the following three categories:

1. Mixture-related parameters
2. Environmental-related parameters
3. Construction-related parameters.

It seems that the protocol is quite feasible. More fieldwork is required to assess the operational related problems with the methodology.

Conclusions

The mixture-related parameters studied were the type of aggregate and the type of admixture. It was found that

a) The strength-maturity relationships from a number of specimens yield a reasonably high degree of correlation independent of the type of aggregate and admixture used. However, as the mix-design changes the strength-maturity relationship changes as well. This is true for compressive as well as tensile strengths.

b) Similar to item a), the modulus-maturity parameters are also highly correlated and mixture dependent.

c) It seems that the type of aggregate has the biggest impact on the strength-modulus relationships developed. All mixtures with limestone from El Paso area, prepared to yield significantly different 28-day strengths, yielded a reasonably unique strength-modulus curve. If this is proven to be appropriate for other mixtures, significantly less calibration effort (as compared to maturity method) will be necessary to predict the strength from seismic modulus.

The environmental-related parameters studied were the temperature and the humidity. It was found that

d) The curing temperature impacted the compressive and tensile strengths of standard cylinders. At early ages, the gain in strength varied significantly with temperature, but the 28-day strengths became similar for the experiments that we conducted. However, for the slabs poured with similar concrete, the strengths after 28 days were still affected by the curing temperature.

e) Patterns similar to those described in item d) were also found true for the measured moduli.

f) The curing temperature less impacted the strength-seismic modulus relationship as compared to strength-maturity relationship. Even though the strength-modulus relationships developed for cylinders were different from those for cores extracted from slabs, the differences were less pronounced than strength-maturity.

g) Moduli measured with the PSPA and free-free resonant column somewhat differed, but most of the difference could be theoretically explained.

h) The air relative humidity did not significantly impact the rate of strength and modulus gain of cylinders, but it impacted the strengths measured from the cores extracted from slabs. Based on very limited data, the strength-modulus relationships for cores and slabs seem to be reasonably similar.

Finally, the construction-related parameters studied were the thickness of the slab, the curing method, the grooving pattern and the existence of rebar. Since these parameters are related to the slab during construction, the focus was on the PSPA measurement. It was found that

i) There was no significant difference in seismic moduli measured from PSPA on slabs of different thickness in the range of 10 in. to 18 in.

j) Based on the Small Slab II study, the method of curing, aside from plastic sheeting, only slightly impacts the gain in strength and modulus, especially after 7 days. Once again, a reasonably unique relationship between the strength (either tensile or compressive) and seismic modulus could be developed.

REFERENCES

- Alexander, D. R. (1996), "In Situ Strength Measurements with Seismic Methods," Report from US Army Engineer Waterways Experiment Station, Vicksburg, Mississippi for the US Air Force Civil Engineering Support Agency, Tyndall AFB, Florida.

- Al-Manaseer, A. and Nasser, K.W. (1987), "New Non-destructive Test for Removal of Concrete Forms," Concrete International, ACI, 9(1), 41.

- Barton, J.P. (1976), "Neutron Radiography – An Overview," Practical Applications of Neutron Radiography and Gaging, ASTM STP 586, Berger, H., Ed., American Society for Testing and Materials, Philadelphia, 5.

- Bartos, M. J. (1979), "Testing Concrete in Place," Civil Engineering, American Society of Civil Engineers, Vol 66.

- Bickley, J. A. (1993), "Field Manual for Maturity and Pullout Testing on Highway Structures," Report SHRP-C-376, Strategic Highway Research Program, Washington DC.

- Bickley, J.A. (1982), "The Variability of Pullout Tests and In-place Concrete Strength," Concrete International, 4(4), 44.

- Cantor, T.R. (1970), "Status Report on the Windsor Probe Test System," presented to Highway Research Board Committee A2-03, Mechanical Properties of Concrete, at 1970 Annual Meeting, Washington DC.

- Carette, G.G. and Malhotra V.M. (1984) "In-Situ Tests: Variability and Strength Prediction of Concrete at Early Ages," Malhotra, V.M., Ed., American Concrete Institute, Spec Publ. SP-82, 111.

- Carino, N. J. (1984), "Closure to Discussion of Reference 32," Journal of American Concrete Institute, 81(1), 98.

- Carino, N.J. (1981), "Temperature Effects on Strength-Maturity Relation of Mortar," NBSIR 81-2244, U.S. National Bureau of Standards.

- Chin, F. K. (1971), "Relation Between Strength and Maturity of Concrete," Journal of American Concrete Institute, 68(3), 196.

- Chung, H.W. (1978), "Effect of Embedded Steel Bars upon Ultrasonic Testing of Concrete," Magazine of Concrete Research, London, 30(102), 19.

- Clemena, G.G. (1987),"Determining Water Content of Fresh Concrete by Microwave Reflection or Transmission Measurement," Report VTRC-88-R3, Virginia Transportation Research Council, Charlottesville, VA.

- Clemena, G.G. and Steele, R.E. (1988), "Inspection of the Thickness of In-Place Concrete with Microwave Reflection Measurements," Report VTRC-88-R16, Virginia Transportation Research Council, Charlottesville, VA.

- Clemena, G.G. (1983), "Microwave Reflection Measurements of the Dielectric Properties of Concrete," Report VTRC-84-R10, Virginia Transportation Research Council, Charlottesville, VA.

- Freiesleben, H. P. and Pederson, E.J. (1985), "Curing of Concrete Structures," CEB Information Bulletin 166.

- Freiesleben, H. P. and Pederson, E.J. (1977), "Maturity Computer for Controlled Curing and Hardening of Concrete," Nordisk Betong, 1, 19.

- Greene, G. W. (1954), "Test Hammer Provides New Method of Evaluating Hardened Concrete," ACI Journal , 51(3), 249.

- Hammond, E. and Robson, T.D. (1955), "Comparison of Electrical Properties of Various Cements and Concretes," The Engineer, 199,78 and 115.

- Huang, Y.H. (1993), "Pavement Analysis and Design," Prentice Hall, Kentucky.

- Jensen, B.C. and Braestrup, M.W. (1976), "Lok-tests Determine the Compressive Strength of Concrete," Nordisk Betong, No. 2, 9.

- Johansen, R. (1976), "A New Method for Determination for In-Place Concrete Strength of Form Removal," 1st European Colloquium On Construction Quality Control, Madrid, Spain.

- Jones, R. (1954), "Testing of Concrete by an Ultrasonic Pulse Technique", RILEM International Symposium On Nondestructive Testing of Materials and Structures," Paris, Vol 1, Paper no. A-17, 137. RILEM Bull. No. 19, 2nd part, November.

- Jones, R. and Facaoaru, I. (1969), "Recommendations for Testing Concrete by the Ultrasonic Pulse Method," Materials and Structures Research and Testing (Paris), 2(19), 275.
- Kolek, J. (1958), "An Appreciation of Schmidt Rebound Hammer," Magazine Concrete Research, London, 10(28, 27).
- Kolek J. (1969), "Non-destructive Testing of Concrete by Hardness Methods," Proceedings of Symposium On Non-destructive Testing of Concrete and Timber, Institution of Civil Engineers, London, 15.
- Kusenberger, F.N. and Barton, J.R. (1981), "Detection of Flaws in Reinforcing Steel in Prestressed Concrete Bridge Members," Report No. FHWA/AD-81/087, Federal Highway Administration, Washington, D.C.
- Malhotra, V.M. (1974), "Evaluation of the Windsor Probe Test for Estimating Compressive Strength of Concrete," RILEM Materials and Structures, Paris; 7:37:3-15.
- Malhotra, V.M. (1976), "Testing Hardened Concrete: Nondestructive Methods," ACI Monogram No. 9, American Concrete Institute, Detroit, 109.
- Malhotra, V.M., Carino, N.J. (1991), "Handbook on Nondestructive Testing of Concrete," CRC Press, Baco Rotan, FL.
- Matzkanin, G.A., De Los Santos, A., and Whiting, D.A. (1982), "Determination of Moisture Levels in Structural Concrete Using Pulsed NMR (Final Report)," Southwest Research Institute, San Antonio, Texas, Federal Highway Administration, Washington, D.C., Report No. FHWA/RD-82-008.
- Mitchell, L.J. and Hoagland, G.G. (1961), "Investigation of the Impact Tube Concrete Test Hammer," Bulletin No. 305, Highway Research Board, 14.
- Nykanen, A. (1956), "Hardening of Concrete at Different Temperatures, Especially Below the Freezing Point," Proceedings, RILEM Symposium on Winter Concreting (Copenhagen, 1956), Danish Institute for Building Research Copenhagen, Session BII.
- Okamoto, P.A., Wu C. L., Tarr, S.M., Darter, M.I., Smith, K.D. (1993) "Performance-Related Specifications for Concrete Pavements," Volume 3-Development of a Prototype Performance Related Specification, Report FHWA-RD-93-044, FHWA, U.S. Department of Transportation.
- Plowman, J.M. (1956), "Maturity and Strength of Concrete," Magazine of Concrete Research, 8(22), 13.
- Ramaiah, S., Dossey, T., McCullough, B.F. (2001), "Estimating In Situ Strength of Concrete Pavements Under Various Field Conditions," Research Report 1700-1, Center for Transportation Research, The University of Texas at Austin.

- Rebut, P. (1962) "Non-destructive Apparatus for Testing Reinforced Concrete: Checking Reinforcement with the Pachometer (in French)," Rev. Malenaux (Paris), 556,31.

- Richart, Jr., F.E., Woods, R. D., Hall Jr., J.R. (1970), Vibrations of Soils and Foundations, Prentice-Hall, Inc., Englewood Cliffs, New Jersey.

- Saul A.G.A. (1951), "Principles Underlying the Steam Curing of Concrete at Atmospheric Pressure," Magazine of Concrete Research, 2(6), 127.

- Schmidt, E. (1950), "The Concrete Test Hammer (Der Beton-Prufhammer)," Schweiz. Bauz. (Zurich), 68(28), 378.

- Shilstone, J. M. (2000), "Performance-Based Specifications for Concrete Portion of Concrete Pavements," Presented in TRB Annual Meeting, Washington D.C.

- Vassie, P.R. (1978), "Evaluation of Techniques for Investigating the Corrosion of Steel in Concrete," Department of the Environment, Department of Transport, TRRL Report SR397, Crowthorne.

- Weaver, J. and Sandgrove, B.M. (1971), "Striking Times of Formwork Tables of Curing Periods to Achieve Given Strengths," Construction Industry Research and Information Association, Rep. 36.

List of ASTM Standards

- ASTM C-1074 "Standard Practice for Estimating Concrete Strength by the Maturity Method," Annual Book of ASTM Standards, Vol 04.02, Concrete and Aggregates.

- ASTM C39 "Standard Test Method for Compressive Strength of Cylindrical Specimens," Annual Book of ASTM Standards, Vol 04.02.

- ASTM C293 "Standard Test Method for Flexural Strength of Concrete (Using Simple Beam with Center-Point Loading)," Annual Book of ASTM Standards, Vol 04.02.

- ASTM C78 "Standard Test Method for Flexural Strength of Concrete (Using Simple Beam with Third-Point Loading)," Annual Book of ASTM Standards, Vol 04.02.

- ASTM C-215 "Standard Test Method for Fundamental Transverse, Longitudinal, and Torsional Frequencies of Concrete Specimens," Vol 04.02.

- ASTM C900 "Standard Test Method for Pullout Strength of Concrete," Annual Book of ASTM Standards, Vol 04.02.

- ASTM C597-83 "Standard Test Method for Pulse Velocity through Concrete," Annual Book of ASTM Standards, Vol 04.02, Philadelphia.

- ASTM C469 "Standard Test Method for Static Modulus of Elasticity and Poisson's Ratio of Concrete in Compression," Annual Book of ASTM Standards, Vol 04.02.
- ASTM C496 "Standard Test Method for Splitting Tensile Strength of Cylindrical Concrete Specimens," Annual Book of ASTM Standards, Vol 04.02.

Appendix A

Introduction to Wave Propagation Theory

Wave Propagation Theory

This appendix introduces the principle of wave propagation and clarifies the relationships between wave velocities and moduli.

For engineering purposes, profiles of most pavement sections can be reasonably approximated by a layered half-space. With this approximation, the profiles are assumed to be homogeneous and to extend to infinity in two horizontal directions. They are assumed to be heterogeneous in the vertical direction, often modeled by a number of layers with constant properties within each layer. In addition, it is assumed that the material in each layer is elastic and isotropic.

Seismic Body Waves

Wave motion created by a disturbance within an ideal whole-space can be described by two kinds of waves: compression waves and shear waves. Collectively, these waves are called body waves, as they travel within the body of the medium. Compression and shear waves can be distinguished by the direction of particle motion relative to the direction of wave propagation.

Compression waves (also called dilatational waves, primary waves, or P-waves) exhibit a push-pull motion. As a result, wave propagation and particle motion are in the same direction. Compression waves travel faster than the other types of waves, and therefore appear first in a direct travel-time record.

Shear waves (also called distortional waves, secondary waves, or S-waves) generate a shearing motion, causing particle motion to occur perpendicular to the direction of wave propagation. Shear waves can be polarized. If the directions of propagation and particle motion are contained in a vertical plane, the wave is "vertically polarized." This wave is called an SV-wave. However, if the direction of particle motion is perpendicular to a vertical plane containing the direction of propagation, the wave is "horizontally polarized." This wave is termed a SH-wave. Shear waves travel more slowly than P-waves and thus appear as the second major wave type in a direct travel-time record.

Seismic Surface Waves

In a half-space, other types of waves occur in addition to body waves. These waves are called surface waves. Many different types of surface waves have been identified and described. The two major types are Rayleigh waves and Love waves.

Surface waves propagate near the surface of a half-space. Rayleigh waves (R-waves) propagate at a speed of approximately 90 percent of S-waves. Particle motion associated with R-waves is composed of both vertical and horizontal components, that when combined, form a retrograde ellipse close to the surface. However, with increasing depth, R-wave particle motion changes to a pure vertical and, finally, to a prograde ellipse. The amplitude of motion attenuates quite rapidly with depth. At a depth equal to about 1.5 times the wavelength, the vertical component of the amplitude is about 10 percent of that at the ground surface.

Particle motion associated with Love waves is confined to a horizontal plane and is perpendicular to the direction of wave propagation. This type of surface wave can exist only when low-velocity layers are underlain by higher velocity layers, because the waves are generated by total multiple reflections between the top and bottom surfaces of the low-velocity layer. As such, Love waves are not generated in pavement sections.

The propagation of body waves (shear and compression waves) and surface waves (Rayleigh waves) are away from a vertically vibrating circular source at the surface of a homogeneous, isotropic, elastic half-space. Miller and Pursey (1955) found that approximately 67 percent of the input energy propagates in the form of R-waves. Shear and compression waves carry 26 and 7 percent of the energy, respectively. Compression and shear waves propagate radically outward from the source. R-waves propagate along a cylindrical wave front near the surface. Although, body waves travel faster than surface waves, body waves attenuate in proportion to $1/r^2$, where r is the distance from the source. Surface wave amplitude decreases in proportion to $1/r^{0.5}$.

Seismic Wave Velocities

Seismic wave velocity is defined as the speed at which a wave advances in the medium. Wave velocity is a direct indication of the stiffness of a material; higher wave velocities are associated with higher stiffness. By employing elastic theory, compression wave velocity can be defined as

$$V_p = [(\lambda + 2G)/\rho]^{0.5} \tag{A.1}$$

where

V_p = compression wave velocity,
λ = Lame's constant,
G = shear modulus, and
ρ = mass density.

Shear wave velocity, V_s, is equal to

$$V_s = (G/\rho)^{0.5} \tag{A.2}$$

Compression and shear wave velocities are theoretically interrelated by Poisson's ratio

$$V_p/V_s = [(1 - \nu)/(0.5 - \nu)]^{0.5} \tag{A.3}$$

where υ is the Poisson's ratio. For a constant shear wave velocity, compression wave velocity increases with an increase in Poisson's ratio. For a υ of 0.0, the ratio of V_p to V_s is equal to $\sqrt{2}$; for a υ of 0.5 (an incompressible material), this ratio goes to infinity.

For a layer with constant properties, R-wave velocity and shear wave velocity are also related by Poisson's ratio. Although, the ratio of R-wave to S-wave velocities increases as Poisson's ratio increases, the change in this ratio is not significant. For Poisson's ratio of 0.0 and 0.5, this ratio changes from approximately 0.86 to 0.95, respectively. Therefore, it can be assumed that the ratio is equal to 0.90 without introducing an error larger than about 5 percent.

Equation A.3 can be rewritten as

$$\nu = [0.5(V_p/V_s)^2 - 1]/[(V_p/V_s)^2 - 1] \tag{A.4}$$

This equation can then be used to calculate Poisson's ratio once V_s and V_p are known.

Elastic Constants

Propagation velocities per se have limited use in engineering applications. In pavement engineering, Young's moduli of the different layers should be measured. Therefore, calculating the elastic moduli from propagation velocities is important.

Shear wave velocity, V_s, is used to calculate the shear modulus, G, by

$$G = \rho V_s^2 \tag{A.5}$$

in which ρ is the mass density. Mass density is equal to γ_t/g, where γ_t is the total unit weight of the material, and g is gravitational acceleration. If Poisson's ratio (or compression wave velocity) is known, other moduli can be calculated for a given V_s.

Young's and shear moduli are related by

$$E = 2G(1 + v) \tag{A.6}$$

or

$$E = 2\rho V_s^2(1 + v) \tag{A.7}$$

In a medium where the material is restricted from deformation in two lateral directions, the ratio of axial stress to axial strain is called constrained modulus. Constrained modulus, M, is defined as

$$M = \rho V_p^2 \tag{A.8}$$

or in terms of Young's modulus and Poisson's ratio

$$M = [(1 - v)E]/[(1 + v)(1 - 2v)] \tag{A.9}$$

The Bulk modulus, B, is the ratio of hydrostatic stress to volumetric strain and can be determined by

$$B = M - (4/3)G \tag{A.10}$$

Appendix B

Test Protocol

ESTIMATING CONCRETE STRENGTH BY MATURITY/SEISMIC METHOD

This test method provides a procedure for estimating concrete strength by means of the combined maturity and seismic methods. The maturity method is based on relating strength gain to temperature and time. The seismic method is in turn based on relating the strength gain to seismic wave velocity and time.

The maturity method consists of three steps:

- Develop strength-maturity relationship
- Estimate in-place strength
- Verify strength-maturity relationship.

The seismic method consists of four steps as well:

- Develop strength-seismic modulus relationship
- Develop modulus-maturity relationship
- Estimate in-place strength
- Verify strength-seismic velocity relationship.

The Nurse-Saul "temperature-time factor (TTF) maturity index shall be used in this test method, with a datum temperature of –10 °C (14 °F).

Apparatus

Maturity

- If the maturity meter has input capability for datum temperature, verify that the proper value of the datum temperature has been selected prior to each use.

- Commercial battery-powered maturity meters that automatically compute and display the maturity index in terms of a temperature-time factor, or both a temperature-time factor and an equivalent age, are acceptable. Batteries in maturity meters are to be adequately charged prior to use.

- The same brand and type of maturity meters shall be used in the field as those used to develop and verify the strength-maturity relationship.

  NOTE 1 – Commercial maturity meters use specific values of datum temperature of activation energy in evaluating the maturity; thus the displayed maturity index may not be the same for different brands and types of maturity meters.

- A minimum of one maturity meter shall be provided for each thermocouple location. The engineer may allow the use of a multi-channel meter when several thermocouples are in close proximity.

- Meters shall be protected from excessive moisture and theft, and the LCD display shall be protected from direct sunlight.

- Thermocouple wire grade shall be greater than or equal to 20 awg.

Seismic

- The automated free-free resonant column test device as described in Appendix I shall be used.

Calibration

- Calibration of the maturity device shall be verified prior to use on a project and, as a minimum, on an annual basis by placing a thermocouple in a controlled-temperature water bath and recording whether the indicated result agrees with the known temperature water bath and recording whether the indicated result agrees with the known temperature of the water bath. At least 3 different temperatures, for example, 5 °C, 25 °C and 40 °C (41 °F, 77 °F, 113 °F), are recommended. The temperature-recording device shall be accurate to within +/- 1 °C (2 °F).

- For seismic tests, no calibration process is needed. However, to ensure that the device is functioning properly, a calibration specimen provided with the device should be tested prior to the use on a project or on annual basis. If the measured modulus of the calibration specimen differs by more than 2% from those reported, the manufacturer shall be contacted.

Procedure to Develop Strength-Maturity/Seismic Relationships

Step	Action
1	For every concrete design that will be evaluated by the maturity/seismic method, prepare a minimum of 15 cylinders or beams in accordance with Test Method Tex-447-A. Additional specimens should be cast to avoid having to repeat the procedure. The mixture proportions and constituents of the concrete shall be the same as those of the job concrete whose strength will be estimated using this practice. The minimum size of each batch shall be approximately 3 m^3 (4 yd^3).
2	Fresh concrete testing for each batch shall include concrete placement temperature, slump, and air content in accordance with Test Method Tex-415-A and Tex-414-A or 416-A.
3	Embed thermocouples in a least two specimens. Thermocouples shall be placed 50-100 mm (2-4 inches) from any surface. Connect the thermocouple to maturity meters. Do not disconnect meters. Data collection must be uninterrupted.
4	Moist cure the specimens in a water bath or in a moist room in accordance with Test Method Tex-447-A.

5	Perform compression or flexural tests at ages of 1, 3, 7, 12, and 28 days in accordance with Test Method Tex-418-A of Tex-448-A, as appropriate. Additional specimens and test ages may be evaluated at the discretion of the engineer. Test three specimens at each age and compute the average strength. The specimens with thermocouples are to be tested last. Prior to conducting compression or flexural tests on each specimen, perform free-free resonant column test according to Test Method *Tex-yyy-A*. If a specimen is obviously defective (for example, out of round, not square, damaged due to handling), the specimen shall be discarded. If an individual cylinder strength is greater than 10 percent (15 percent for beams) outside the average of three specimens, the specimen can be considered defective and be discarded. When two of the three specimens are defective, a new batch must be evaluated unless additional acceptable specimens are available.
6	At each test age, record the individual and average values of maturity, seismic velocity, seismic modulus and strength for each batch on a permanent data sheet.
7	Plot the average strengths as a function of the average maturity values, with data points shown. Using a computer spreadsheet program such as Microsoft Excel, calculate a logarithmic best-fit curve through the data. Record the equation of the curve as well as the R^2 value. The resulting curve is the strength-maturity relationship to be used for estimating the strength of the concrete mixture placed in the field. Plot the average strengths as a function of the average seismic values, with data points shown. Using a computer spreadsheet program such as Microsoft Excel, calculate a logarithmic best-fit curve through the data. Record the equation of the curve as well as the R^2 value. The resulting curve is the strength-seismic relationship to be used for estimating the strength of the concrete mixture placed in the field. Plot also the average seismic modulus as a function of the average maturity values, with data points shown. Using a computer spreadsheet program such as Microsoft Excel, calculate a logarithmic best-fit curve through the data. Record the equation of the curve as well as the R^2 value. The resulting curve is the seismic modulus-maturity relationship to be used for estimating the modulus of the concrete mixture placed in the field.
8	The plot, with data points, of the strength-maturity, strength-seismic value, and seismic modulus-maturity relationships for each concrete mixture shall be circulated and signed by the Contractor or his representative and reviewed by the District Materials Engineer or the Construction Division, Materials Section. Copies are to be provided to the Engineer, the District Materials Laboratory, and the Contractor.

Procedure to Estimate In-Place Strength

Step	Action
1	When placing concrete that will be evaluated by the combined maturity/seismic methods, a TxDOT inspector shall be present at the concrete plant. For structural and Pavement Concrete, the inspector shall be at the plant on a daily basis, and shall verify batching operations using a checklist. For Miscellaneous Concrete, the inspector shall be at the plant a minimum of once per week on a random basis, and shall verify batching operations using a checklist.
2	Prior to concrete placement, install thermocouples at the frequency specified in the pertinent item of work. Install a minimum of two thermocouples at locations in the structure that are critical in terms of structural considerations or exposure conditions as directed by the engineer. Thermocouples shall be placed 50-100 mm (2-4 inches) from any formed surface, or at mid-depth of the section for sections less than 50 mm (4 inches). Thermocouples may be tied to reinforcing steel, but should not be in direct contact with the reinforcing steel or framework.
3	When Verification Tests are required or when combined maturity/seismic method will be used to estimate strength for removal of structurally critical formwork or falsework, or for steel stressing of other safety-related operations, specimen strength tests shall be done in accordance with “Procedure to Verify Strength-Maturity/Seismic Relationships” in this test method.
4	As soon as practical after concrete placement, connect and activate the maturity meter(s). Do not disconnect meters until the required maturity values are achieved. Data Collection must be uninterrupted.
5	Record maturity data on a permanent data sheet. The permanent data sheet shall show the Required Strength and the Required TTF for the specified Operation. Also perform a PSPA test Using Test Method *Tex-zzz-A*. When applicable perform *12* PSPA tests between two consecutive maturity testing stations.
6	When the maturity/seismic values are at values that are equal to or greater than the required strength for that concrete mixture, as determined by the strength-maturity/ seismic relationships, record the maturity/seismic values, verify the specimen strength in accordance with “Procedure to Verify Strength-Maturity/Seismic Relationship” in this test method as appropriate, and then remove the meter. Clip the thermocouple wires at the concrete surface.

Procedure to Verify Strength-Maturity Relationship

NOTE: When maturity is used to estimate strength for removal of structurally-critical formwork of falsework, or for steel stressing of other safety-critical operations, the specimen strength tests may be included as Verification Tests.

Step	Action
1	Make a minimum of either three cylinders or three beams in accordance with Test Method Tex-418-A or Tex-448-A, respectively, at the frequency specified in the pertinent item of work.
2	Fresh concrete testing shall include concrete placement temperature, slump, and air content in accordance with Test Method Tex-415-A and Tex-414-A or 416-A.
3	Embed thermocouples in two specimens. Thermocouples shall be placed 50-100 mm (2-4 inches) from any surface. Connect the thermocouples to maturity meters. Do not disconnect meters. Data collection must be uninterrupted.
4	Moist cure the specimens in a water bath or in a moist room in accordance with Test Method Tex-447-A.
5	Perform compression or flexural strength tests, as appropriate, when the specimen achieves the TTF corresponding to the design strength, or when the required TTF of the member is achieved in the field if estimating strength for removal of structurally-critical formwork or falsework, or for steel stressing of other safety-related operations. Test the three specimens in accordance with Test Method Tex-418-A or Tex-448-A, and compute the average strength of the specimens. Prior to conducting compression or flexural tests on each specimen, perform free-free resonant column test according to Test Method *Tex-yyy-A*. If a specimen is obviously defective,for example, out of round, not square, damaged due to handling), the specimen shall be discarded. If and individual cylinder strength is grater than 10 percent (15 percent for beams) outside the average of three specimens, the specimen can be considered defective and be discarded. When two of the three specimens are defective, a new batch must be evaluated unless additional acceptable specimens are available.
6	Record the individual and average values of maturity, individual and average strengths, seismic velocity, and seismic modulus established from the specimen breaks on a permanent data sheet. Also record the predicted strength based on the strength-maturity/seismic relationships established for that particular concrete design, and the percent difference between average and predicted values. See Table 3 for sample record log. Compare the average strength determined from the specimen breaks to the strength predicted by the strength-maturity/seismic relationships. The average strength of the specimens shall be within the verification tolerance specified for the item of work.

ESTIMATING MODULUS OF PORTLAND CEMENT CONCRETE WITH FREE-FREE RESONANT COLUMN (FFRC) METHOD

This test method provides a procedure for determining seismic modulus and possibly Poisson's ratio by means of the free-free resonant column (FFRC) method. The FFRC method is based on determining the velocity of propagation of waves in the material.

The background behind the test method is included in Appendix I.

Apparatus

The free-free resonant column device consists of a data acquisition system, an instrumented hammer and an accelerometer.

Calibration

Calibration of the free-free resonant column device shall be verified prior to use on a project using a fully matured concrete specimen. If the measured modulus of the calibration specimen differs by more than 2% from established values, the manufacturer shall be contacted.

Sample Preparation

Prepare standard 6-in. or 4-in. diameter cylinders or standard beams as per TxDOT procedures. Alternatively, cores or beams extracted from slabs can be used provided the length-to-diameter ratio of the specimens is greater than 2.

Procedure

Step	Action
1	Start the data collection program by double-clicking on the Desktop Link for the Concrete Free-free Resonant Column test program. Click on continue and you will see a screen like Figure 1.
2	For each specimen, determine the diameter, length, and mass of the specimen being tested. Enter the Specimen ID, Sample Type (cylinder, beam or core), Length, Diameter and the Mass of the specimen being tested in appropriate locations in the program. Note: This information can be updated in an Excel spreadsheet along with the results when exiting the program. However, it is recommended to enter it before testing the specimen to minimize the possibility for error.
3	Place each specimen on testing stand and attach the accelerometer to one end of the specimen. A convenient way of attaching the accelerometer to the specimen is to use a glue gun (see Figure II-2).
4	Press the RUN/ENABLE button to start the acquisition cycle.

Step	Action
5	Trigger the data acquisition by tapping the hammer near the center of the end of the specimen opposite to the accelerometer. Note: If the trigger times out, click on the red square beneath the CALC PEAK button to re-queue the data acquisition cycle. The square will turn green when re-queued. The screen will then look somewhat like Figure II-3.
6 (Optional)	Note: This step is more appropriate for specimens with length-to-diameter of about 2. Ignore this step when you are using shorter specimens. Drag the cursor to the resonant frequency associated with torsional (shear) wave. Press CALC PEAK for the program to place the cursor in the vicinity of the frequency where the resonant peak should be. Move the cursor either by pressing NEXT PEAK or PREV PEAK, by dragging the cross hair, or by depressing the diamonds under the graph, to the appropriate resonant frequency. The value for this resonant frequency, f_S is automatically adjusted as the cursor is positioned on the peak. The resonant frequency associated with the shear waves should be less than that of the compression frequency.
7	If the data is of high quality, save the resonant frequencies of the compression and/or shear waves by pressing the YES button. The values are stored in the Average Frequency Displays and the LED shows the number of samples taken for the specimen. If the specimen is not struck properly, press NO to repeat this step.
8	Repeat Steps 5 and 7 at least two more times to obtain a good average on the specimen. The frequency readings should be within 5% among the three repeats. The SAVE AVG FREQ buttons are enabled as soon as the process is repeated correctly 3 times Note: Make sure that if the shear frequency is being measured that it is recorded in all three samples taken. If a shear frequency is only measured once or twice, a "false" shear frequency will be reported. If this happens, click on RESET to restart the testing (sometimes you will have to trigger the hammer by tapping it on a hard surface so that the system will reset). If the results do not seem reasonable, simply press the NO button to discard the record.
9	To save the average frequencies click on the SAVE AVG FREQ button (refer to Figure II-4). The button will become disabled and grayed out as an indication that the averages for this specimen have been stored in memory. If you want to save the raw data as well, click on the TIME HISTORY button *after* the SAVE AVG FREQ button. If you click on the TIME HISTORY button, a window will come up for you to choose a name for the data file and to save it (refer to Figure II-5).

Step	Action
10	If there is another specimen to test, click on NEW SPECIMEN (Figure II-6) and repeat Steps 2-8 (omit Step 3). When finished testing click on the STOP button, the data acquisition program will close and will ask you to select the filename to save the test results. Notice that the default name is "NewFile.xls". If this is the first time this particular specimen has been tested, select the default filename. If however, the specimen was previously tested and a file already exists with those results, choose that file to update the data (Figure II-7).
	In Excel, click on FILE, then SAVE AS and name the file. Testing is done (Figure II-8).

Calculations

All calculations are done automatically and are reported in the Excel sheet above. The nature of the calculations is included in Appendix I.

Test Record Forms

Typical sample preparation and testing data, which are automatically input to the data collection program, is transferred to an Excel sheet. The final results are also shown and summarized in the same Excel sheet. An example of the Excel sheet is shown below. The yellow zone contains data input by the operator during testing. The green zone contains the results that are useful to the user. The white zone contains intermediate results for advanced and expert users. The turquoise zone contains the summary results.

Test No.	ID No.	Age	TTF	Diameter	Length	Mass	Compress. Frequency	Shear Frequency	Mass Density	Young's Modulus	Poisson's Ratio	Strength	√Strength
		days	°C·hr	mm	mm	kg	Hz	Hz	kg/m³	MPa		lb/in²	√lb/in²
1	Sample1	1	0	152.40	304.80	13.344	6265.22	3790.08	[illegible]	[illegible]	[illegible]		
2	Sample2	1	0	152.40	304.80	13.344	6253.61	3790.08	[illegible]	[illegible]	[illegible]		
3													
4													
5													
6													
7													
8													
9													
10													
11													
12													
13													
14													
15													
16													
17													
18													
19													
20													
Average									[illegible]	[illegible]	0.23	N/A	N/A
Standard Deviation									0	45.1	0.00	N/A	N/A
Coeff. Of Variation									0.0%	0.1%	0.2%	N/A	N/A

Appendix I

Background

Aside from traffic and environmental loading, the primary parameters that affect the performance of pavements are the modulus of each layer. Current mechanistic-empirical design procedures for structural design of flexible pavements consider these parameters. Unfortunately, the construction specifications are not based on these engineering properties. To successfully implement any mechanistic pavement design procedure and to move toward performance-based specifications, it is essential to develop tools that can measure the modulus of each layer.

Significance and Use

The free-free resonant column test is a simple laboratory test for determining the modulus and possibly Poisson's ratio of pavement materials. The modulus measured with this method is the low-strain seismic modulus. The method is applicable to specimens of Portland cement concrete, asphalt concrete, stabilized base and subgrade, compacted subgrade and granular base provided the length is greater than the diameter. A length-to-diameter of 2 is strongly recommended. Since the seismic tests are nondestructive, a membrane can be placed around the specimen so that the specimen can be tested later for strength or stiffness (resilient modulus).

Performing this test on pavement materials will allow districts to develop a database that can be used to smoothly unify the design procedures and construction quality control. As in any other quality management program, acceptance criteria for quality control should be developed. The proposed acceptance criteria can be based on free-free resonant column testing of specimens prepared in the lab. The specimens used for this purpose are similar to those used for determining the optimum moisture/maximum dry density tests for base and subgrade.

Theoretical Background

When a cylindrical specimen is subjected to an impulse load at one end, seismic energy over a large range of frequencies will propagate within the specimen. Depending on the dimensions and the stiffness of the specimen, energy associated with one or more frequencies are trapped and magnified (resonate) as they propagate within the specimen. The goal with this test is to determine these resonant frequencies. Since the dimensions of the specimen are known, if one can determine the frequencies that are resonating (i.e. the resonant frequencies), one can readily determine the modulus of the specimen using principles of wave propagation in a solid rod (see Richart et al., 1970 for the theoretical background).

What to expect?

A schematic of the test set-up is shown in the figure. An accelerometer is securely placed on one end of the specimen, and the other end is impacted with a hammer instrumented with a load cell. The signals from the accelerometer and load cell are used to determine the resonant frequencies.

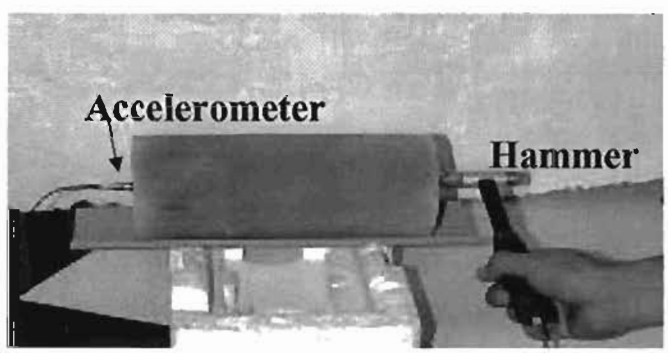

Results from an ideal condition are shown here. Resonant frequencies appear as peaks in a so-called amplitude spectrum. Two peaks are evident, one corresponding to the longitudinal propagation of waves in the specimen, and the other corresponding to the shear mode of vibration. It is simple to distinguish the two peaks. The longitudinal resonance always occurs at a higher frequency than the shear resonance.

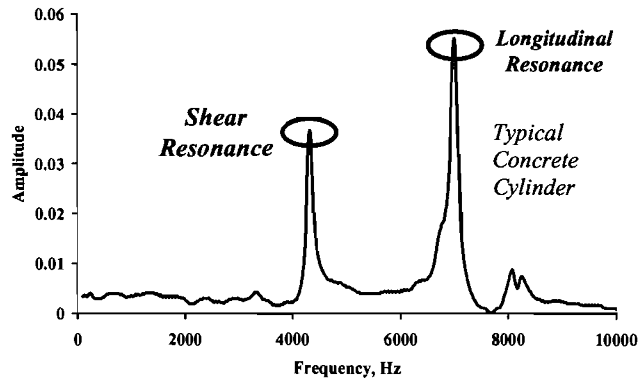

For our application, the longitudinal resonance is essential but the shear resonance is a nicety. As we will see later, the longitudinal resonance that provides the modulus, and the ratio of the longitudinal to shear resonant frequencies, provides the Poisson's ratio. For specimens with length-to-diameter of about 2, the frequency ratio cannot be less than 1.4.

Even though the resonant frequencies are not sensitive to the locations of the accelerometer and to the impact on the specimen ends, the amplitude associated with each resonance varies with these two parameters. Fortunately, the amplitudes are not important at all. Only the frequencies at which the peak amplitudes (resonant frequencies) occur are significant.

If the accelerometer is placed exactly at the center of one end, and the other end is impacted exactly at the center, the shear resonance totally disappears. The best compromise for getting adequate energy for both resonant frequencies is to place the accelerometer about 1/3 to 1/2 the radius from the center and impact the other end in the center.

How "sharp" (narrow and tall) a resonant peak is depends on the material being tested. The softer and the more absorbent (having higher damping properties) the material is, the less sharp the peak will be.

Calculations

Once the longitudinal resonant frequency, f_L, and the length of the specimen, L, are known, Young's modulus, E, can be found from the following relation:

$$E = \rho\ (2\ f_L\ L)^2. \tag{I-1}$$

where ρ is mass density. The mass density is calculated from:

$$\rho = M / L\ A_s \tag{I-2}$$

where A_s is the cross-sectional area of the specimen. Poisson's ratio, ν, is determined from

$$\nu = (0.5\,\alpha - 1) / (\alpha - 1) \tag{I-3}$$

where

$$\alpha = (f_L / f_S)^2 C_{L/D} \tag{1-4}$$

with $C_{L/D}$ being a correction factor when the length-to-diameter ratio differs from 2. These equations are implemented in an excel worksheet shown below. The yellow zone contains data input by the operator during testing. The green zone contains the results that are concern to the user. The white zone contains intermediate results for advanced and expert users. The turquoise zone contains the summary results.

Test No.	ID No.	Age days	TTF °C·hr	Diameter mm	Length mm	Mass kg	Compress. Frequency Hz	Shear Frequency Hz	Mass Density Kg/m³	Young's Modulus MPa	Poisson's Ratio	Strength [illegible]	Strength [illegible]
1	Sample1	1	0	152.40	304.80	13.244	[illegible]	3750.00	[illegible]	[illegible]	[illegible]		
2	Sample2	1	0	152.40	304.80	13.244	[illegible]	3750.00	[illegible]	[illegible]	[illegible]		
3													
4													
5													
6													
7													
8													
9													
10													
11													
12													
13													
14													
15													
16													
17													
18													
19													
20													
Average									2400	[illegible]	0.22	N/A	N/A
Standard Deviation									[illegible]	45.1	0.00	N/A	N/A
Coeff. Of Variation									0.0%	0.1%	0.2%	N/A	N/A

Appendix II

Figures

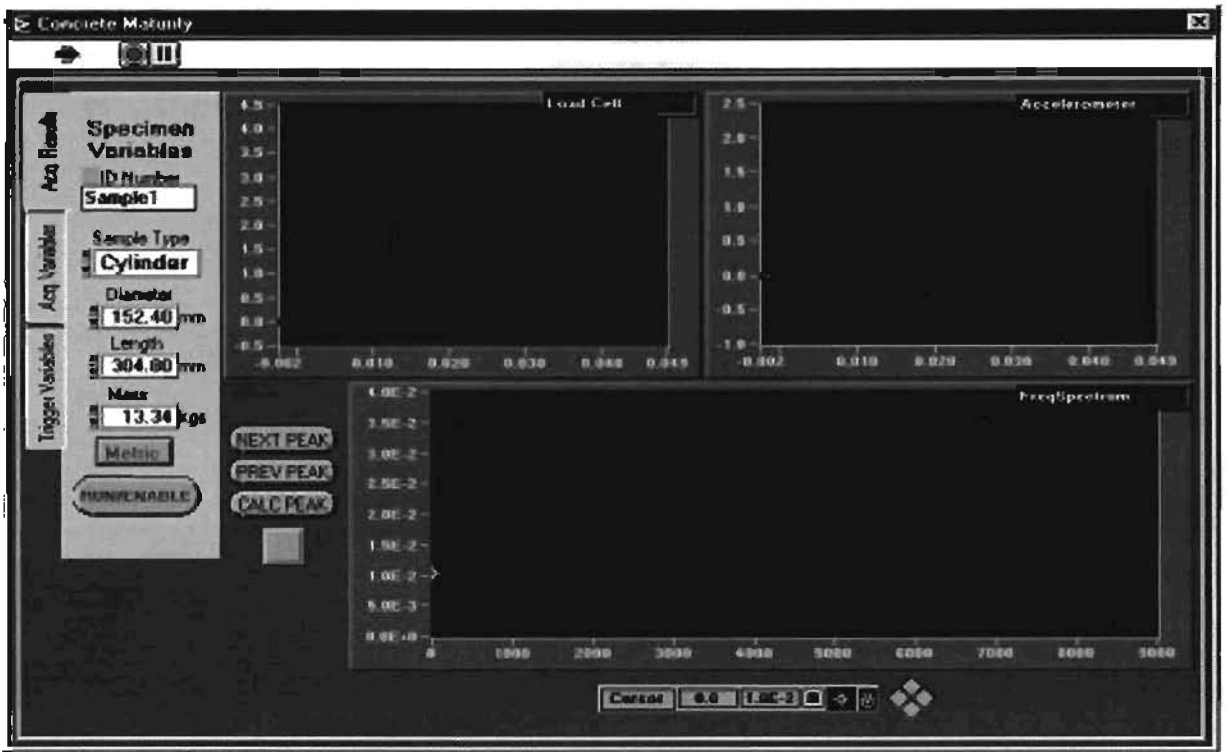

Figure II-1 – Initial Screen for Concrete Free-free Resonant Test

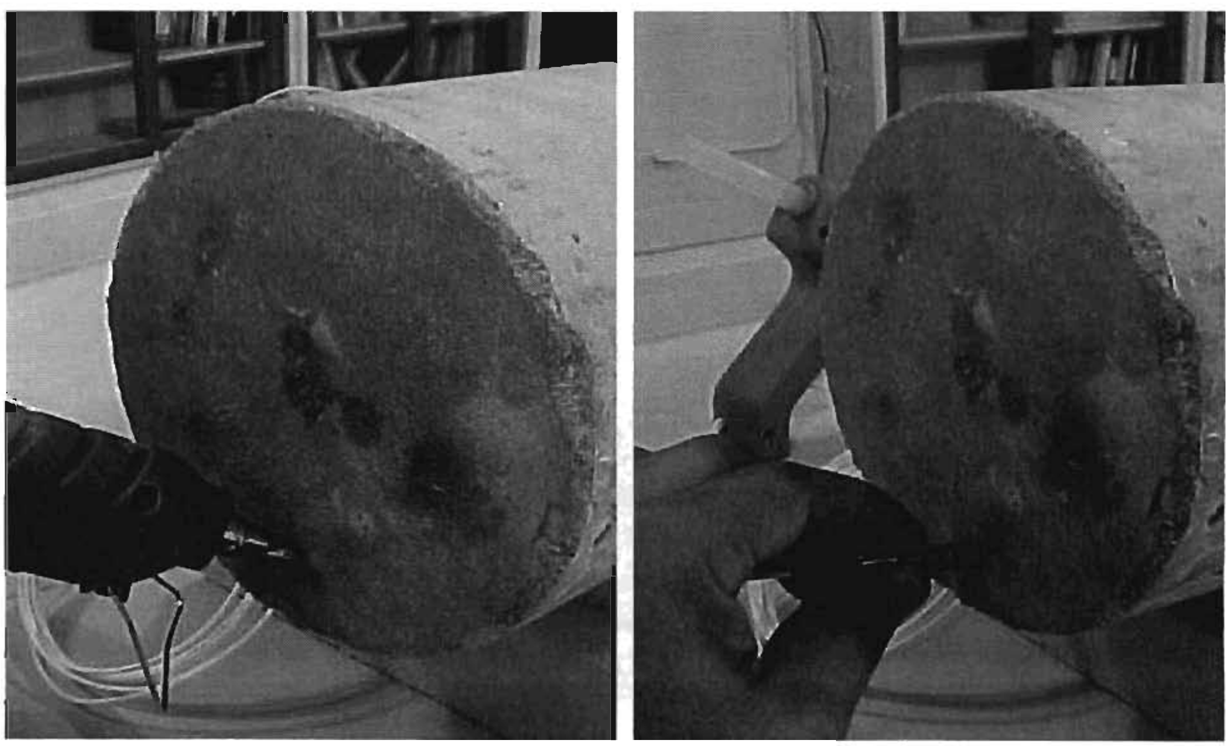

Figure II-2 – Attaching Sensor to Concrete Specimen.

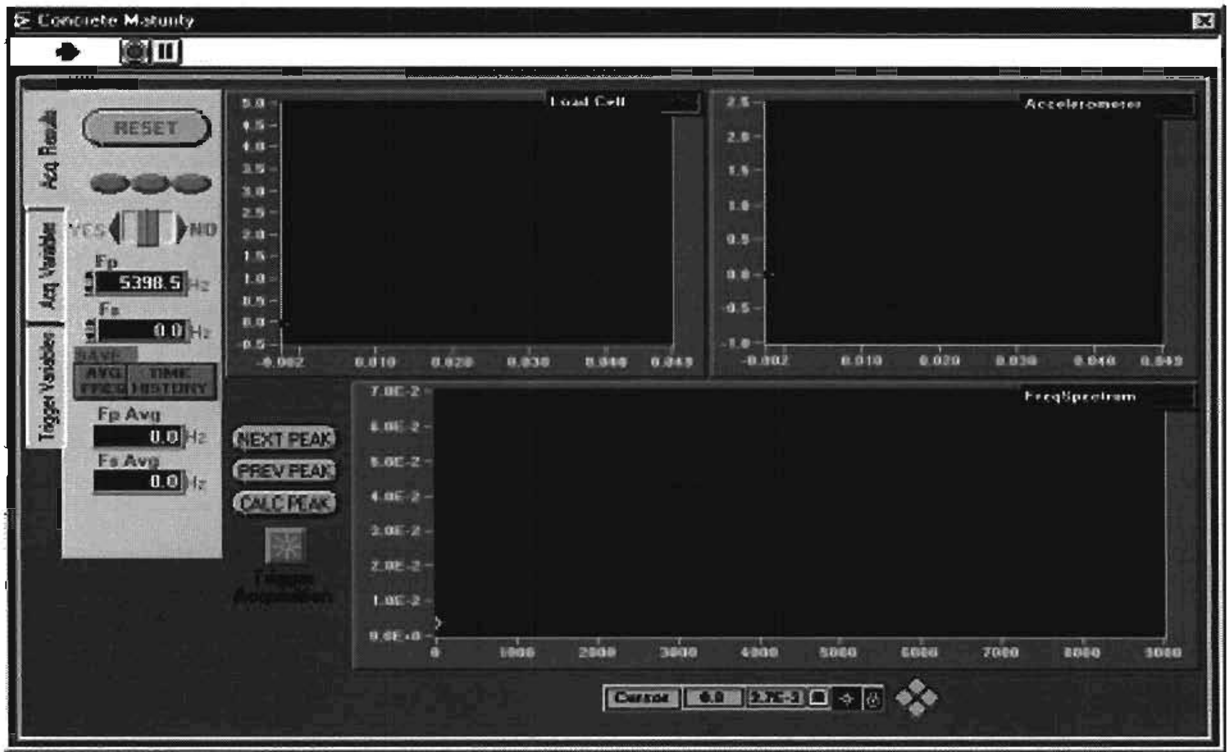

Figure II-3 – Waiting to trigger acquisition.

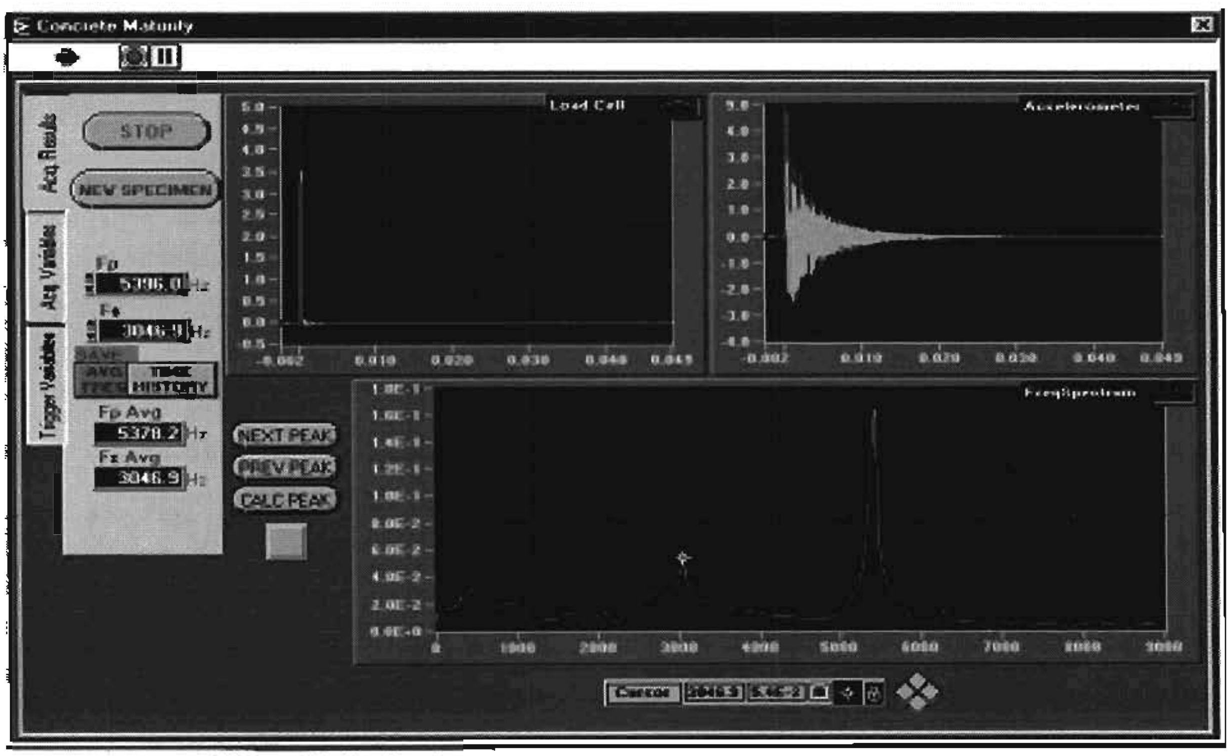

Figure II-4 – Saving Average Resonant Frequencies to cache.

Figure II-5 – Saving Time History to tab delimited excel file.

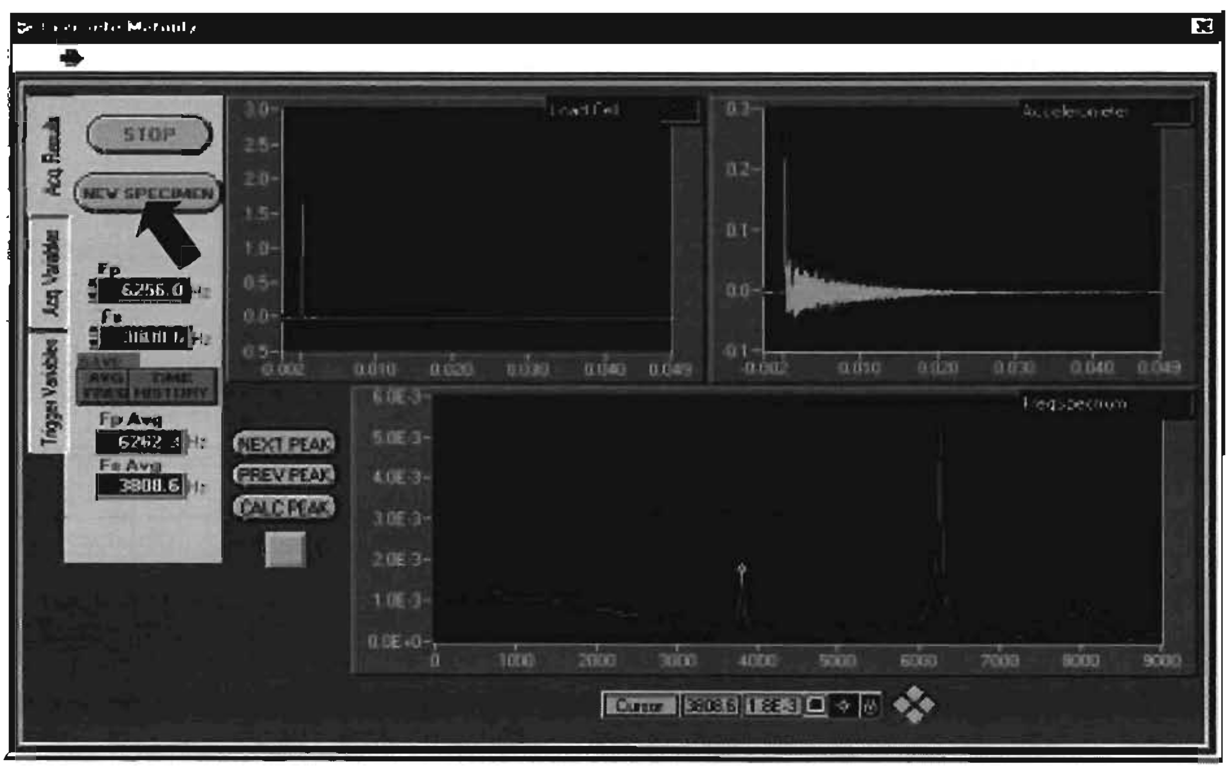

Figure II-6 – Click on "New Specimen" to Continue Testing.

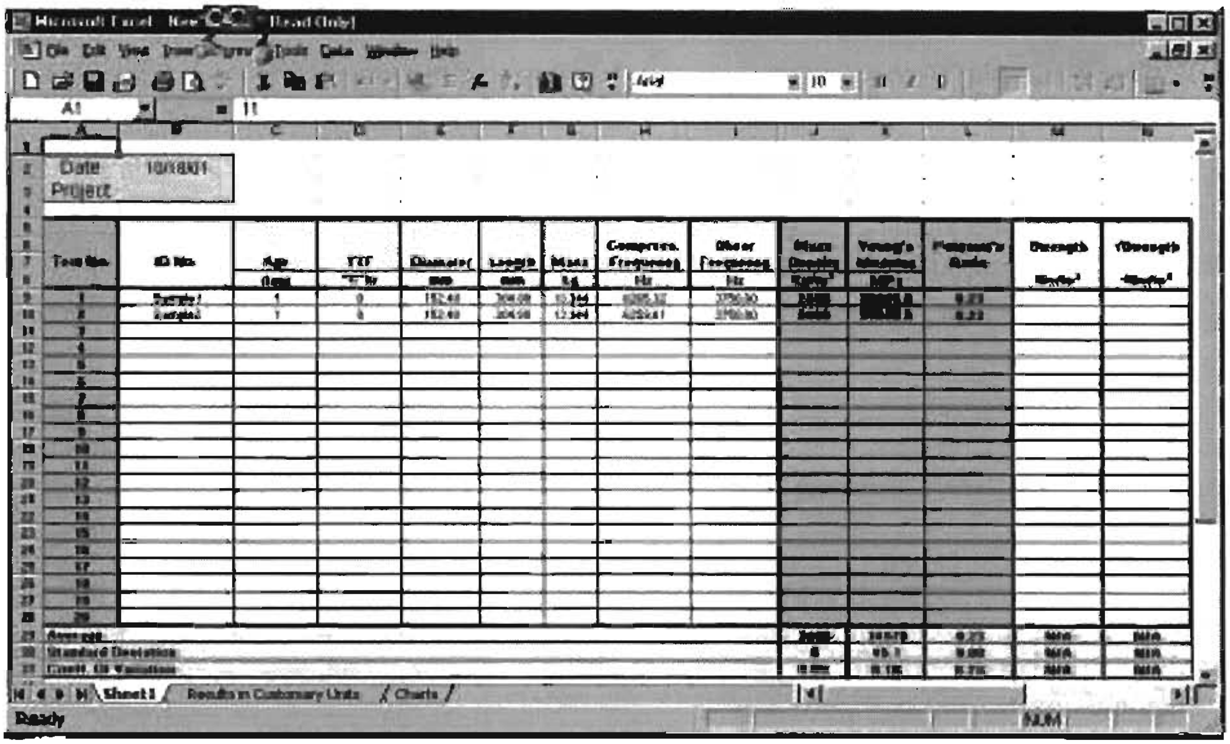

Figure II-7 – Excel sheet used for Concrete Maturity data calculation.

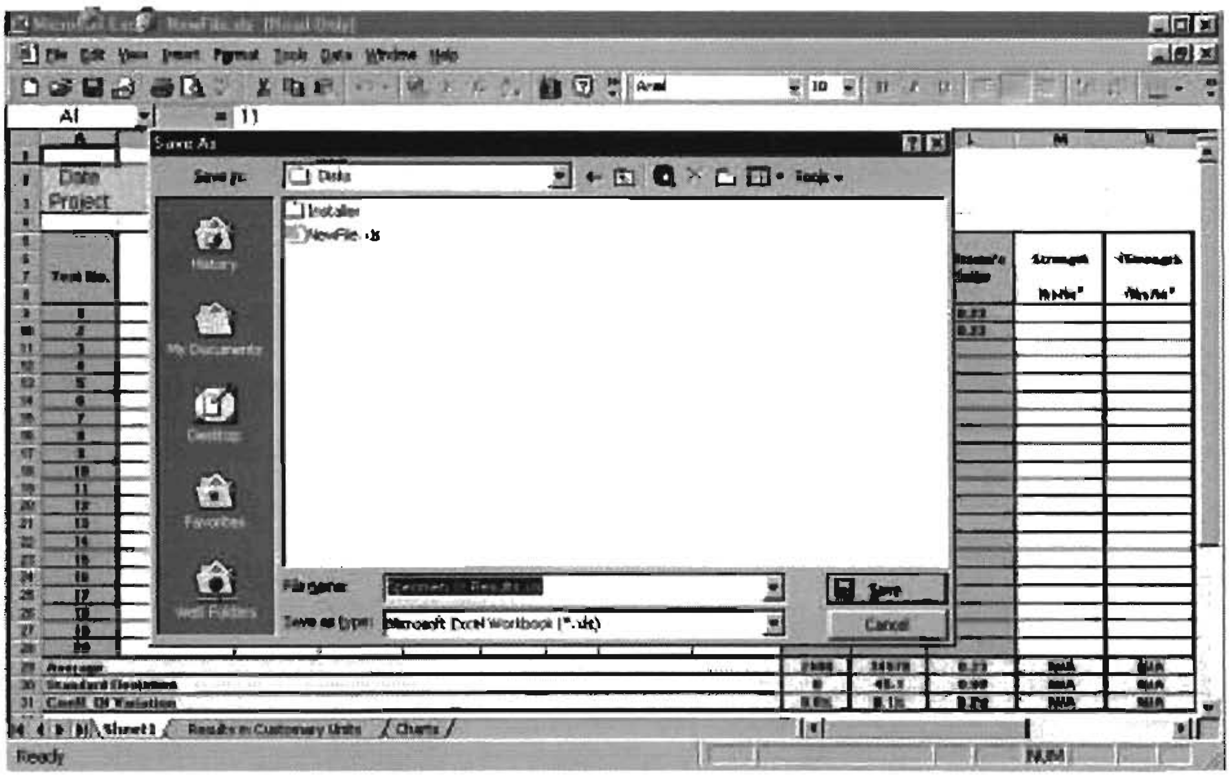

Figure II-8 – Saving Concrete Maturity results with different filename.

Appendix C

FIGURE NO.	CASE STUDY	SPECIMEN TYPE	RELATION	TYPE OF AGGREGATE	DEVELOPED CORRELATION	R^2 VALUE
6.1	Small Slab I Study	Standard Cylinders	Compressive Strength vs. Maturity	Limestone	Y=840.6Ln(X)-3434.5	0.97
				Gravel	Y=844.44Ln(X)-3263.1	0.98
6.2	Small Slab I Study	Standard Cylinders	Tensile Strength vs. Maturity	Limestone	Y=61.762Ln(X)-148.48	0.82
				Gravel	Y=62.844Ln(X)-143.22	0.95
6.3	Small Slab I Study	Standard Cylinders	Flexural Strength vs. Maturity	Limestone	Y=85.509Ln(X)-96.379	0.96
				Gravel	Y=92.653Ln(X)-206.55	0.85
6.4	Small Slab I Study	Standard Cylinders	Seismic Modulus vs. Maturity	Limestone	Y=485.71Ln(X)+1291.1	0.94
				Gravel	Y=372.82Ln(X)+1330.8	0.94
6.5.a	Small Slab I Study	Standard Cylinders	Compressive Strength vs. Seismic Modulus	Limestone	$Y=2E\text{-}07X^{2.7699}$	0.99
				Gravel	$Y=4E\text{-}07X^{2.7476}$	0.99

FIGURE NO.	CASE STUDY	SPECIMEN TYPE	RELATION	TYPE OF MIXTURE/ AGGREGATE	DEVELOPED CORRELATION	R^2 VALUE
6.5.b	Small Slab I Study	Standard Cylinders	Tensile Strength vs. Seismic Modulus	Limestone	$Y=4E\text{-}06X^{2.1382}$	0.95
				Gravel	$Y=1E\text{-}05X^{2.0671}$	0.99
6.5.c	Small Slab I Study	Standard Cylinders	Flexural Strength vs. Seismic Modulus	Limestone	$Y=4E\text{-}06X^{2.1825}$	0.81
				Gravel	$Y=5E\text{-}06X^{2.1969}$	0.72
6.6	Laboratory Study	Standard Cylinders	Compressive Strength vs. Maturity	Mix With AEA	Y=1416.6Ln(X)-8477	0.99
				Mix Without AEA	Y=2083Ln(X)-13061	0.99
6.7	Laboratory Study	Standard Cylinders	Seismic Modulus vs. Maturity	Mix With AEA	Y=838.62Ln(X)-2189.1	0.85
				Mix Without AEA	Y=1088.4Ln(X)-3902.9	0.97
6.8	Laboratory Study	Standard Cylinders	Compressive Strength vs. Seismic Modulus	Mix with AEA and Without AEA	$Y=2E\text{-}07X^{2.7861}$	0.94

FIGURE NO.	CASE STUDY	SPECIMEN TYPE	RELATION	TYPE OF AGGREGATE/ TEMPERATURE	DEVELOPED CORRELATION	R^2 VALUE
6.9	Combined Study	Standard Cylinders	Compressive Strength vs. Seismic Modulus	Limestone	$Y=3E\text{-}07X^{2.6997}$	0.90
				Gravel	$Y=8E\text{-}07X^{2.6552}$	0.99
6.10	Combined Study	Standard Cylinders	Compressive Strength vs. Maturity	Limestone	Y=1139Ln(X)-6359.4	0.67
7.1	Environmental Study	Standard Cylinders	Compressive Strength vs. Actual Age	5°C	Y=1030.1Ln(X)+607.06	0.99
				25°C	Y=592.28Ln(X)+1840.8	0.99
				40°C	Y=510.92Ln(X)+2242	0.99
			Compressive Strength vs. Maturity	5°C	Y=1076.1Ln(X)-5907.4	0.99
				25°C	Y=604.41Ln(X)-2232.2	0.99
				40°C	Y=529.13Ln(X)-1565	0.98
			Compressive Strength vs. Equivalent Age	5°C	Y=1075.6Ln(X)-2033.1	0.99
				25°C	Y=635.6Ln(X)-410.66	0.99
				40°C	Y=540.85Ln(X)-134.95	0.98
7.2	Environmental Study	Standard Cylinders	Seismic Modulus vs. Actual Age	5°C	Y=951.59Ln(X)+2906	0.95
				25°C	Y=438.3Ln(X)+4584.6	0.95
				40°C	Y=307.48Ln(X)+4694.2	0.87
			Seismic Modulus vs. Maturity	5°C	Y=989.55Ln(X)-3077.5	0.94
				25°C	Y=447.34Ln(X)+1570	0.95
				40°C	Y=317.04Ln(X)+2415.3	0.86
			Seismic Modulus vs. Equivalent Age	5°C	Y=989.47Ln(X)+483.63	0.94
				25°C	Y=470.21Ln(X)+2919.2	0.95
				40°C	Y=323.33Ln(X)+3276.5	0.86

FIGURE NO.	CASE STUDY	SPECIMEN TYPE	RELATION	TEMPERATURE/ HUMIDITY/TYPE OF CURING	DEVELOPED CORRELATION	R^2 VALUE
7.3	Environmental Study	Standard Cylinders	Compressive Strength vs. Seismic Modulus	5°C, 25°C and 40°C	$Y=1E\text{-}05X^{2.2633}$	0.99
7.4	Environmental Study	Slabs	Seismic Modulus vs. Maturity	5°C	Y=204.97Ln(X)+2989	0.47
				25°C	Y=205.771Ln(X)+2858.6	0.7
				40°C	Y=106.28Ln(X)+3338.2	0.61
7.5	Environmental Study	Standard Cylinders	Compressive Strength vs. Maturity	100%	Y=726.561Ln(X)-3202.7	0.99
				35%	Y=604.41Ln(X)-2232.2	0.99
7.6	Environmental Study	Standard Cylinders	Seismic Modulus vs. Maturity	100%	Y=376.27Ln(X)+2145.3	0.83
				35%	Y=447.341Ln(X)+1570	0.95
7.7	Environmental Study	Slabs	Seismic Modulus vs. Maturity	100%	Y=276.03Ln(X)+2742.6	0.78
				35%	Y=205.771Ln(X)+2858.6	0.7
7.8	Environmental Study	Standard Cylinders	Compressive Strength vs. Maturity	Ideal Curing	Y=726.56Ln(X)-3202.7	0.99
				Natural Curing	Y=647.53Ln(X)-2460.8	0.95

FIGURE NO.	CASE STUDY	SPECIMEN TYPE	RELATION	TYPE OF CURING/ SPECIMEN/ THICKNESS OF SLAB	DEVELOPED CORRELATION	R^2 VALUE
7.9	Environmental Study	Standard Cylinders	Seismic Modulus vs. Maturity	Ideal Curing	Y=376.27Ln(X)+2145.3	0.83
				Natural Curing	Y=359.47Ln(X)+2356.2	0.84
7.10	Environmental Study	Slabs	Seismic Modulus vs. Maturity	Ideal Curing	Y=276.03Ln(X)+2742.6	0.78
				Natural Curing	Y=206.3Ln(X)+2840.6	0.87
7.11	Environmental Study	Standard Cylinders and Slabs	Compressive Strength vs. Seismic Modulus	Standard Cylinders	$Y=6E\text{-}06X^{2.3378}$	0.68
				Slabs	$Y=1E\text{-}08X^{3.101}$	0.95
8.1	Environmental Study	Slabs	Seismic Modulus vs. Maturity	10 in.	Y=161.04Ln(X)+3149.3	0.77
				14 in.	Y=148.4Ln(X)+3420.5	0.44
				18 in.	Y=308.48Ln(X)+1999.7	0.76
8.2	Small Slab I Study	Slabs	Seismic Modulus vs. Actual Age	Gravel with Curing	Y=196.92Ln(X)+3703.7	0.85
				Gravel w/o Curing	Y=243.19Ln(X)+3506.9	0.90
				Limestone with Curing	Y=270.17Ln(X)+4261.1	0.89
				Limestone w/o Curing	Y=319.49Ln(X)+3932.8	0.96

FIGURE NO.	CASE STUDY	SPECIMEN TYPE	RELATION	SLAB SECTION	DEVELOPED CORRELATION	R^2 VALUE
8.3.a	Small Slab II Study	Cores	Compressive Strength vs. Maturity	'N'	Y=557.49Ln(X)-2894.8	0.99
				'O'	Y=562.63Ln(X)-2911.9	0.97
				'S'	Y=669.75Ln(X)-3852.4	0.99
				'2'	Y=533.78Ln(X)-2657.8	0.99
				'8'	Y=519.03Ln(X)-2424.9	0.96
				'P'	Y=433.5Ln(X)-1752.5	0.99
8.3.b	Small Slab II Study	Cores	Tensile Strength vs. Maturity	'N'	Y=75.229Ln(X)-313.16	0.98
				'O'	Y=99.163Ln(X)-512.91	0.97
				'S'	Y=84.172Ln(X)-370.93	0.99
				'2'	Y=106.26Ln(X)-570.85	0.84
				'8'	Y=84.523Ln(X)-349.76	0.79
8.4.a	Small Slab II Study	Cores	Seismic Modulus vs. Maturity	'N'	Y=353.07Ln(X)+1200.3	0.94
				'O'	Y=419.63Ln(X)+539.65	0.97
				'S'	Y=454.17Ln(X)+258.26	0.98
				'2'	Y=418.81Ln(X)+676.6	0.97
				'8'	Y=406.33Ln(X)+838.46	0.99
				'P'	Y=513.39Ln(X)+138.5	0.99
8.4.b	Small Slab II Study	Slabs	Seismic Modulus vs. Maturity	'N'	Y=462.09Ln(X)-254.13	0.85
				'O'	Y=327.2Ln(X)+1136.2	0.99
				'S'	Y=399.91Ln(X)+307.44	0.88
				'2'	Y=216.16Ln(X)+2018.3	0.93
				'8'	Y=411.42Ln(X)+295.26	0.94
				'P'	Y=442.33Ln(X)+383.63	0.99
8.5.a	Small Slab II Study	Cores	Compressive Strength vs. Seismic Modulus	N, O, S, 2,8 and P Sections	$Y=1E\text{-}06X^{2.5285}$	0.90
8.5.b	Small Slab II Study	Cores	Tensile Strength vs. Seismic Modulus	N, O, S, 2,8 and P Sections	$Y=3E\text{-}06X^{2.2414}$	0.74

FIGURE NO.	CASE STUDY	SPECIMEN TYPE	RELATION	SLAB SECTION	DEVELOPED CORRELATION	R^2 VALUE
8.6.a	Small Slab II Study	Slabs	Compressive Strength vs. Seismic Modulus	N, O, S, 2,8 and P Sections	$Y=7E\text{-}05X^{2.068}$	0.76
8.6.b	Small Slab II Study	Slabs	Tensile Strength vs. Seismic Modulus	N, O, S, 2,8 and P Sections	$Y=7E\text{-}05X^{1.8696}$	0.64
8.7	Small Slab II Study	Standard Cylinders	Compressive Strength vs. Seismic Modulus	N, O, S, 2,8 and P Sections	$Y=3E\text{-}06X^{2.4198}$	0.97
		Cores			$Y=1E\text{-}06X^{2.5285}$	0.90
		Slabs			$Y=7E\text{-}05X^{2.068}$	0.77
8.8	Small Slab II Study	Standard Cylinders	Tensile Strength vs. Seismic Modulus	N, O, S, 2,8 and P Sections	$Y=0.0002X^{1.7143}$	0.82
		Cores			$Y=2E\text{-}05X^{2.0149}$	0.73
		Slabs			$Y=7E\text{-}05X^{1.8696}$	0.64

Appendix D

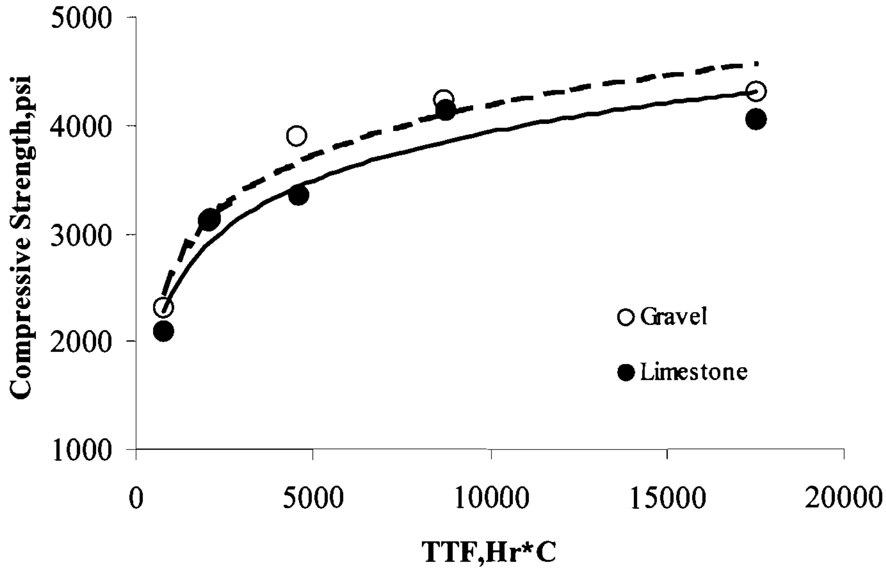

Figure D-1-Variation in Compressive Strength with Maturity for Sand-cured Specimens

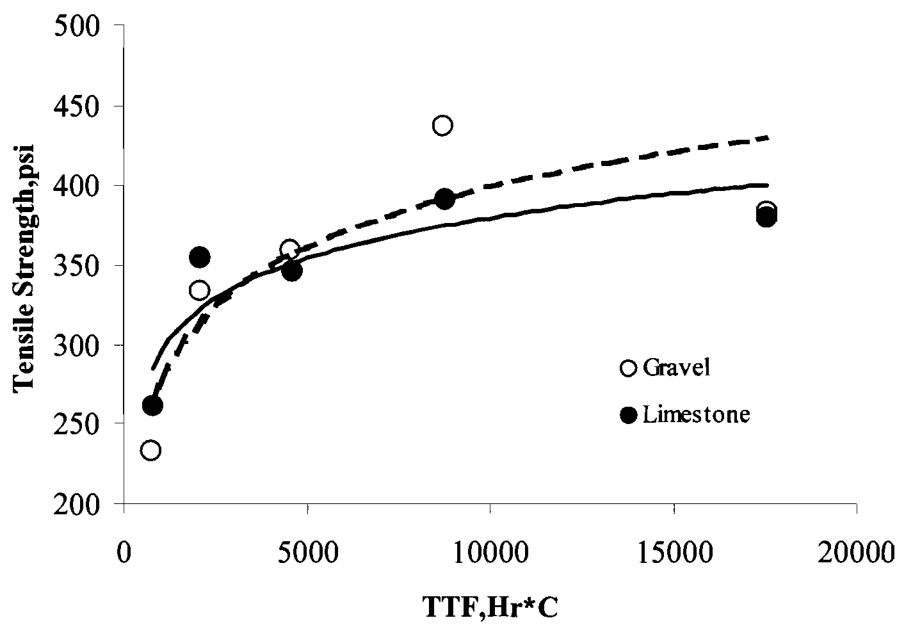

Figure D-2 –Variation in Tensile Strength with Maturity for Sand-cured Specimens

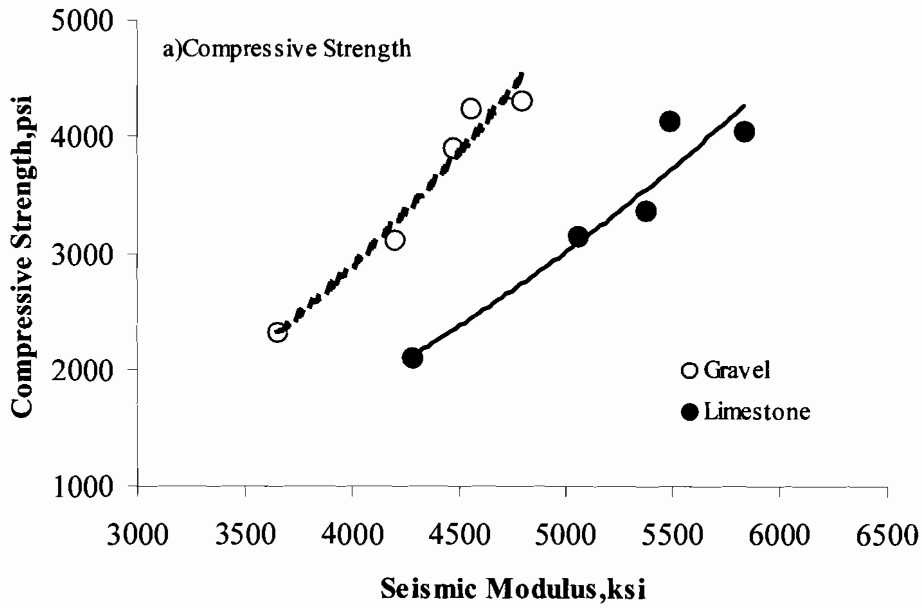

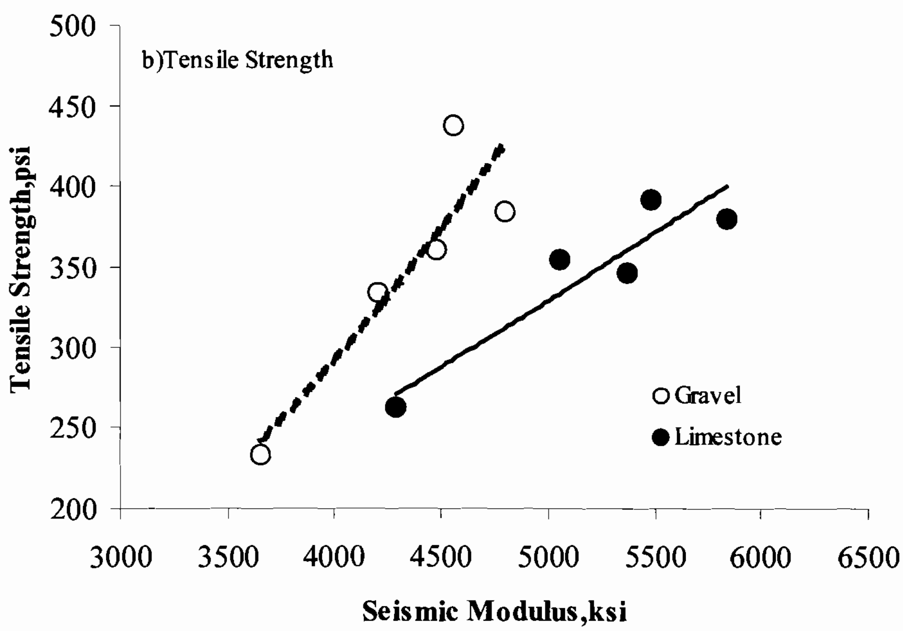

Figure D-3 –Variation in Strength Parameters with Seismic Modulus for Sand-cured Specimens

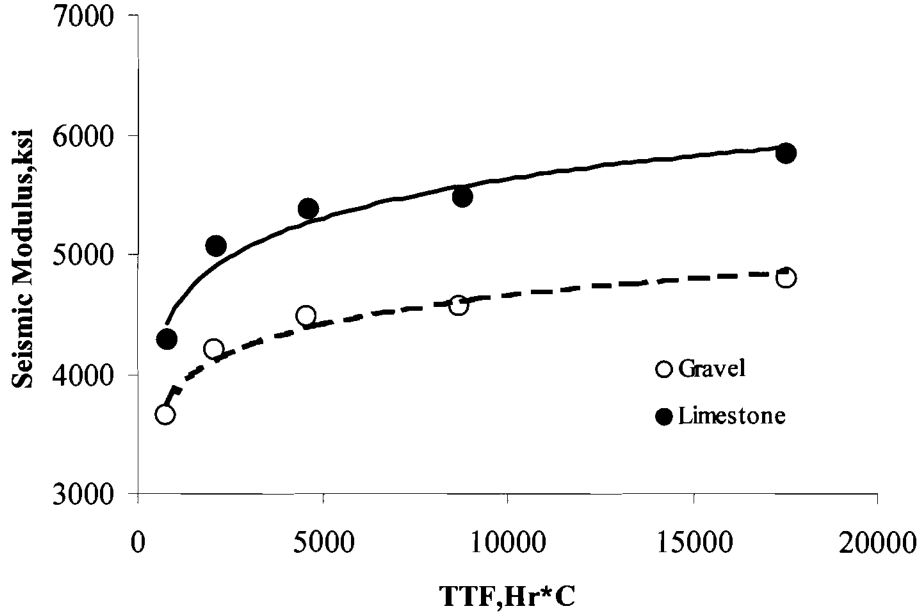

Figure D-4-Variation in Seismic Modulus with Maturity for Sand-cured Specimens

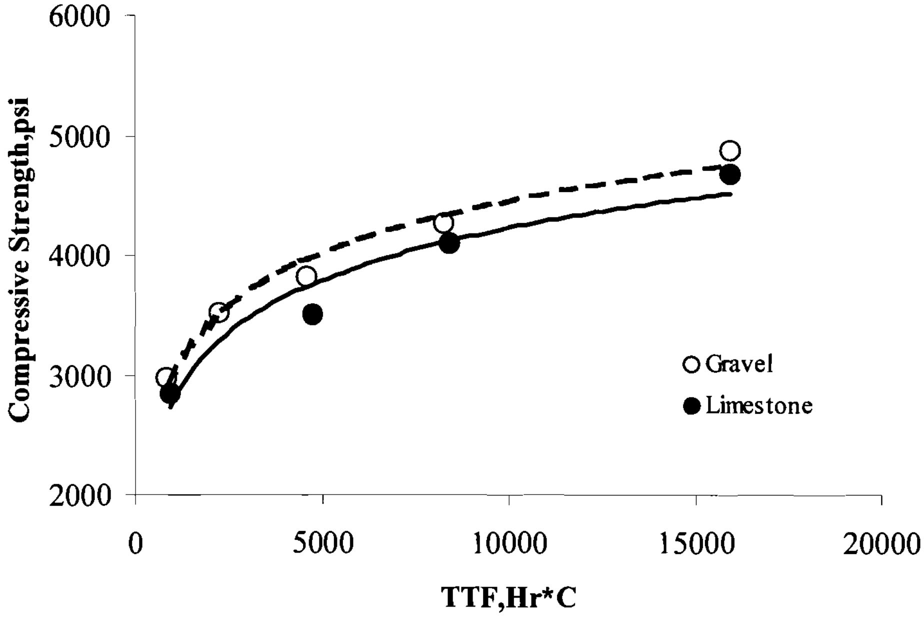

Figure D-5 – Variation in Compressive Strength with Maturity for the 4-in-diameter Cores

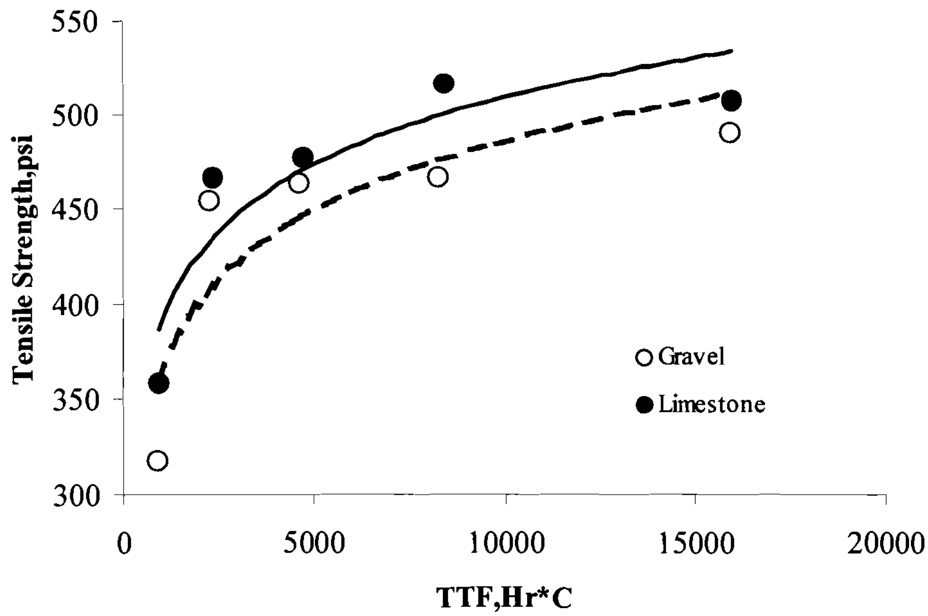

Figure D-6 – Variation in Tensile Strength with Maturity for the 4-in-diameter Cores

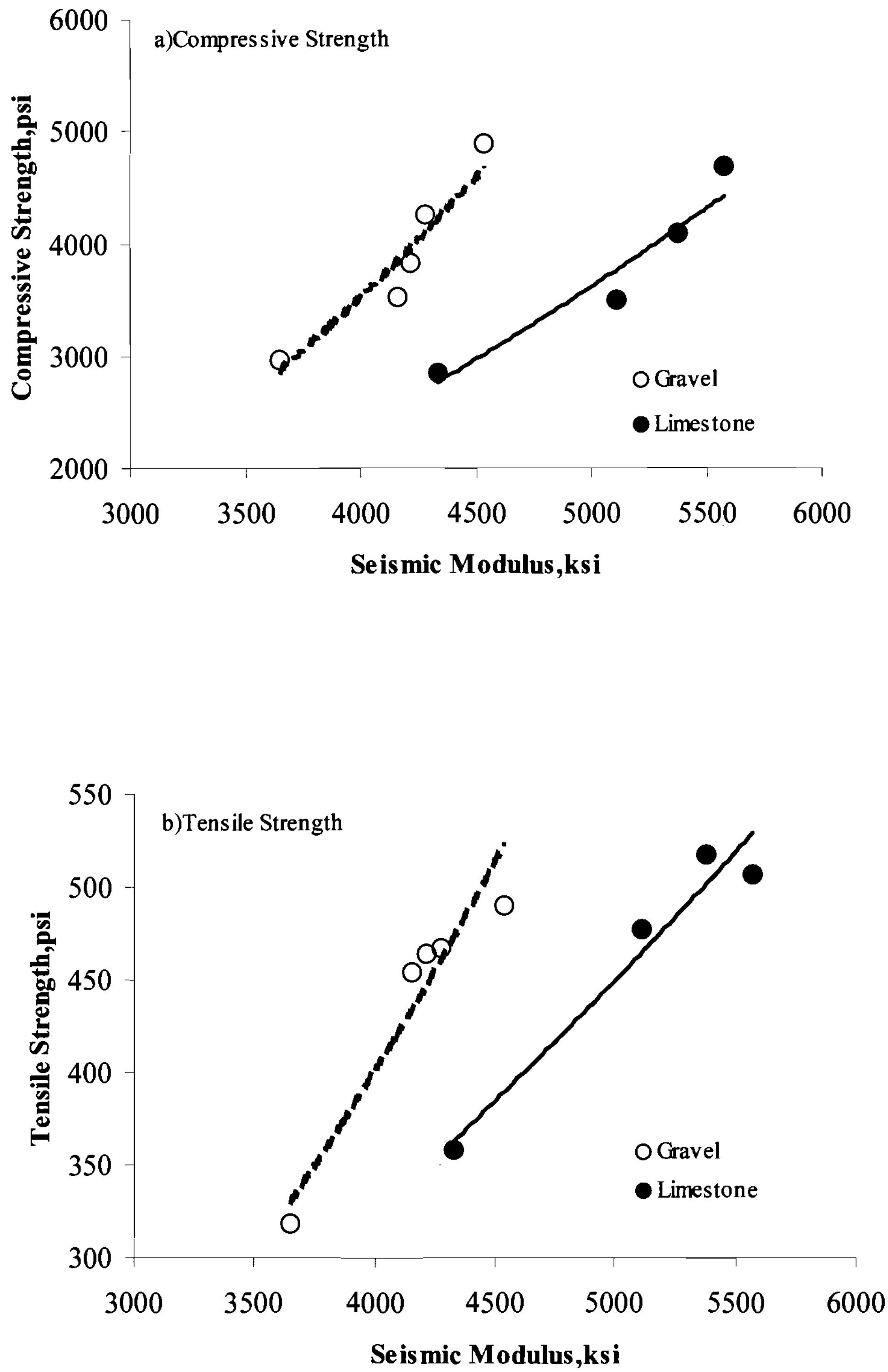

Figure D-7– Variation in Strength Parameters with Seismic Modulus for the 4-in-diameter Cores

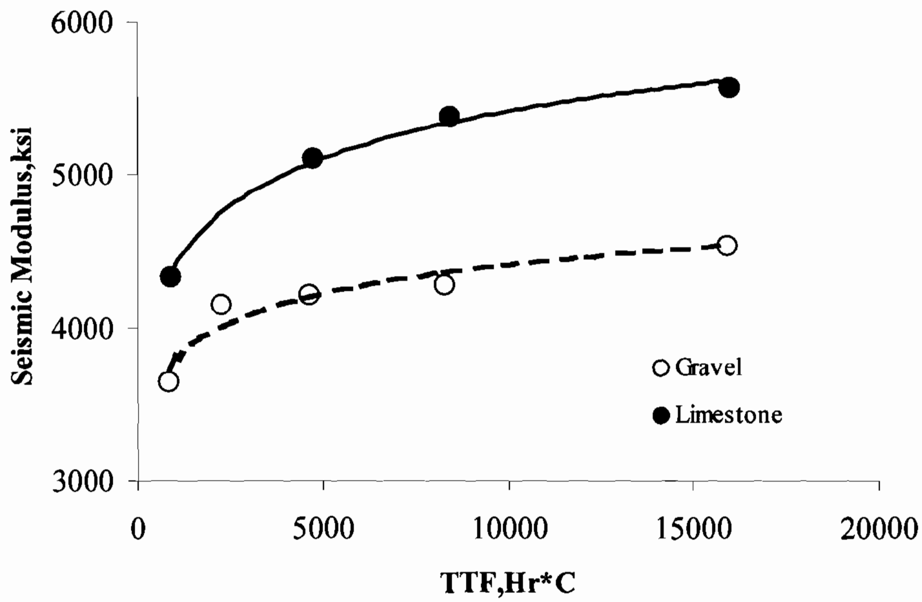

Figure D-8 – Variation in Seismic Modulus with Maturity for the 4-in-diameter Cores

FIGURE NO.	CASE STUDY	SPECIMEN TYPE	RELATION	TYPE OF AGGREGATE	DEVELOPED CORRELATION	R^2 VALUE
D-1	Small Slab I Study	Standard Sand-cured Cylinders	Compressive Strength vs. Maturity	Limestone	Y=650.53Ln(X)-2052.9	0.92
				Gravel	Y=671.44Ln(X)-1997.1	0.94
D-2	Small Slab I Study	Standard Sand-cured Cylinders	Tensile Strength vs. Maturity	Limestone	Y=37.008Ln(X)+39.215	0.78
				Gravel	Y=54.158Ln(X)-99.841	0.77
D-3.a	Small Slab I Study	Standard Sand-cured Cylinders	Compressive Strength vs. Seismic Modulus	Limestone	$Y=1E\text{-}05X^{2.2658}$	0.94
				Gravel	$Y=4E\text{-}06X^{2.4721}$	0.97
D-3.b	Small Slab I Study	Standard Sand-cured Cylinders	Tensile Strength vs. Seismic Modulus	Limestone	$Y=0.0063X^{1.2761}$	0.88
				Gravel	$Y=7E\text{-}06X^{2.1105}$	0.86
D-4	Small Slab I Study	Standard Sand-cured Cylinders	Seismic Modulus vs. Maturity	Limestone	Y=469.37Ln(X)+1305.1	0.95
				Gravel	Y=346.95Ln(X)+1459.7	0.96

FIGURE NO.	CASE STUDY	SPECIMEN TYPE	RELATION	TYPE OF AGGREGATE	DEVELOPED CORRELATION	R^2 VALUE
D-5	Small Slab I Study	4-in-diameter Cores	Compressive Strength vs. Maturity	Limestone	Y=629.17Ln(X)-1569.9	0.94
				Gravel	Y=631.25Ln(X)-1362.7	0.98
D-6	Small Slab I Study	4-in-diameter Cores	Tensile Strength vs. Maturity	Limestone	Y=51.826Ln(X)+32.368	0.82
				Gravel	Y=53.158Ln(X)-3.5419	0.76
D-7.a	Small Slab I Study	4-in-diameter Cores	Compressive Strength vs. Seismic Modulus	Limestone	$Y=0.0004X^{1.8669}$	0.93
				Gravel	$Y=3E\text{-}05X^{2.2323}$	0.91
D-7.b	Small Slab I Study	4-in-diameter Cores	Tensile Strength vs. Seismic Modulus	Limestone	$Y=0.0013X^{1.5001}$	0.96
				Gravel	$Y=9E\text{-}06X^{2.1175}$	0.93
D-8	Small Slab I Study	4-in-diameter Cores	Seismic Modulus vs. Maturity	Limestone	Y=444.44Ln(X)+1320.8	0.99
				Gravel	Y=273.06Ln(X)+1894	0.91